Compact and Full Polarimetric SAR techniques

Presenter

Marco Lavalle, DISP, Tor Vergata University, Rome, Italy

D. Solimini, Tor Vergata University, E. Pottier, University of Rennes 1

OUTLINE

1. FULL POLARIMETRY AND FULL POLINSAR

2. COMPACT POLARIMETRY AND COMPACT POLINSAR

RADAR POLARIMETRY

what is polarimetry

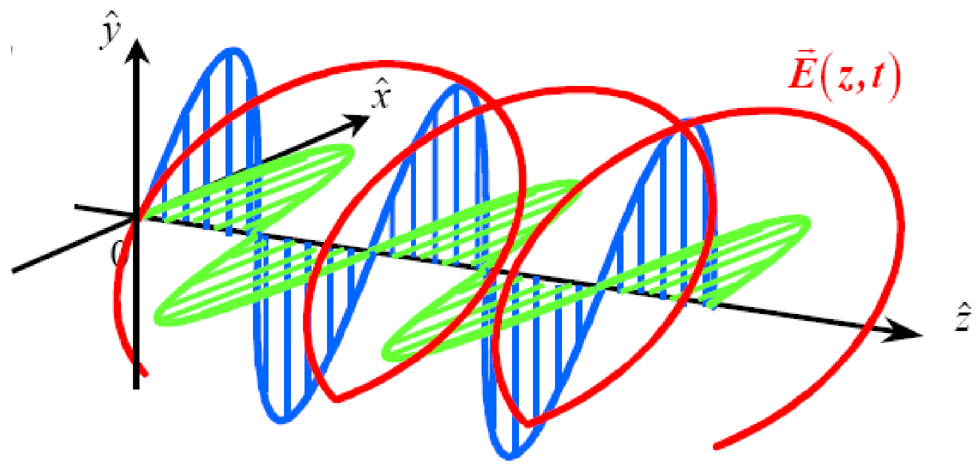

Radar Polarimetry (Polar : polarisation Metry: measure) is the science of acquiring, processing and analysing the polarization state of an electromagnetic field

Radar Polarimetry deals with the full vector nature of polarized electromagnetic waves

what is polarimetry

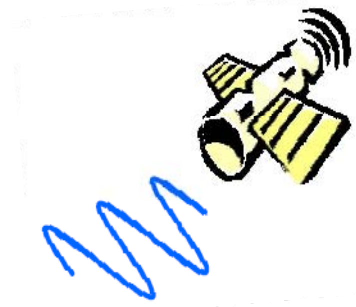

The information contained into backscattered waves from a given target is highly related to:

- → geometrical structure
- → reflectivity
- → shape
- → orientation
- → geophysical properties
- → umidity
- → roughness
- → etc.

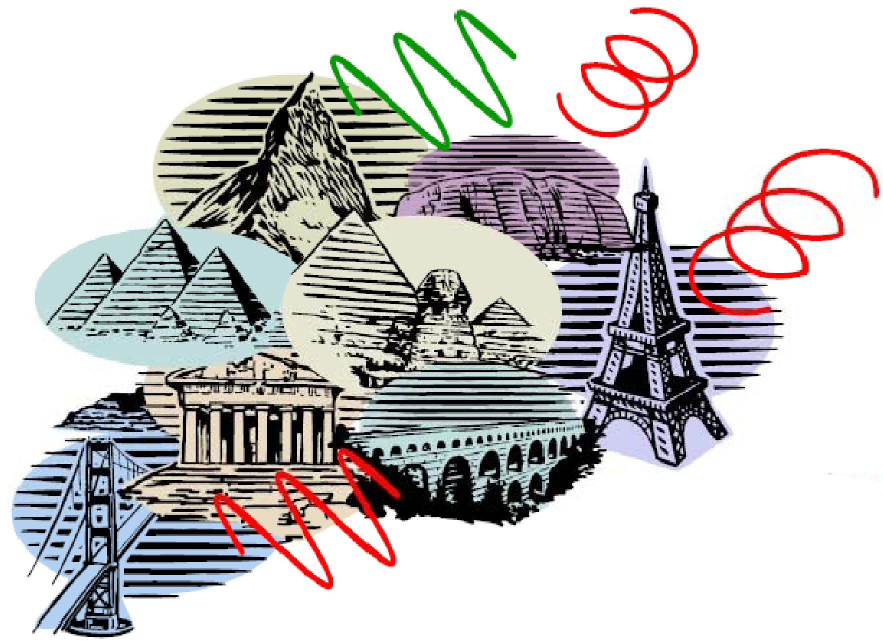

RADAR POLARIMETRY
space-borne sensors

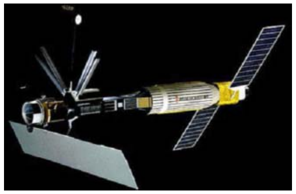

SEASAT
NASA/JPL (USA)
L-Band, 1978

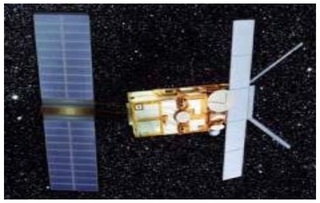

ERS-1
European Space Agency (ESA)
C-Band, 1991-2000

J-ERS-1
Japanese Space Agency (NASDA)
L-Band, 1992-1998

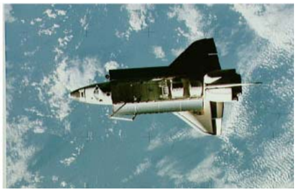

SIR-C/X-SAR
NASA/JPL, L- and C-Band (quad)
DLR / ASI, X-band
April and October 1994

RadarSAT-1
Canadian Space Agency (CSA)
C-Band, 1995-today

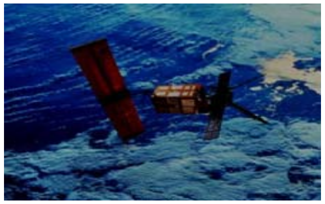

ERS-2
European Space Agency (ESA)
C-Band, 1995-today

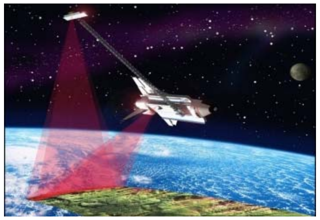

Shuttle Radar Topography Mission (SRTM)
NASA/JPL (C-Band), DLR (X-Band)
February 2000

ENVISAT / ASAR
European Space Agency (ESA)
C-Band (dual), 2002-today

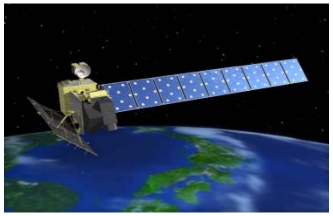

ALOS / PALSAR
Japanese Space Agency (JAXA)
L-Band (quad), 2006

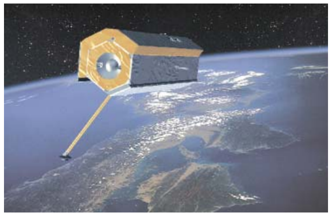

TerraSAR-X
German Aerospace Center (DLR) / Astirum
X-Band (quad), 2007

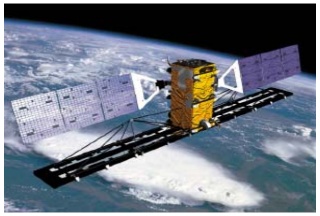

RadarSAT-II
Canadian Space Agency (CSA)
C-Band (quad), 2007

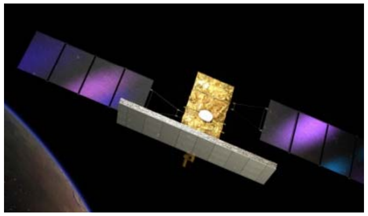

COSMO-SkyMed
Italian Space Agency (ASI)
X-Band, 2007

SCATTERING COEFFICIENT

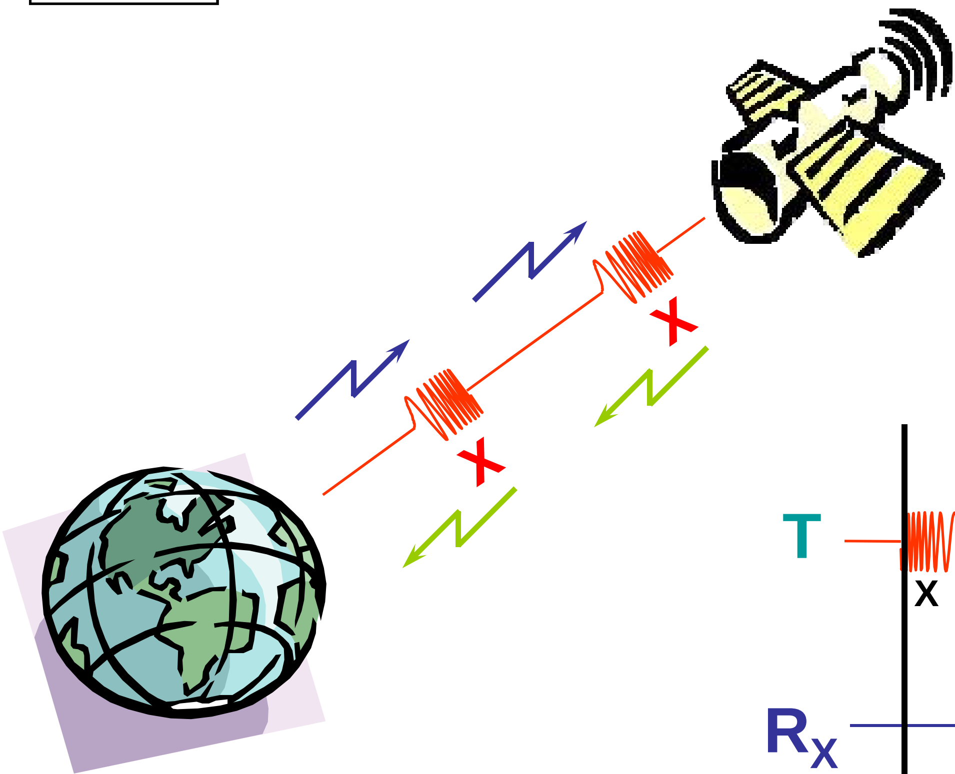

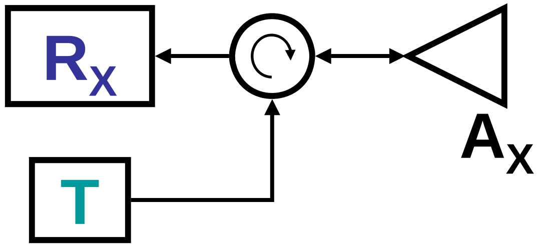

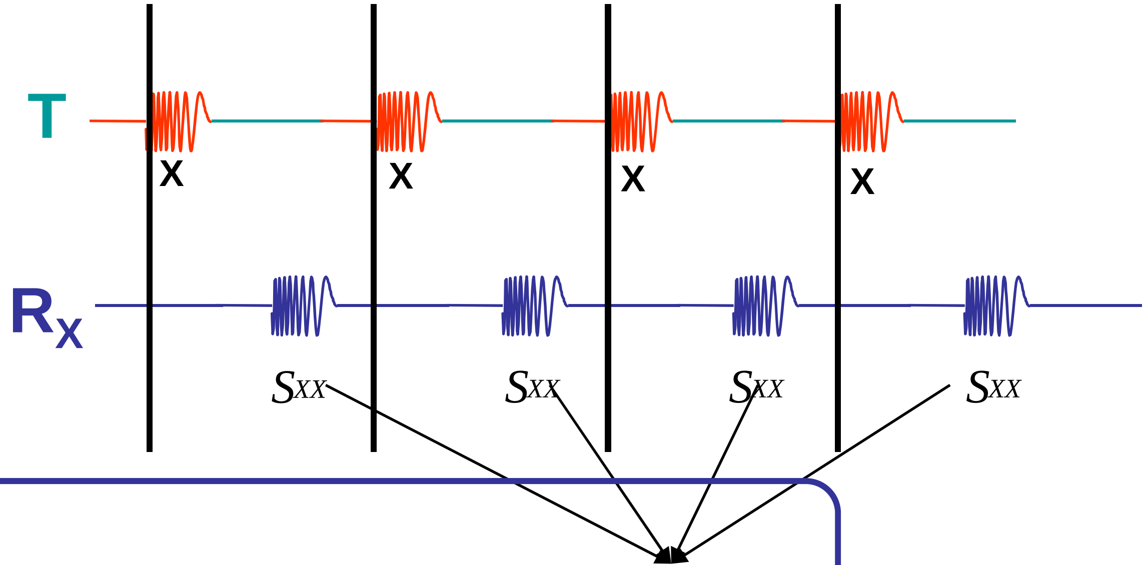

TRANSMITTER: X
RECEIVER: X

SCATTERING COEFFICIENT S_{XX}

RADAR POLARIMETRY

space-borne sensors

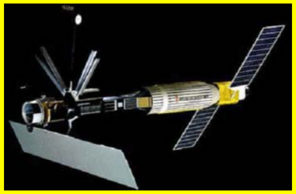

SEASAT
NASA/JPL (USA)
L-Band, 1978

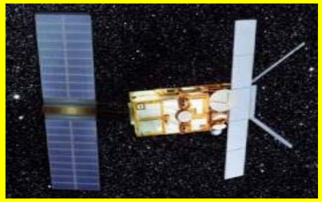

ERS-1
European Space Agency (ESA)
C-Band, 1991-2000

J-ERS-1
Japanese Space Agency (NASDA)
L-Band, 1992-1998

SIR-C/X-SAR
NASA/JPL, L- and C-Band (quad)
DLR / ASI, X-band
April and October 1994

RadarSAT-1
Canadian Space Agency (CSA)
C-Band, 1995-today

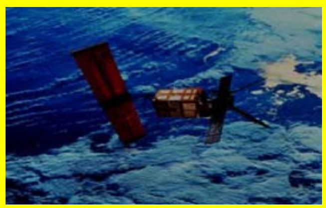

ERS-2
European Space Agency (ESA)
C-Band, 1995-today

Shuttle Radar Topography Mission (SRTM)
NASA/JPL (C-Band), DLR (X-Band)
February 2000

ENVISAT / ASAR
European Space Agency (ESA)
C-Band (dual), 2002-today

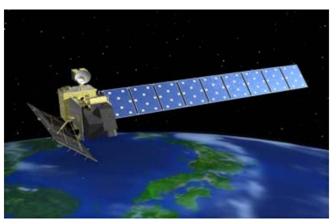

ALOS / PALSAR
Japanese Space Agency (JAXA)
L-Band (quad), 2006

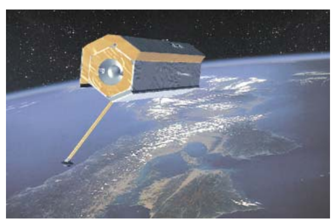

TerraSAR-X
German Aerospace Center (DLR) / Astirum
X-Band (quad), 2007

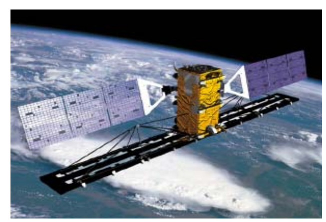

RadarSAT-II
Canadian Space Agency (CSA)
C-Band (quad), 2007

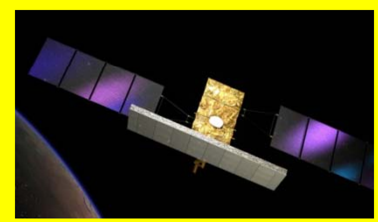

COSMO-SkyMed
Italian Space Agency (ASI)
X-Band, 2007

DUAL-POLARIMETRY

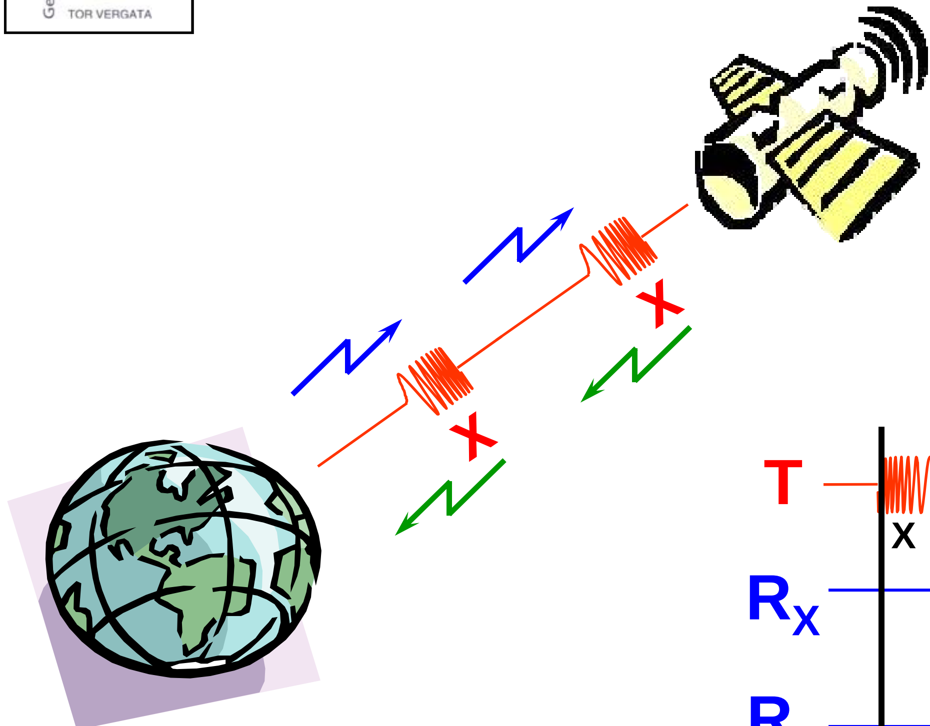

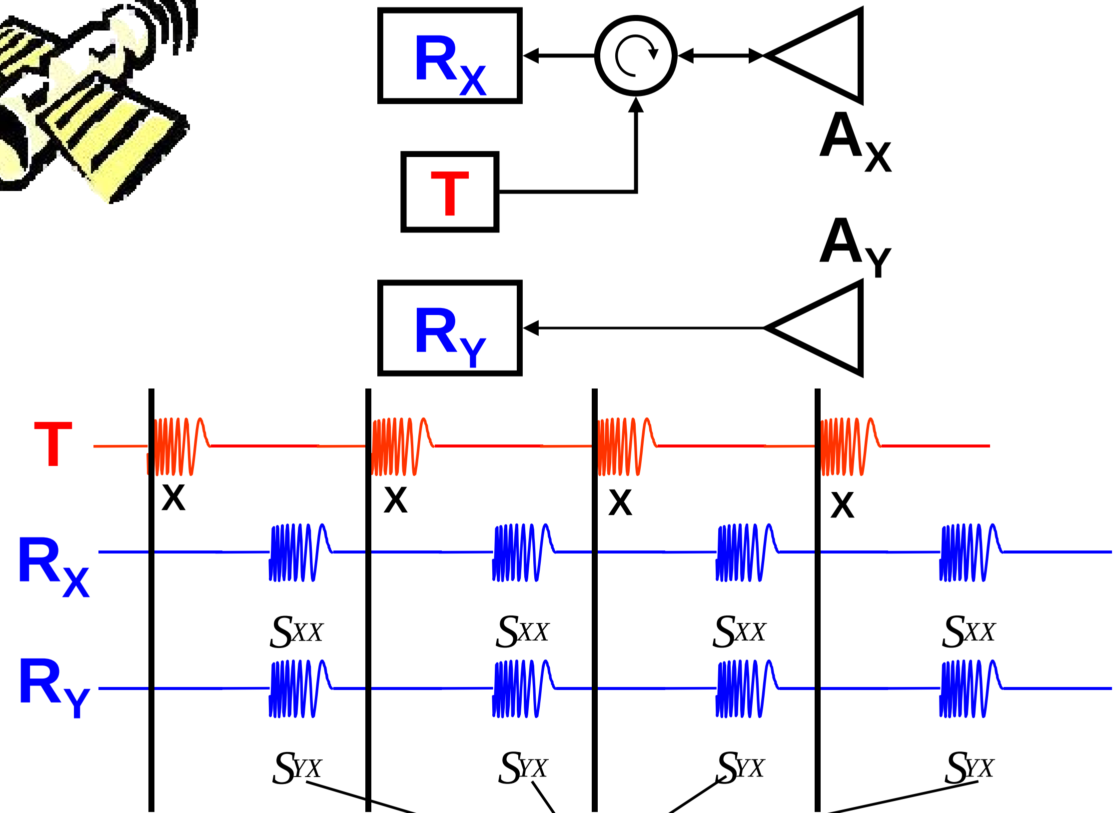

TRANSMITTER: X

RECEIVERS: X & Y

JONES VECTORS $\left\{ \underline{E}_S = \begin{bmatrix} S_{XX} \\ S_{YX} \end{bmatrix} \right\}$

RADAR POLARIMETRY
space-borne sensors

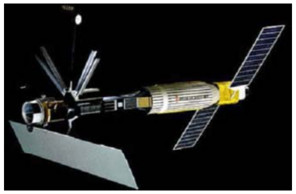

SEASAT
NASA/JPL (USA)
L-Band, 1978

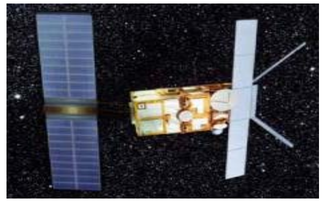

ERS-1
European Space Agency (ESA)
C-Band, 1991-2000

J-ERS-1
Japanese Space Agency (NASDA)
L-Band, 1992-1998

SIR-C/X-SAR
NASA/JPL, L- and C-Band (quad)
DLR / ASI, X-band
April and October 1994

RadarSAT-1
Canadian Space Agency (CSA)
C-Band, 1995-today

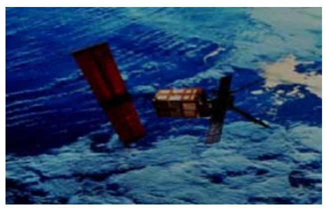

ERS-2
European Space Agency (ESA)
C-Band, 1995-today

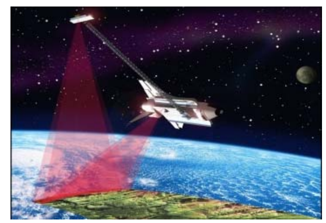

Shuttle Radar Topography Mission (SRTM)
NASA/JPL (C-Band), DLR (X-Band)
February 2000

ENVISAT / ASAR
European Space Agency (ESA)
C-Band (dual), 2002-today

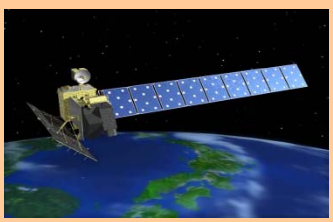

ALOS / PALSAR
Japanese Space Agency (JAXA)
L-Band (quad), 2006

TerraSAR-X
German Aerospace Center (DLR) / Astirum
X-Band (quad), 2007

RadarSAT-II
Canadian Space Agency (CSA)
C-Band (quad), 2007

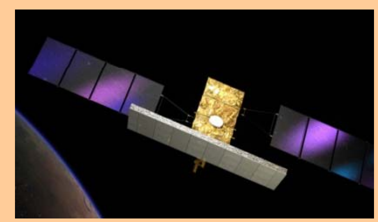

COSMO-SkyMed
Italian Space Agency (ASI)
X-Band, 2007

SCATTERING SAR POLARIMETRY

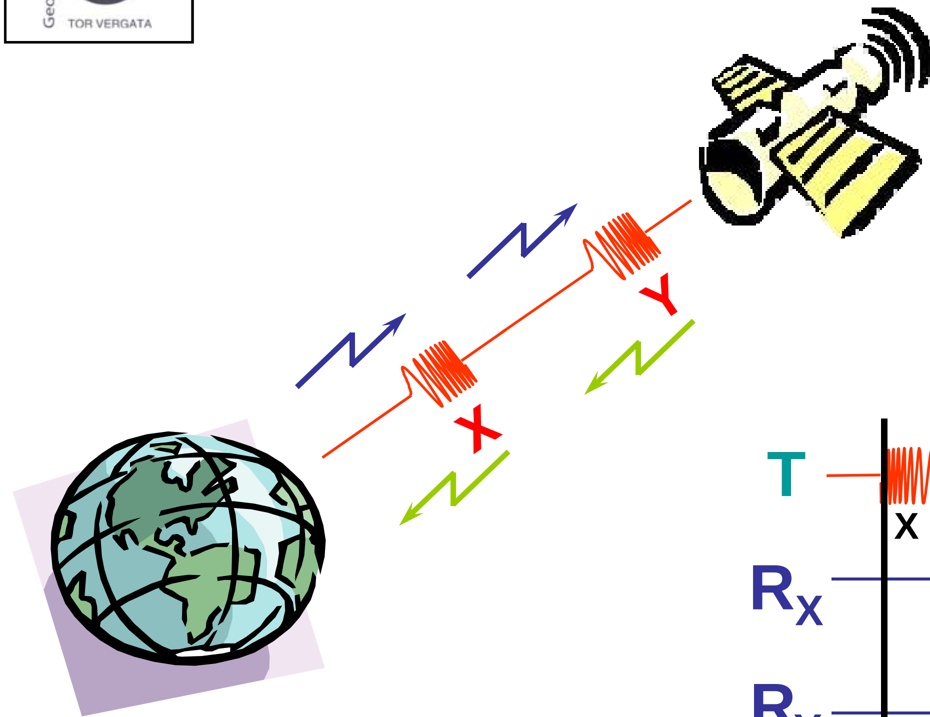

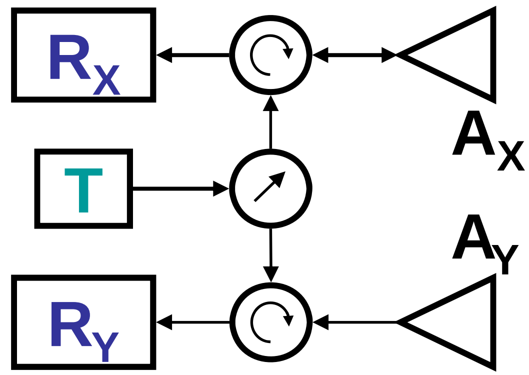

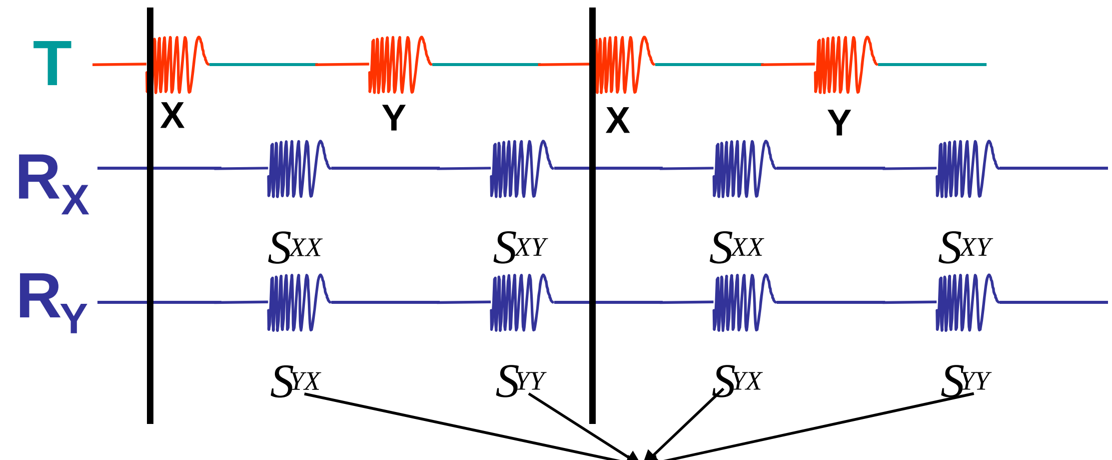

TRANSMITTER: X & Y

RECEIVERS: X & Y

SINCLAIR MATRICES $\left\{[S]=\begin{bmatrix}S_{XX} & S_{XY}\\ S_{YX} & S_{YY}\end{bmatrix}\right\}$

RADAR POLARIMETRY

space-borne sensors

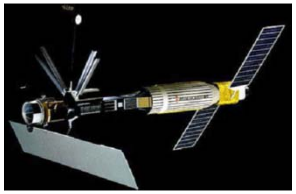

SEASAT
NASA/JPL (USA)
L-Band, 1978

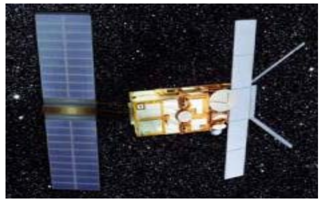

ERS-1
European Space Agency (ESA)
C-Band, 1991-2000

J-ERS-1
Japanese Space Agency (NASDA)
L-Band, 1992-1998

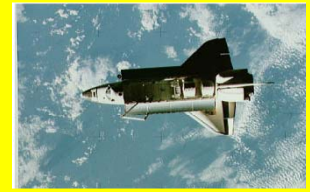

SIR-C/X-SAR
NASA/JPL, L- and C-Band (quad)
DLR / ASI, X-band
April and October 1994

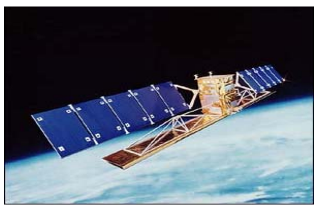

RadarSAT-1
Canadian Space Agency (CSA)
C-Band, 1995-today

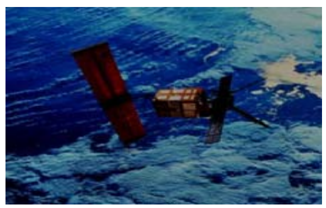

ERS-2
European Space Agency (ESA)
C-Band, 1995-today

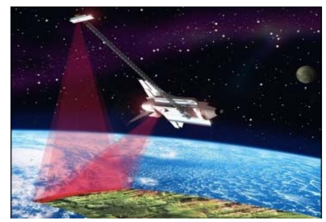

Shuttle Radar Topography Mission (SRTM)
NASA/JPL (C-Band), DLR (X-Band)
February 2000

ENVISAT / ASAR
European Space Agency (ESA)
C-Band (dual), 2002-today

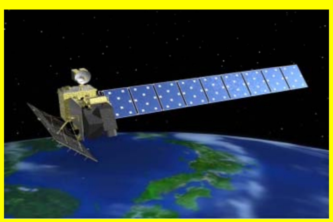

ALOS / PALSAR
Japanese Space Agency (JAXA)
L-Band (quad), 2006

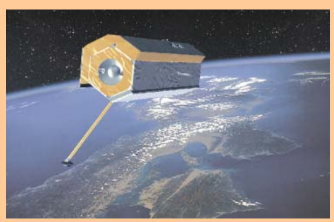

TerraSAR-X
German Aerospace Center (DLR) / Astrium
X-Band (quad), 2007

RadarSAT-II
Canadian Space Agency (CSA)
C-Band (quad), 2007

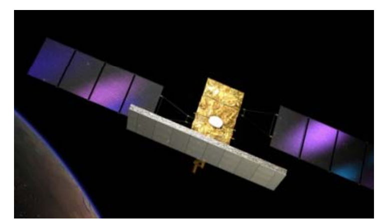

COSMO-SkyMed
Italian Space Agency (ASI)
X-Band, 2007

FULL PolSAR SPACEBORNE SENSORS

	ALOS-PALSAR	RADARSAT-1	TERRASAR-X
	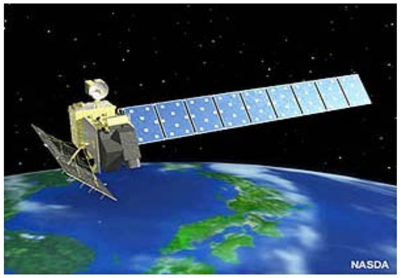	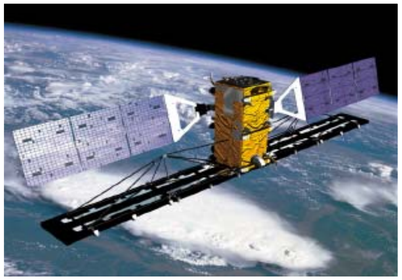	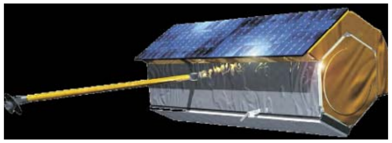
Orbit: LEO, Circular	**Sun-synchronous**	**Sun-synchronous**	**Sun-synchronous**
Repeat Period	**46 days**	**24 days**	**11 days**
Equatorial Crossing Time (*hrs*)	**22:30 (ascending)**	**18:00 (ascending)**	**18:00 (ascending)**
Inclinaison (*deg*)	**98.16**	**98.60**	**97.44**
Equatorial Altitude (*km*)	**692**	**798**	**515**
Wavelegth - Band	**23cm (L)**	**5.6 cm (C)**	**3 cm (X)**

FUTURE SPACEBORNE SENSORS

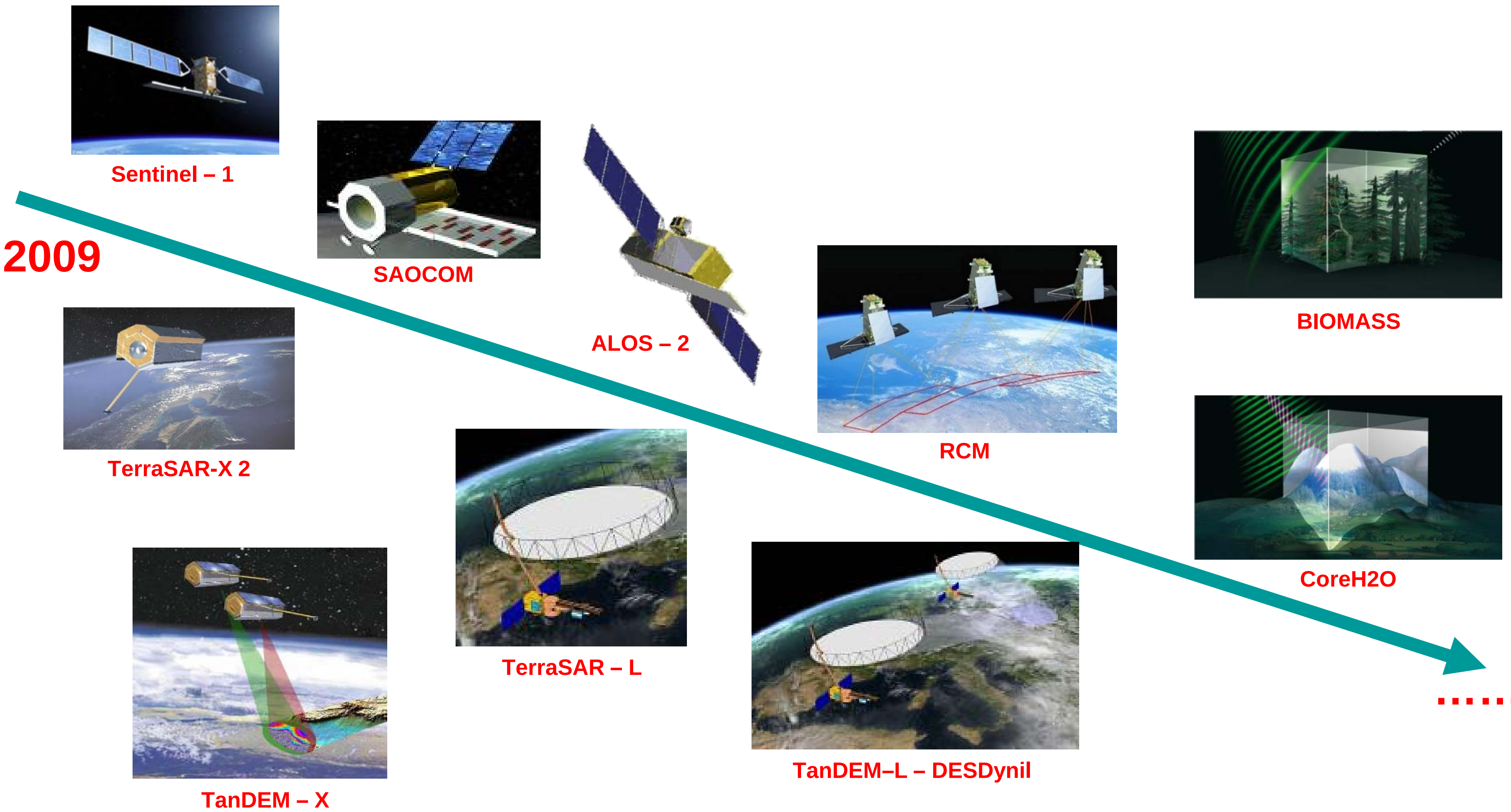

SAR POLARIMETRY APPLICATIONS

Forest Vegetation

- Forest Height
- Forest Biomass
- Forest Structure
- Canopy Extinction
- Underlying Topography

- Forest Ecology
- Forest Management
- Ecosystem Change
- Carbon Cycle

Agriculture

- Soil Moisture Content
- Soil roughness
- Height of Vegetation Layer
- Extinction of Vegetation Layer
- Moisture of Vegetation Layer

- Farming Management
- Water Cycle
- Desretification

Snow and Ice

- Topography
- Penetration Depth / Density
- Snow Ice Layer
- Snow Ice Extinction
- Water Equivalent

- Ecosystem Change
- Water Cycle
- Water Management

Urban Areas

- Geometric Properties
- Dielectric Properties

- Urban Monitoring

Courtesy of Dr. I. Hajnsek

SAN FRANCISCO BAY

AIRSAR

DC8

P, L, C-Band (Quad)

© Google Earth

SAN FRANCISCO BAY

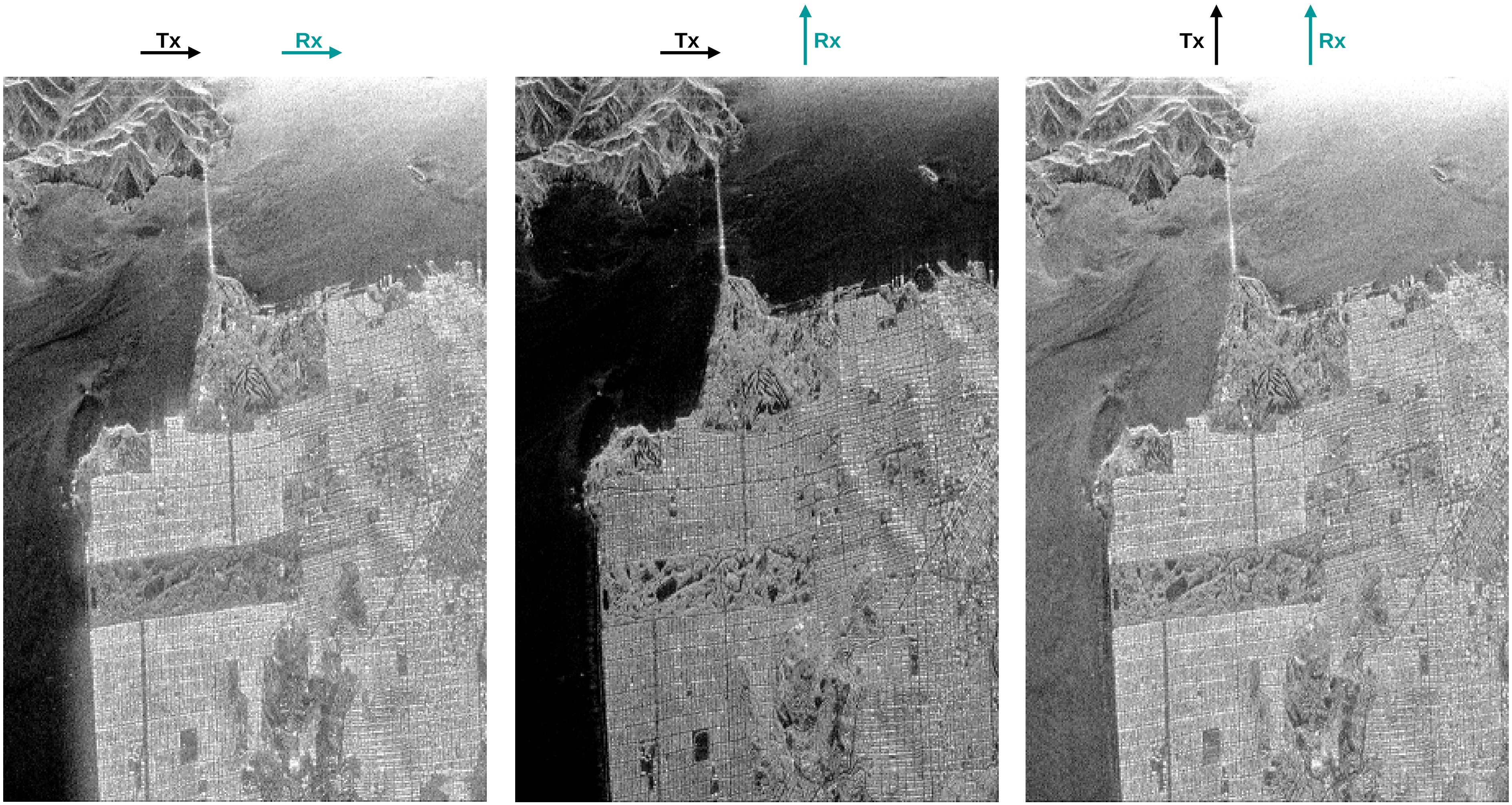

$|HH|_{dB}$ $|HV|_{dB}$ $|VV|_{dB}$

-30dB -15dB 0dB

SAN FRANCISCO BAY

© Google Earth

Sinclair Color Coding

|HH| |HV| |VV|

POLARIMETRIC DESCRIPTORS

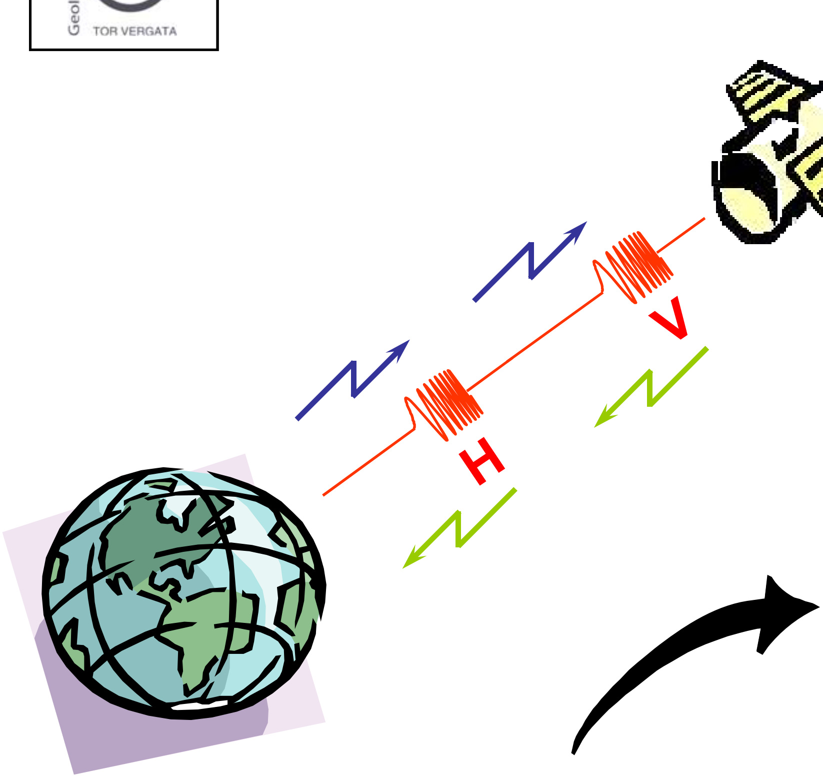

TRANSMITTER: H & V
RECEIVERS: H & V

POLARIMETRIC DESCRIPTORS

[S] SINCLAIR Matrix

$$[S] = \begin{bmatrix} S_{HH} & S_{HV} \\ S_{VH} & S_{VV} \end{bmatrix}$$

$\underline{k}$ Target Vector

[T] 3x3 COHERENCY Matrix

POLARIMETRIC DESCRIPTORS

VECTORIZATION OF [S]

$$[S] = \begin{bmatrix} S_{HH} & S_{HV} \\ S_{HV} & S_{VV} \end{bmatrix} \Rightarrow \underline{k} = V([S]) = \frac{1}{2} Trace([S][\psi])$$

SET OF 2x2 COMPLEX MATRICES FROM THE PAULI MATRICES GROUP

$$[\psi_P] = \left\{ \sqrt{2}\begin{bmatrix} 1 & 0 \\ 0 & 1 \end{bmatrix}, \sqrt{2}\begin{bmatrix} 1 & 0 \\ 0 & -1 \end{bmatrix}, \sqrt{2}\begin{bmatrix} 0 & 1 \\ 1 & 0 \end{bmatrix} \right\}$$

⬇

TARGET VECTOR

$$\underline{k} = \frac{1}{\sqrt{2}} \begin{bmatrix} S_{HH} + S_{VV} & S_{HH} - S_{VV} & 2S_{HV} \end{bmatrix}^T$$

POLARIMETRIC DESCRIPTORS

TARGET VECTOR $\underline{k}$

$$\underline{k} = \frac{1}{\sqrt{2}} \left[S_{HH} + S_{VV} \quad S_{HH} - S_{VV} \quad 2S_{HV} \right]^T$$

COHERENCY MATRIX [*T*]

$$[T] = \underline{k} \cdot \underline{k}^{*T} = \begin{bmatrix} 2A_0 & C - jD & H + jG \\ C + jD & B_0 + B & E + jF \\ H - jG & E - jF & B_0 - B \end{bmatrix}$$

HERMITIAN MATRIX - RANK 1

A0, B0+B, B0-B : HUYNEN TARGET GENERATORS

[*T*] is closer related to Physical and Geometrical Properties of the Scattering Process, and thus allows a better and direct physical interpretation

TARGET GENERATORS

PHYSICAL INTERPRETATION

SINGLE BOUNCE SCATTERING (ROUGH SURFACE)

DOUBLE BOUNCE SCATTERING

VOLUME SCATTERING

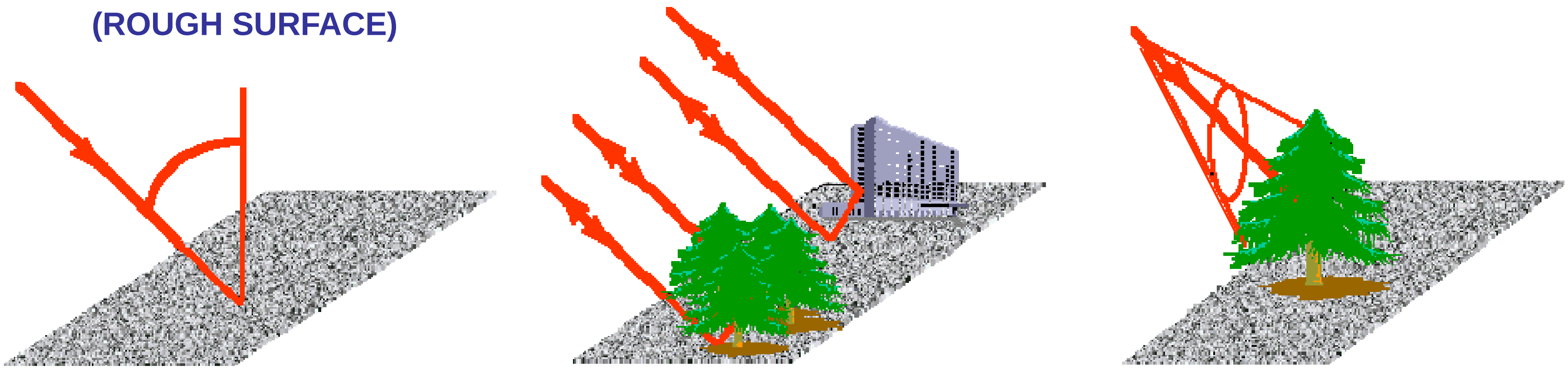

$$T_{11} = 2A_0 = \left|S_{HH} + S_{VV}\right|^2$$

$$T_{33} = B_0 - B = 2\left|S_{HV}\right|^2$$

$$T_{22} = B_0 + B = \left|S_{HH} - S_{VV}\right|^2$$

SAN FRANCISCO BAY

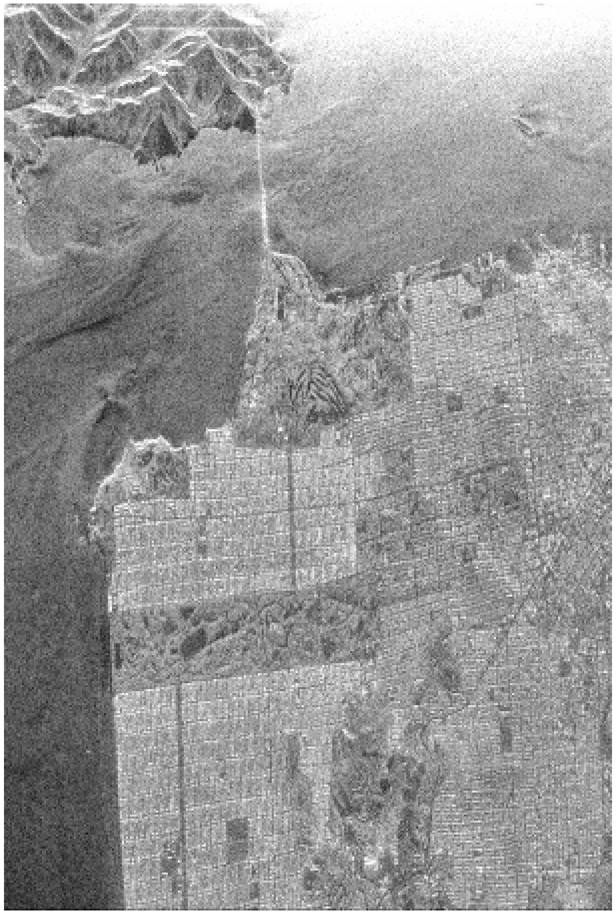

$|HH+VV|_{dB}$

$|HV|_{dB}$

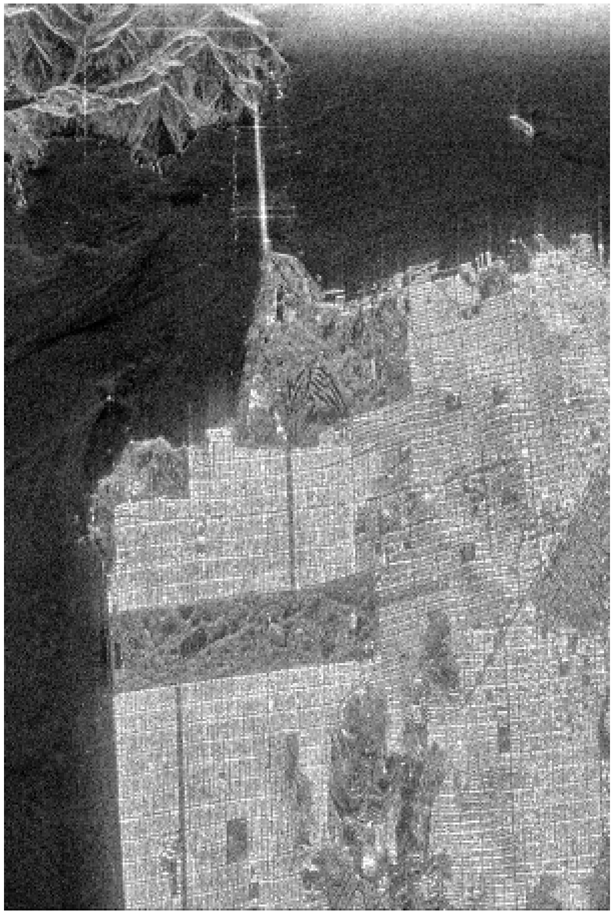

$|HH-VV|_{dB}$

-30dB -15dB 0dB

SAN FRANCISCO BAY

© Google Earth

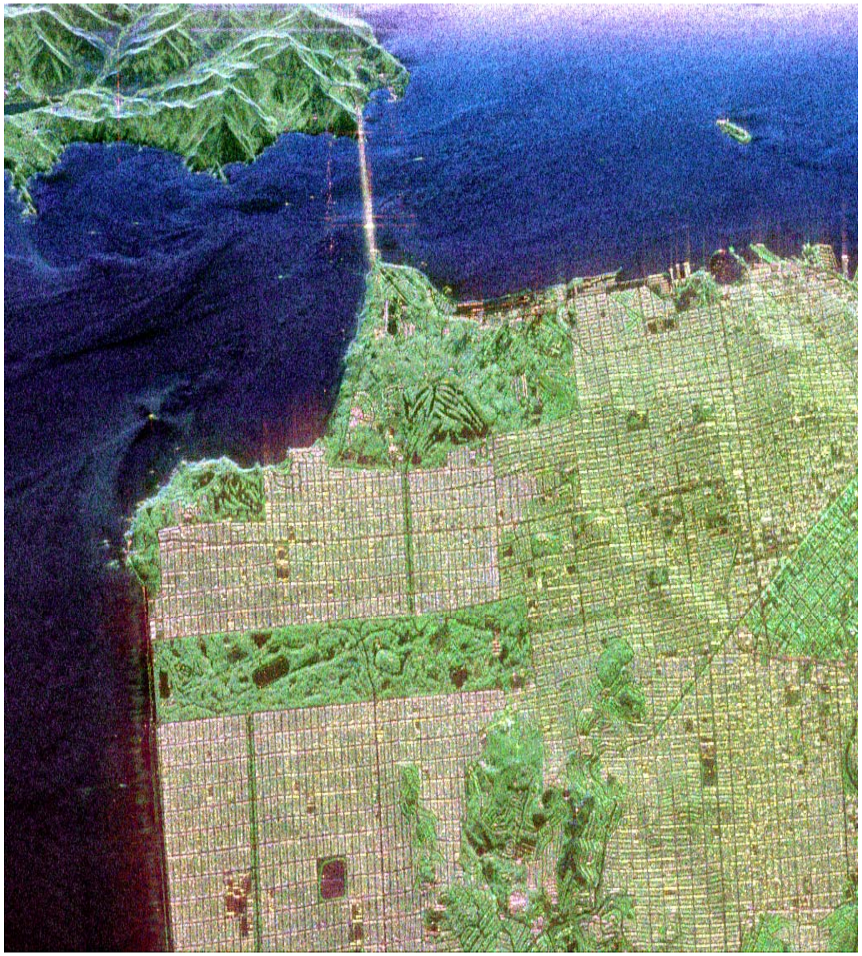

|HH+VV| |HV| |HH-VV|

$T_{11}=2A_0$ $T_{33}=B_0-B$ $T_{22}=B_0+B$

ELLIPTICAL BASIS TRANSFORMATION

SINCLAIR MATRIX

$$\left[S_{(B,B_\perp)}\right] = \left[U_{(A,A_\perp)\mapsto(B,B_\perp)}\right]^T \left[S_{(A,A_\perp)}\right]\left[U_{(A,A_\perp)\mapsto(B,B_\perp)}\right]$$

CON-SIMILARITY TRANSFORMATION

$$\left[U_{2(A,A_\perp)\mapsto(B,B_\perp)}\right]$$

U(2) SPECIAL UNITARY ELLIPTICAL BASIS TRANSFORMATION MATRIX

COHERENCY MATRIX

$$\left[T_{(B,B_\perp)}\right] = \left[U_{3(A,A_\perp)\mapsto(B,B_\perp)}\right]\left[T_{(A,A_\perp)}\right]\left[U_{3(A,A_\perp)\mapsto(B,B_\perp)}\right]^{-1}$$

SIMILARITY TRANSFORMATION

$$\left[U_{3(A,A_\perp)\mapsto(B,B_\perp)}\right]$$

U(3) SPECIAL UNITARY ELLIPTICAL BASIS TRANSFORMATION MATRIX

ELLIPTICAL BASIS TRANSFORMATION

SPECIAL UNITARY SU(2) GROUP

$$[U] = \begin{bmatrix} cos(\phi) & -sin(\phi) \\ sin(\phi) & cos(\phi) \end{bmatrix} \begin{bmatrix} cos(\tau) & j\,sin(\tau) \\ j\,sin(\tau) & cos(\tau) \end{bmatrix} \begin{bmatrix} e^{-j\alpha} & 0 \\ 0 & e^{j\alpha} \end{bmatrix}$$

$$[U_2(\phi)] \qquad [U_2(\tau)] \qquad [U_2(\alpha)]$$

SPECIAL UNITARY SU(3) GROUP

$$\begin{bmatrix} 1 & 0 & 0 \\ 0 & cos(2\phi) & sin(2\phi) \\ 0 & -sin(2\phi) & cos(2\phi) \end{bmatrix} \begin{bmatrix} cos(2\tau) & 0 & j\,sin(2\tau) \\ 0 & 1 & 0 \\ j\,sin(2\tau) & 0 & cos(2\tau) \end{bmatrix} \begin{bmatrix} cos(2\alpha) & -j\,sin(2\alpha) & 0 \\ -j\,sin(2\alpha) & cos(2\alpha) & 0 \\ 0 & 0 & 1 \end{bmatrix}$$

$$[U_3(2\phi)] \qquad [U_3(2\tau)] \qquad [U_3(2\alpha)]$$

(ϕ, τ, α) **POLARIZATION ELLIPSE PARAMETERS**

ELLIPTICAL BASIS TRANSFORMATION

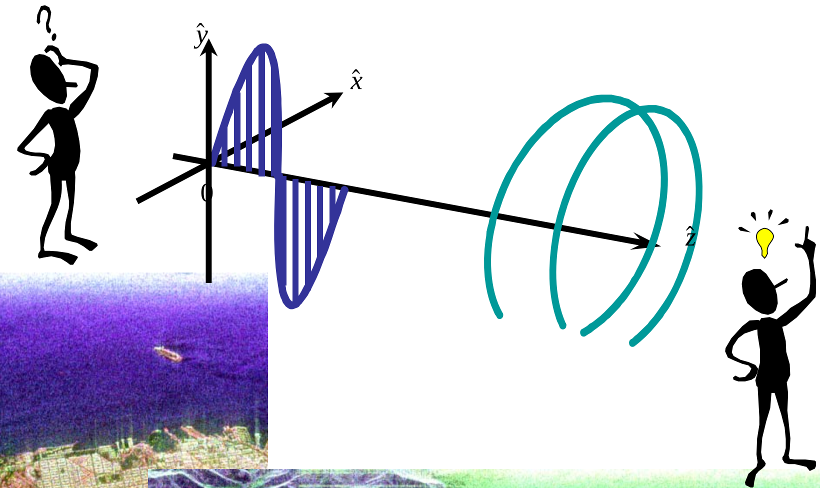

Pauli Color Coding (H,V)

Ernst LÜNEBURG
(PIERS95 - Pasadena)

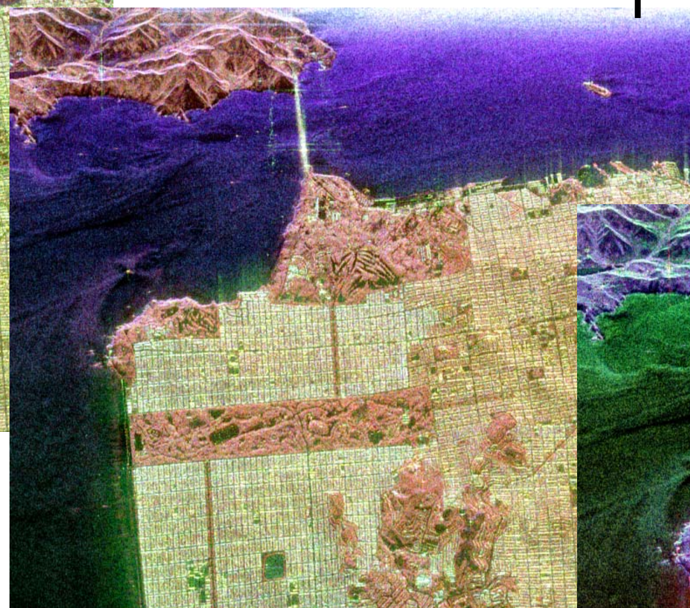

Pauli Color Coding (+45,-45)

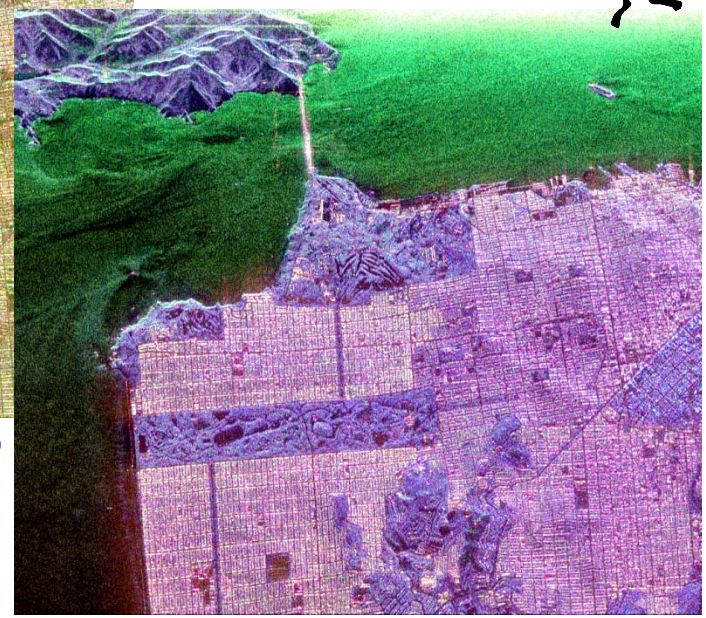

Pauli Color Coding (L,R)

SPECKLE FILTERING

$$[T] = \underline{k}\,\underline{k}^{*T}$$

SPECKLE FILTER

AVERAGING DATA

SECOND ORDER STATISTICS

COHERENCY MATRICES

SMOOTHING AVERAGING

CONCEPT OF THE DISTRIBUTED TARGET

$$\langle [T] \rangle = \frac{1}{N} \sum_{i=1}^{N} \underline{k}_i \underline{k}_i^{*T}$$

TARGET DECOMPOSITIONS

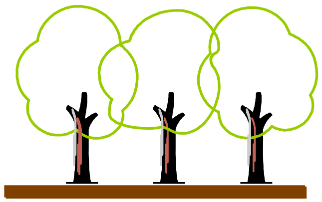

PURE TARGET

COHERENCY MATRIX [T]

9 REAL DEPENDANT HUYNEN PARAMETERS
(A0,B0,B,C,D,E,F,G,H)

POLARIMETRIC DISTRIBUTED TARGET « *DIMENSION* » = 5

9 - 5 = 4 TARGET EQUATIONS

$$2A_0(B_0+B) = C^2+D^2$$
$$2A_0(B_0-B) = G^2+H^2$$
$$2A_0E = CH-DG$$
$$2A_0F = CG+DH$$

TARGET DECOMPOSITIONS

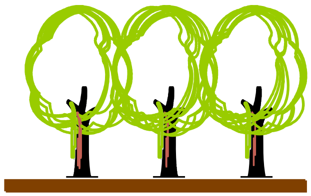

DISTRIBUTED TARGET

POLARIMETRIC DISTRIBUTED TARGET « *DIMENSION* » = 9

COHERENCY MATRIX $<[T]>$

9 REAL INDEPENDANT HUYNEN PARAMETERS

(<A0>,<B0>,<B>,<C>,<D>,<E>,<F>,<G>,<H>)

9 TARGET INEQUATIONS

$$2\langle A_0\rangle\left(\langle B_0\rangle+\langle B\rangle\right)\geq\langle C\rangle^2+\langle D\rangle^2$$

$$2\langle A_0\rangle\left(\langle B_0\rangle-\langle B\rangle\right)\geq\langle G\rangle^2+\langle H\rangle^2$$

$$2\langle A_0\rangle\langle E\rangle\geq\langle C\rangle\langle H\rangle-\langle D\rangle\langle G\rangle$$

$$2\langle A_0\rangle\langle F\rangle\geq\langle C\rangle\langle G\rangle+\langle D\rangle\langle H\rangle$$

$$\langle B_0\rangle^2\geq\langle B\rangle^2+\langle E\rangle^2+\langle F\rangle^2$$

$$\langle H\rangle\left(\langle B_0\rangle+\langle B\rangle\right)\geq\langle C\rangle\langle E\rangle+\langle D\rangle\langle F\rangle$$

$$\langle G\rangle\left(\langle B_0\rangle+\langle B\rangle\right)\geq\langle C\rangle\langle F\rangle-\langle D\rangle\langle E\rangle$$

$$\langle C\rangle\left(\langle B_0\rangle-\langle B\rangle\right)\geq\langle H\rangle\langle E\rangle+\langle F\rangle\langle G\rangle$$

$$\langle D\rangle\left(\langle B_0\rangle-\langle B\rangle\right)\geq\langle F\rangle\langle H\rangle-\langle G\rangle\langle E\rangle$$

TARGET DECOMPOSITIONS

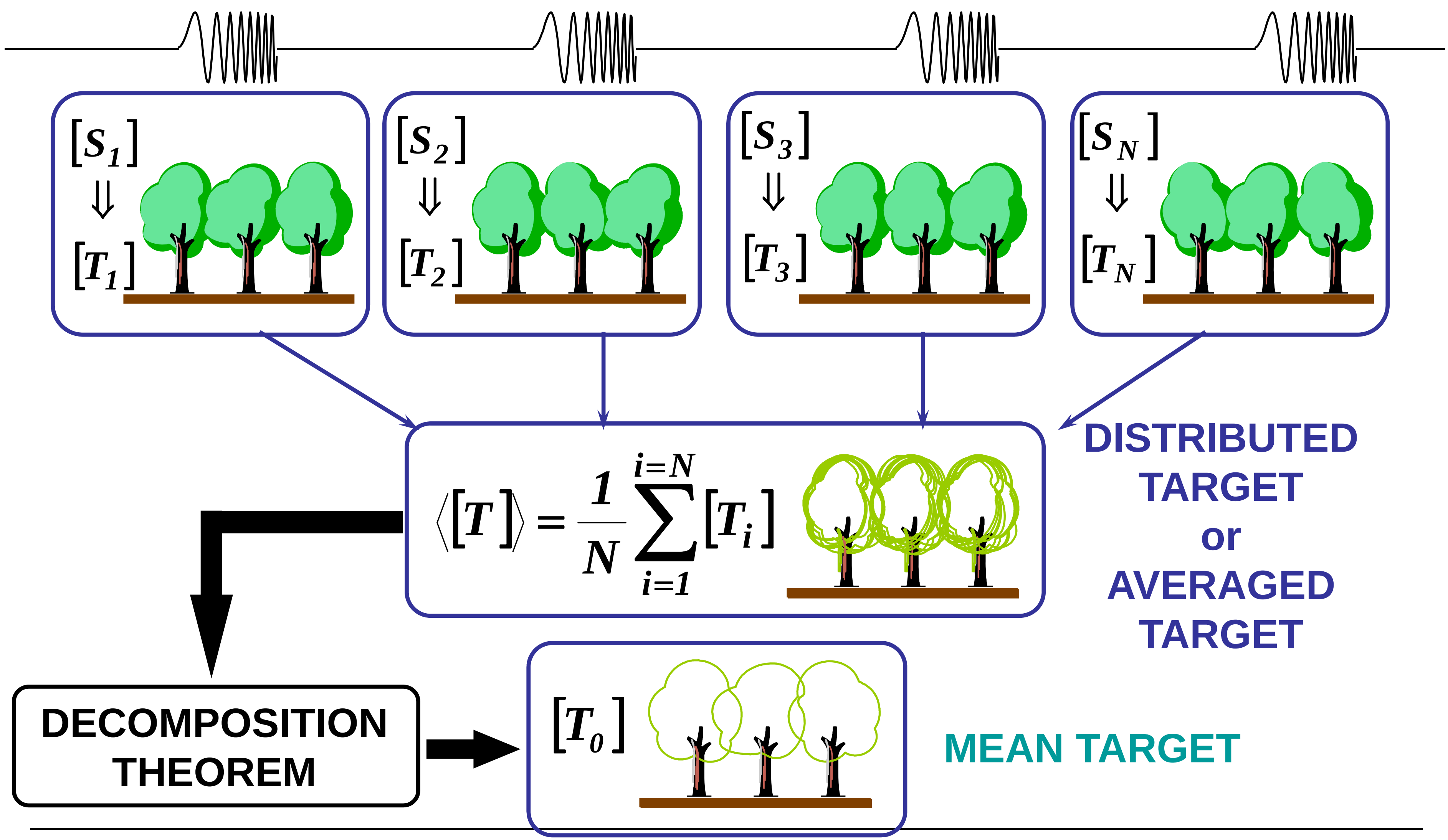

TARGET DECOMPOSITIONS

[S]

COHERENT DECOMPOSITION

E. KROGAGER (1990)

W.L. CAMERON (1990)

[K]

TARGET DICHOTOMY

J.R. HUYNEN (1970)

R.M. BARNES (1988)

[T] **[C]**

AZIMUTHAL SYMMETRY

EIGENVECTORS BASED DECOMPOSITION

S.R. CLOUDE (1985)

W.A. HOLM (1988)

MODEL BASED DECOMPOSITION

A.J. FREEMAN – S.L. DURDEN (1992)
Y. YAMAGUSHI (2005)

EIGENVECTORS / EIGENVALUES ANALYSIS
&
MODEL BASED DECOMPOSITION

J.J. VAN ZYL (1992 - 2008)

EIGENVECTORS / EIGENVALUES ANALYSIS
ENTROPY / ANISOTROPY / ALPHA

S.R. CLOUDE - E. POTTIER (1996-1997)

H / A / α DECOMPOSITION

TARGET VECTOR

$$\underline{k} = \frac{1}{\sqrt{2}}\left[S_{XX}+S_{YY} \quad S_{XX}-S_{YY} \quad 2S_{XY}\right]^T$$

LOCAL ESTIMATE OF THE COHERENCY MATRIX

$$\langle [T] \rangle = \frac{1}{N}\sum_{i=1}^{N} \underline{k}_i \cdot \underline{k}_i^{*T} = \frac{1}{N}\sum_{i=1}^{N}[T_i]$$

EIGENVECTORS / EIGENVALUES ANALYSIS

$$\langle [T] \rangle = [U_3][\Sigma][U_3]^{-1} = \begin{bmatrix} \underline{u}_1 & \underline{u}_2 & \underline{u}_3 \end{bmatrix} \begin{bmatrix} \lambda_1 & 0 & 0 \\ 0 & \lambda_2 & 0 \\ 0 & 0 & \lambda_3 \end{bmatrix} \begin{bmatrix} \underline{u}_1 & \underline{u}_2 & \underline{u}_3 \end{bmatrix}^{*T}$$

ORTHOGONAL EIGENVECTORS

REAL EIGENVALUES
$\lambda_1 > \lambda_2 > \lambda_3$

$$P_i = \frac{\lambda_i}{\sum_{k=1}^{3}\lambda_k}$$

H / A / α DECOMPOSITION

PARAMETERISATION OF THE SU(3) UNITARY MATRIX

$$[U_3] = \begin{bmatrix} \cos(\alpha_1) & \cos(\alpha_2) & \cos(\alpha_3) \\ \sin(\alpha_1)\cos(\beta_1)e^{j\delta_1} & \sin(\alpha_2)\cos(\beta_2)e^{j\delta_2} & \sin(\alpha_3)\cos(\beta_3)e^{j\delta_3} \\ \sin(\alpha_1)\sin(\beta_1)e^{j\gamma_1} & \sin(\alpha_2)\sin(\beta_2)e^{j\gamma_2} & \sin(\alpha_3)\sin(\beta_3)e^{j\gamma_3} \end{bmatrix}$$

3 ROLL INVARIANT PARAMETERS

ENTROPY — **$\underline{\alpha}$ PARAMETER** — **ANISOTROPY**

$$H = -\sum_{i=1}^{3} P_i \log_3(P_i) \qquad \underline{\alpha} = P_1\alpha_1 + P_2\alpha_2 + P_3\alpha_3 \qquad A = \frac{\lambda_2 - \lambda_3}{\lambda_2 + \lambda_3}$$

S.R. CLOUDE - E. POTTIER (1995 - 1996)

H / A / α DECOMPOSITION

$$\underline{\alpha} = P_1\alpha_1 + P_2\alpha_2 + P_3\alpha_3$$: ROLL INVARIANT

PHYSICAL INTERPRETATION

SINGLE BOUNCE SCATTERING (ROUGH SURFACE)	DOUBLE BOUNCE SCATTERING	VOLUME SCATTERING
$\underline{\alpha} \mapsto 0$	$\underline{\alpha} \mapsto \frac{\pi}{2}$	$\underline{\alpha} \mapsto \frac{\pi}{4}$

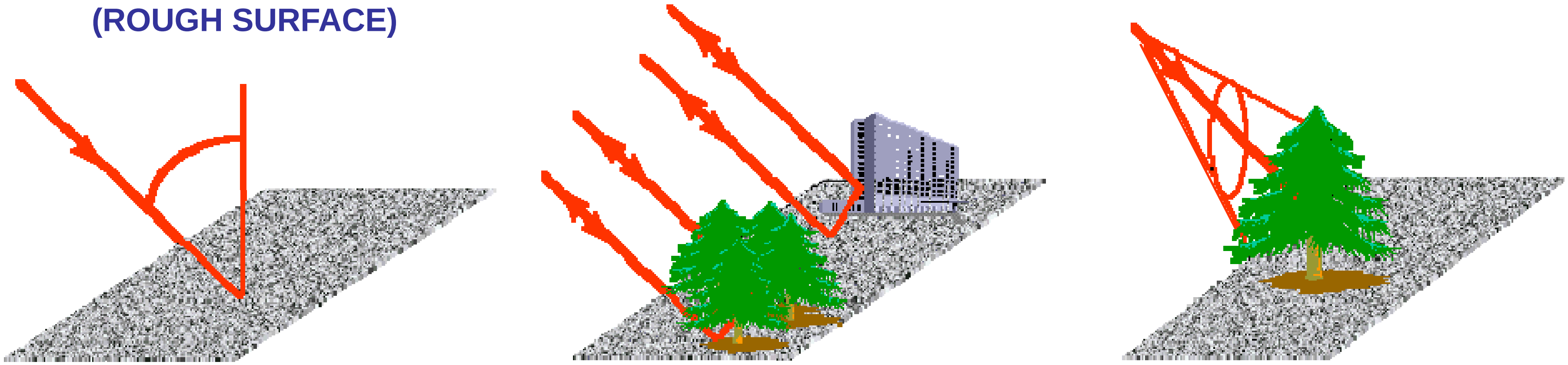

H / A / α DECOMPOSITION

α PARAMETER

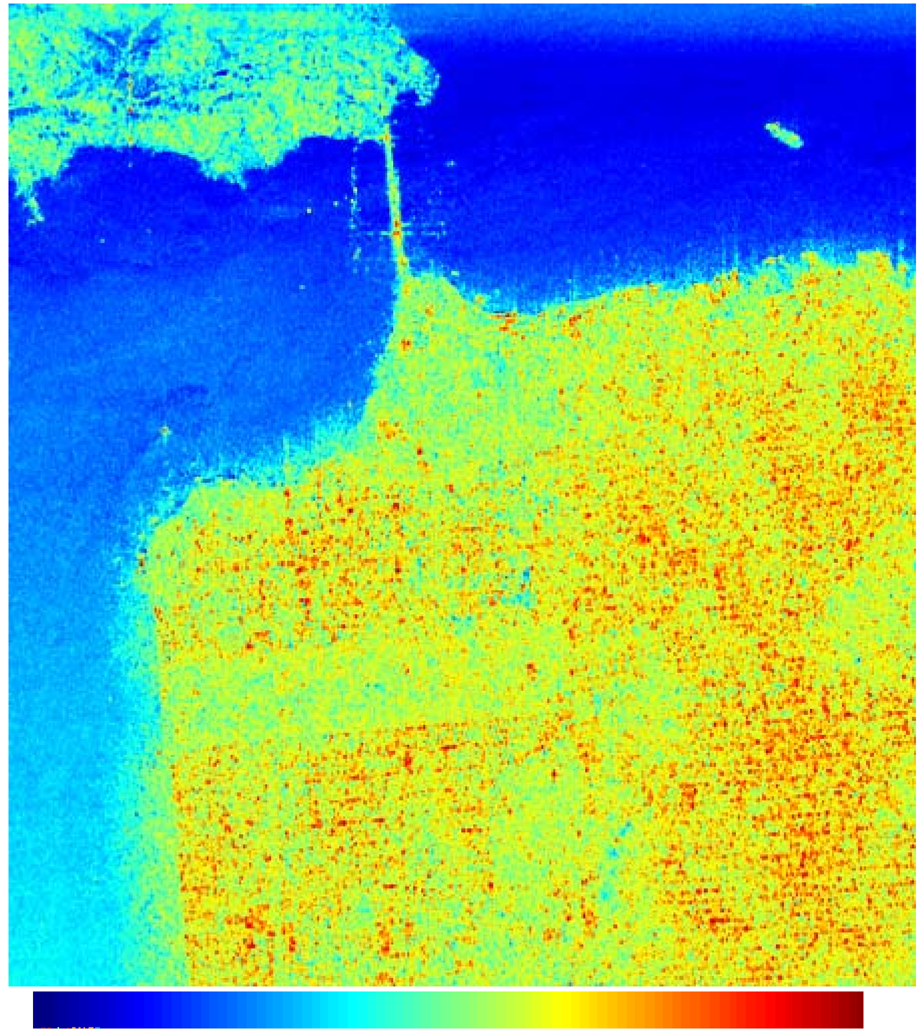

$2A_0$ $B_0 + B$ $B_0 - B$

H / A / α DECOMPOSITION

ENTROPY (H)

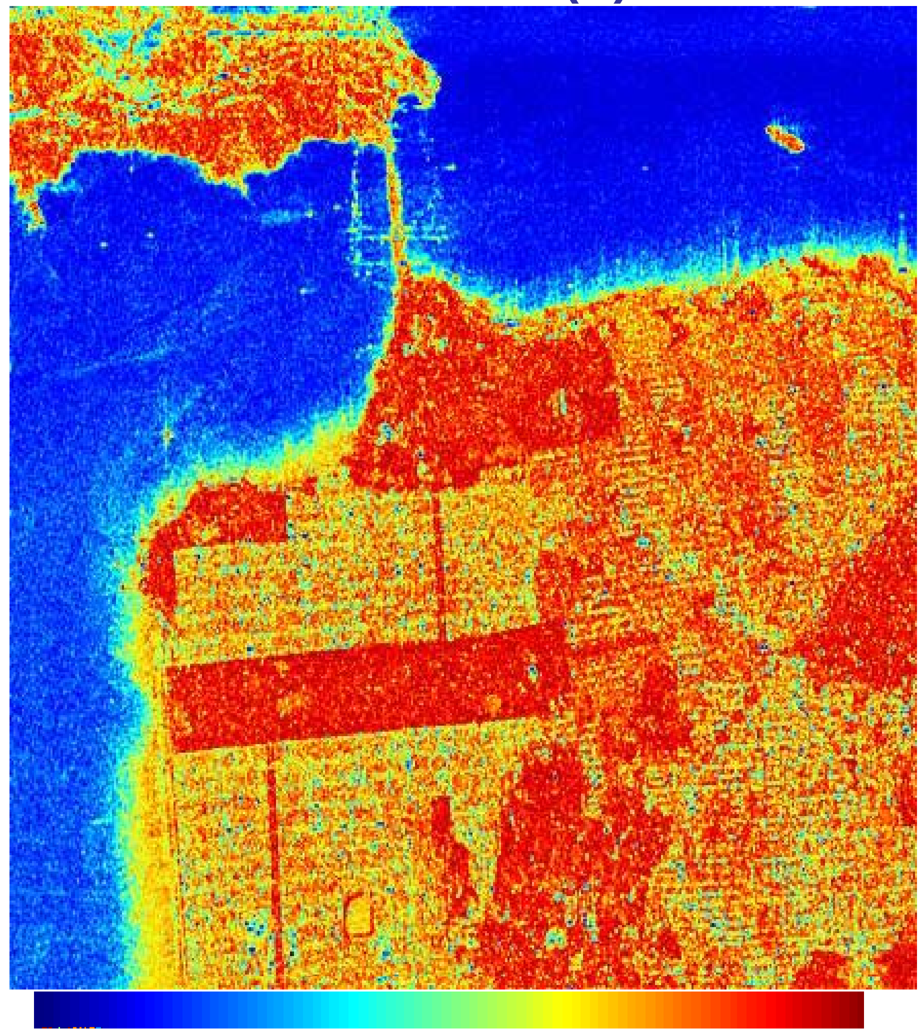

$2A_0$ $B_0 + B$ $B_0 - B$

H / A / α DECOMPOSITION

SEGMENTATION OF THE H / α SPACE

MULTIPLE SCATTERING

VOLUME SCATTERING

SURFACE SCATTERING

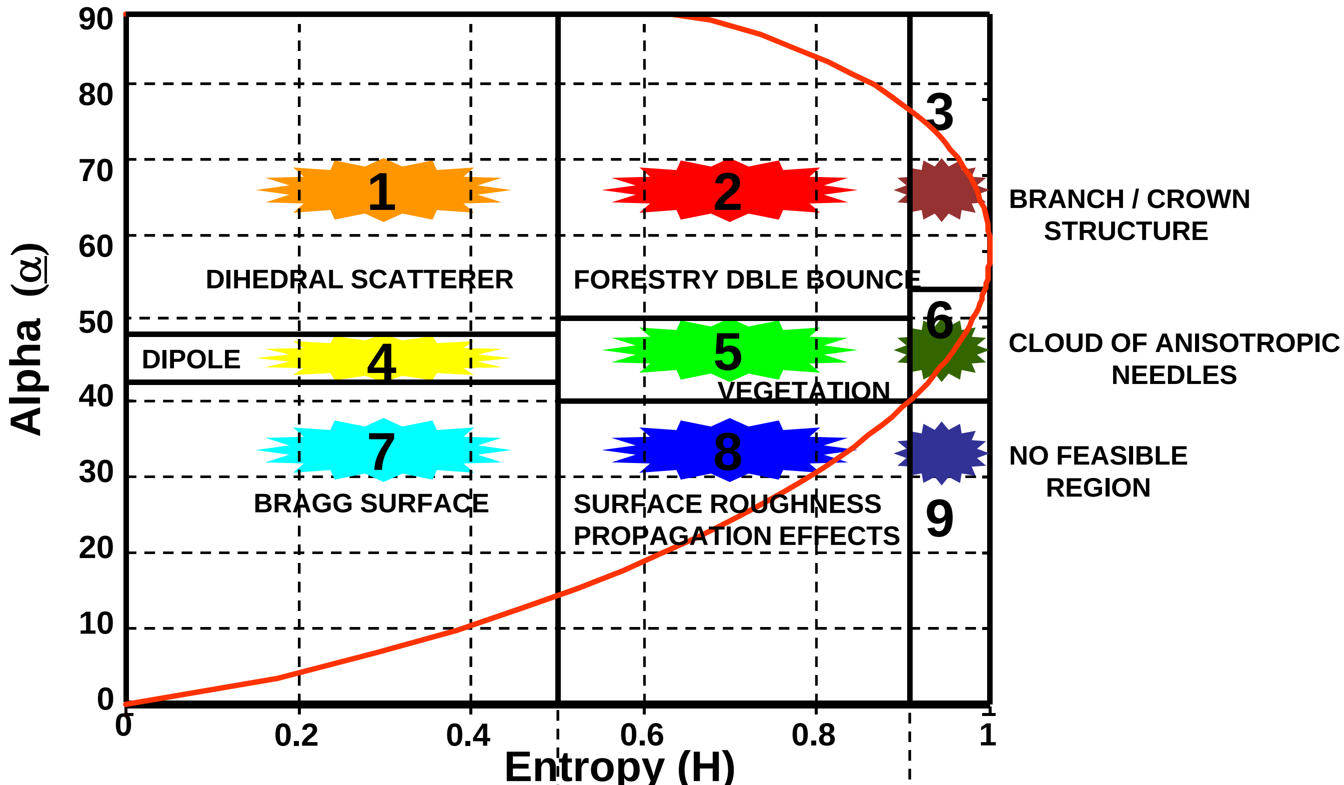

LOW ENTROPY

MEDIUM ENTROPY

HIGH ENTROPY

PERTURBATION OF 1st ORDER SCATTERING THEORIES DUE TO 2nd ORDER EVENTS

DEGREE OF ARBITRARINESS (SCATTERING PROCESSES RANDOM NOISE

H / A / α DECOMPOSITION

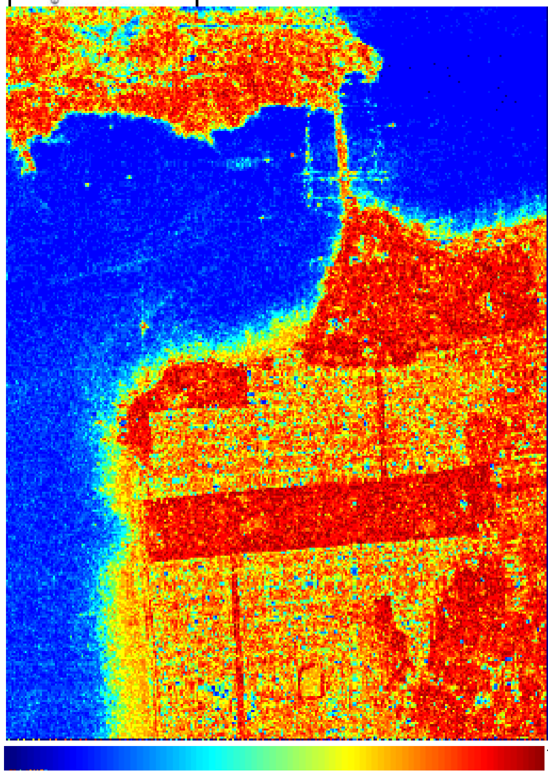

POLSAR DATA DISTRIBUTION IN THE H / $\underline{\alpha}$ PLANE

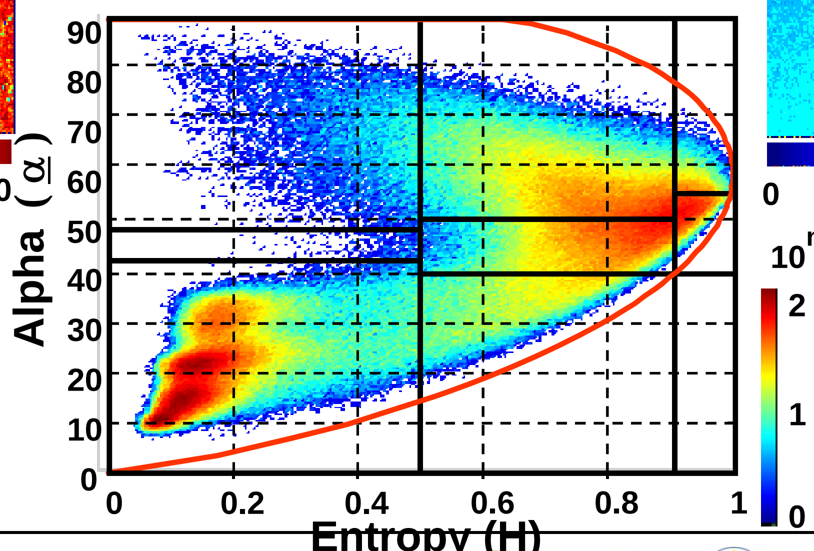

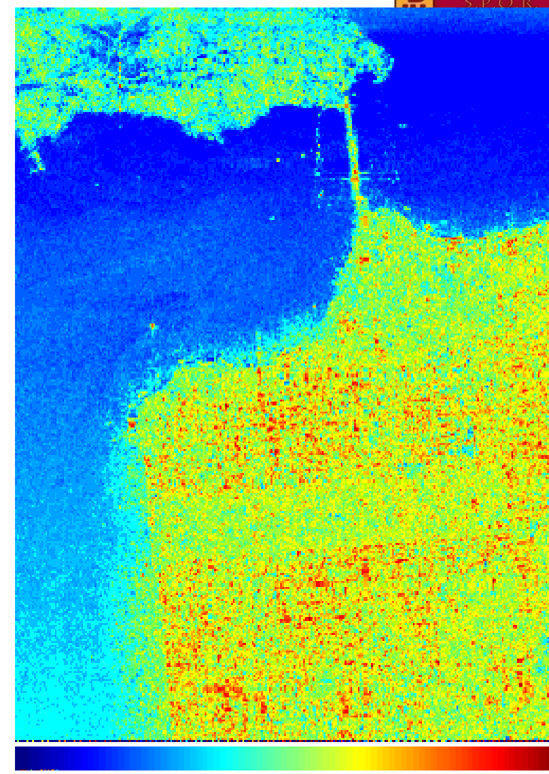

ALOS - PALSAR

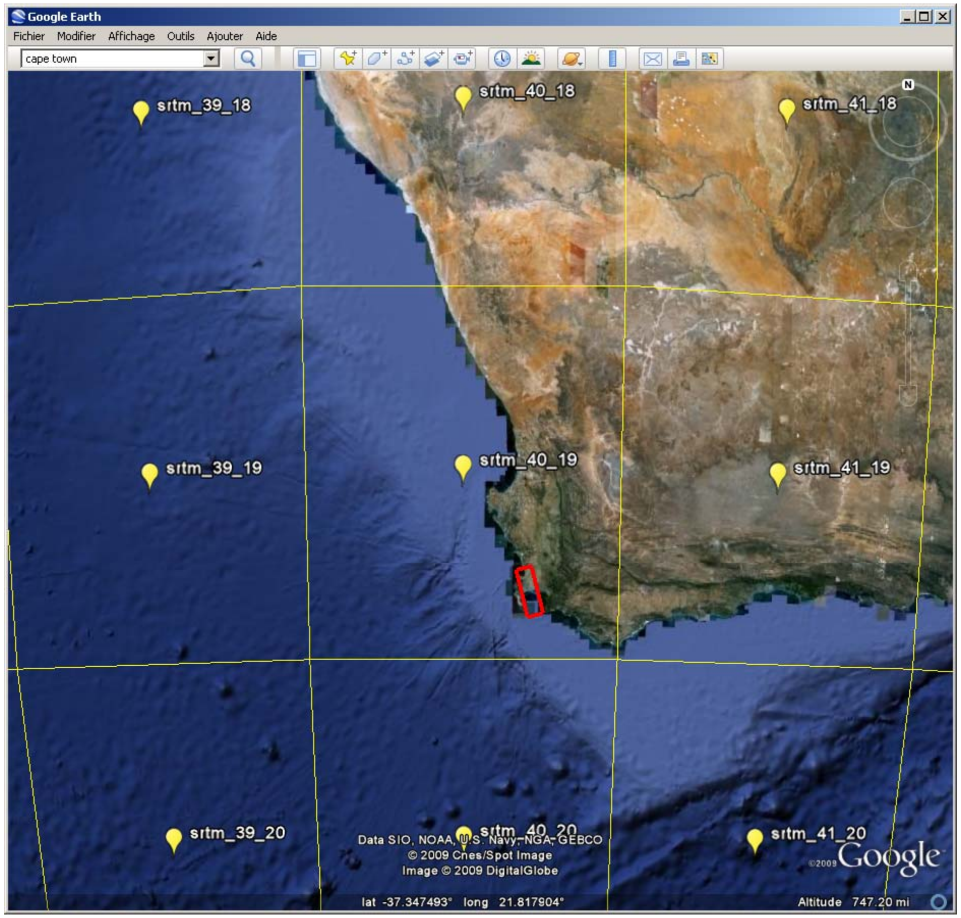

- **PALSAR Quad POL**
- **PALSAR Data Level 1.1**

Cape Town – February 2009

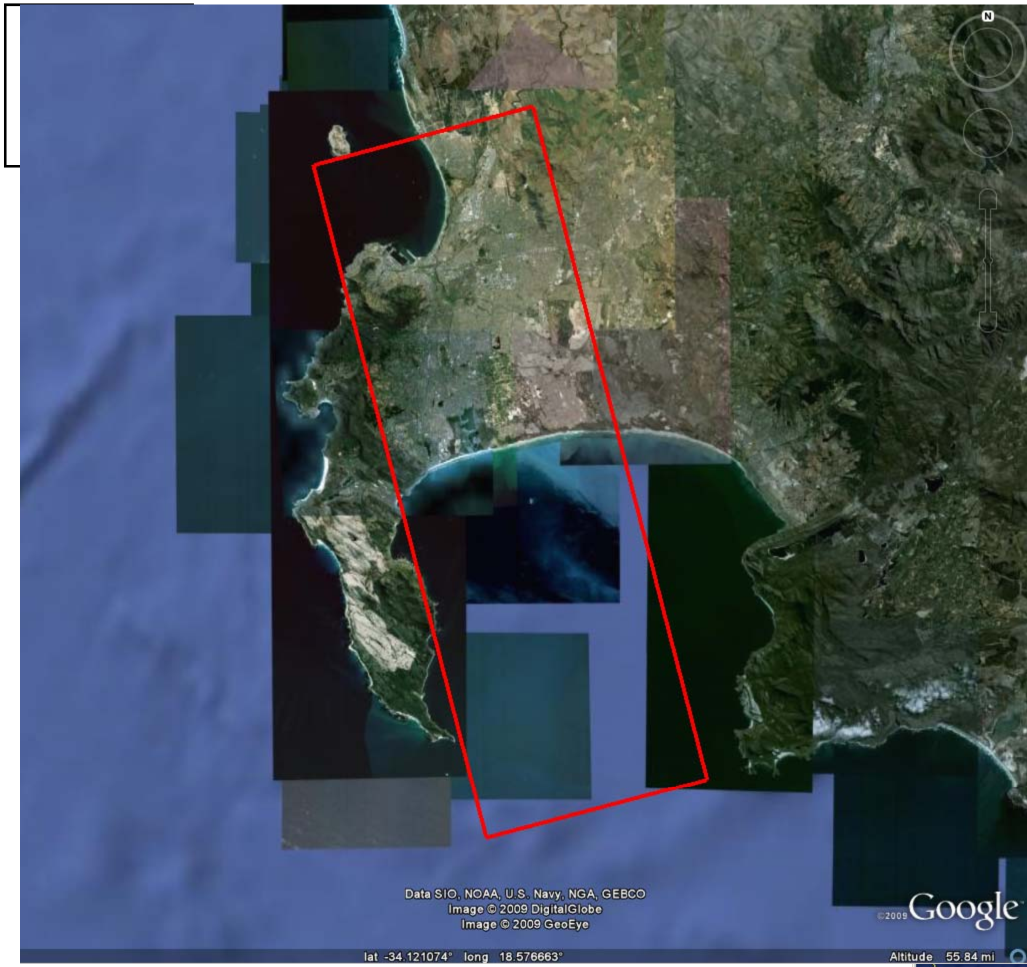

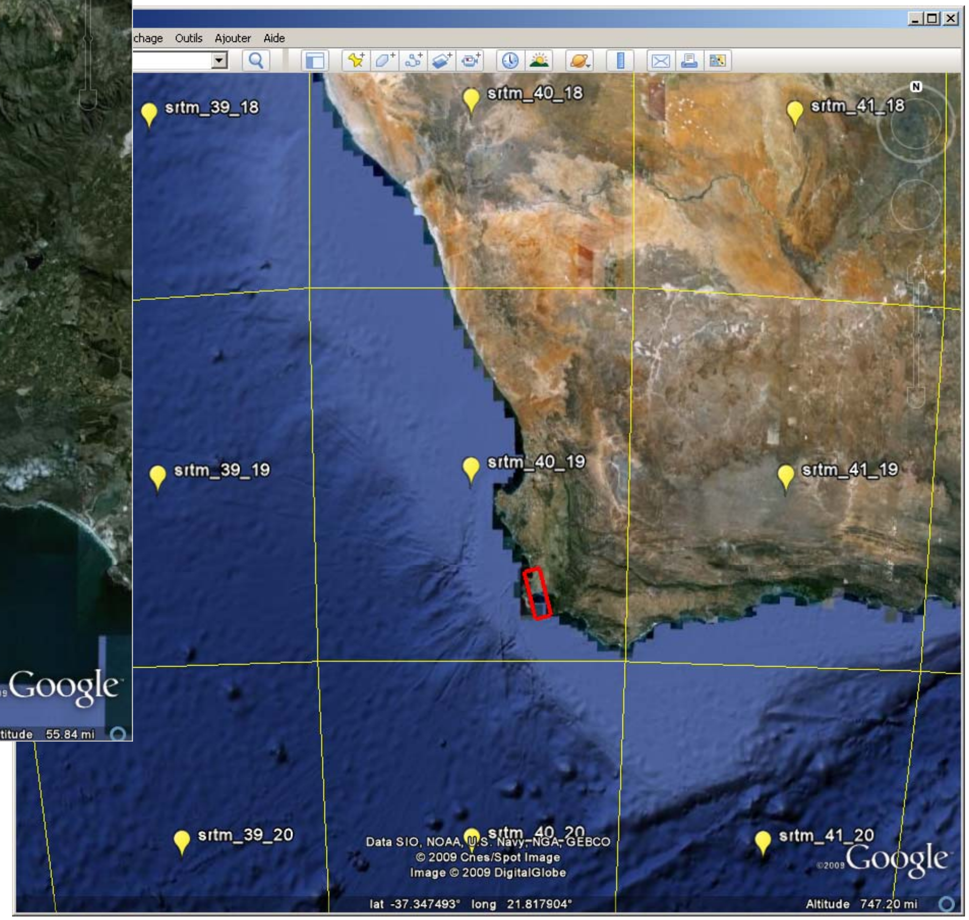

Cape Town – February 2009


Downtown
Waterfront
University
Cape Town
Data SIO, NOAA, U.S. Navy, NGA, GEBCO
Image © 2009 DigitalGlobe
Image © 2009 GeoEye
©2009 Google
Dates des images satellite : 21 juin 2005 - 23 févr. 2009 lat -33.966672° long 18.516714°
Altitude 22.30 mi

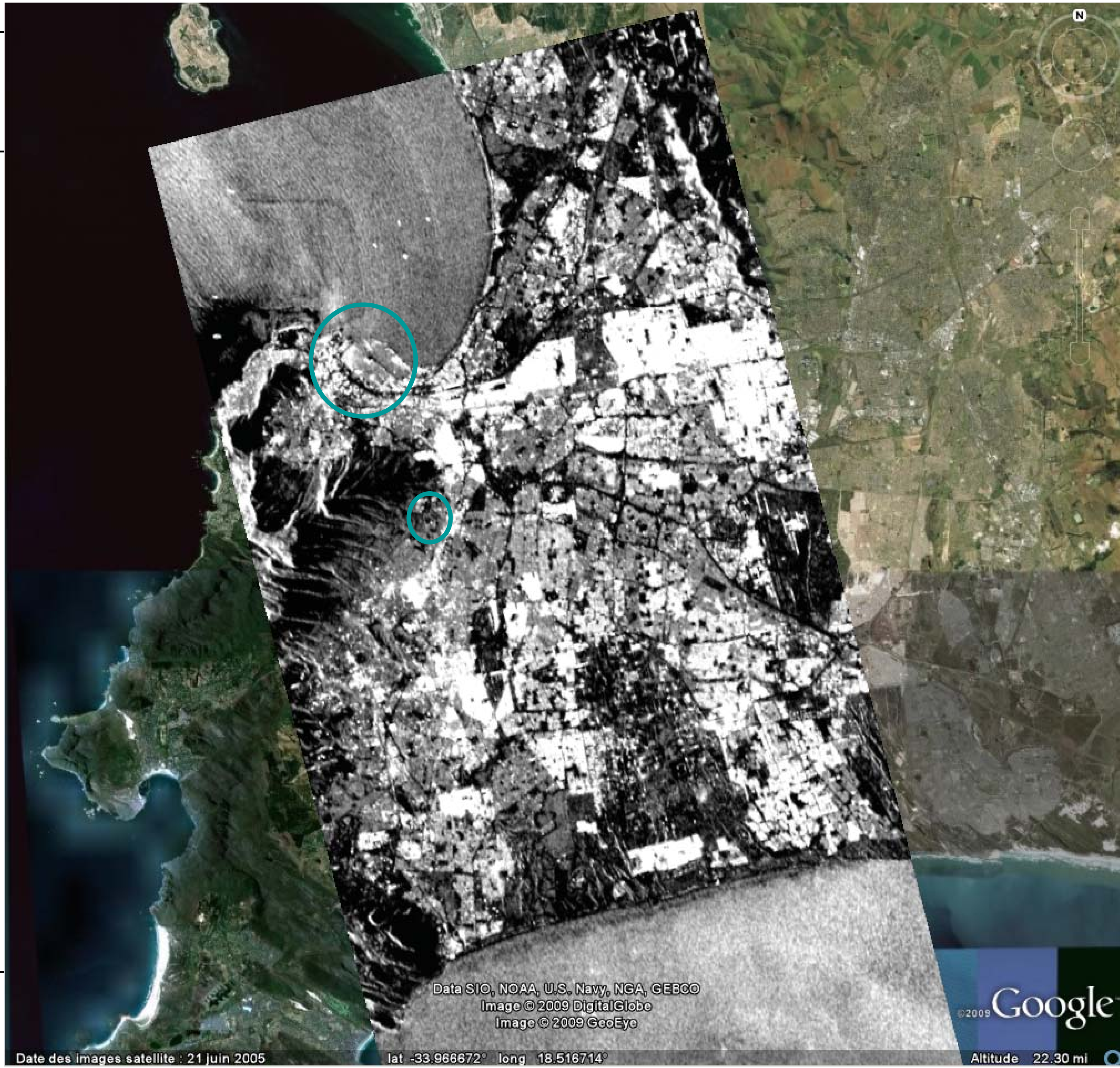
Data SIO, NOAA, U.S. Navy, NGA, GEBCO
Image © 2009 DigitalGlobe
Image © 2009 GeoEye
©2009 Google
Date des images satellite : 21 juin 2005
lat -33.966672° long 18.516714°
Altitude 22.30 mi

|HH+VV|
|HV|
|HH-VV|

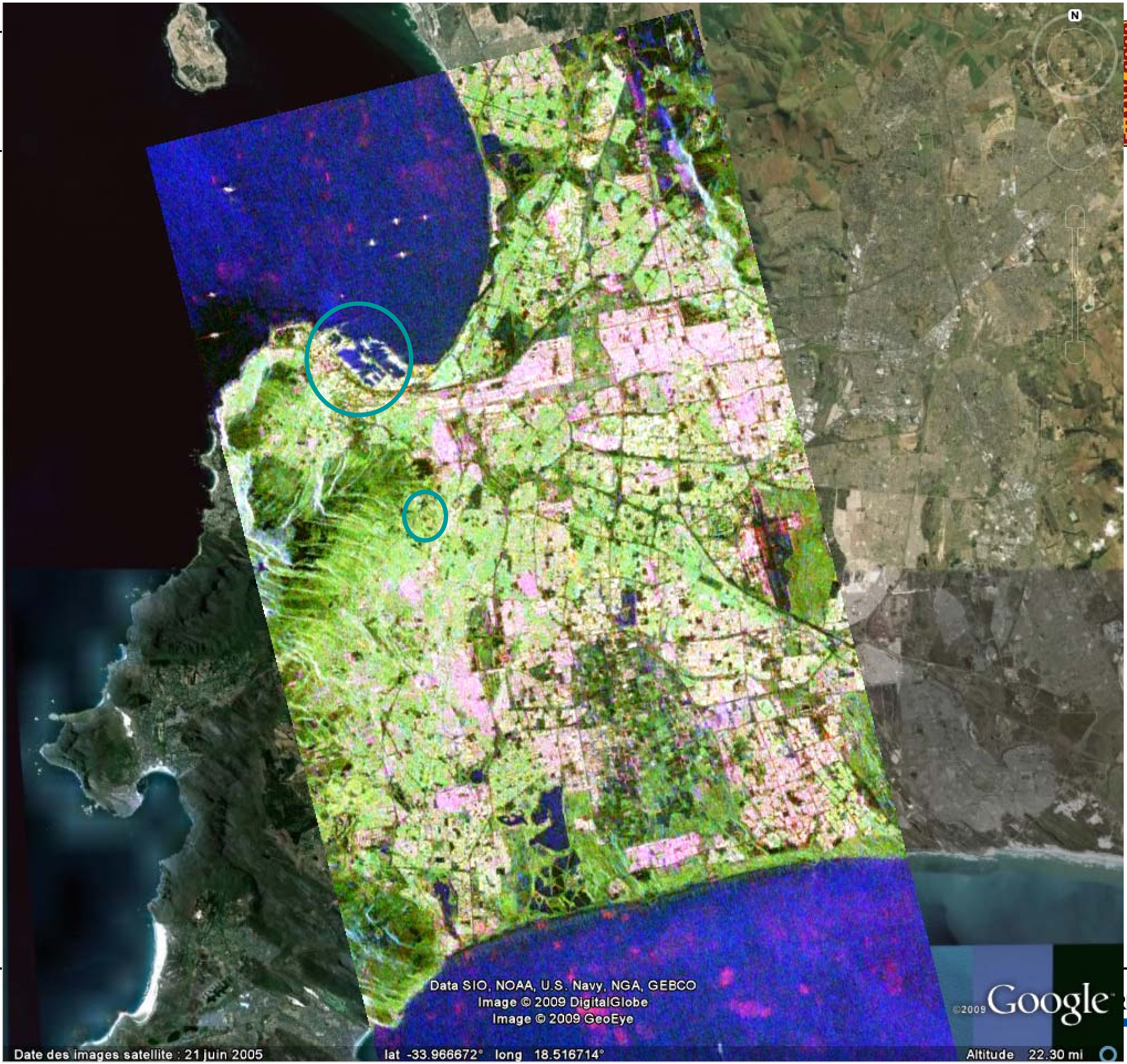
Data SIO, NOAA, U.S. Navy, NGA, GEBCO
Image © 2009 DigitalGlobe
Image © 2009 GeoEye
©2009 Google
Date des images satellite : 21 juin 2005
lat -33.966672° long 18.516714°
Altitude 22.30 mi

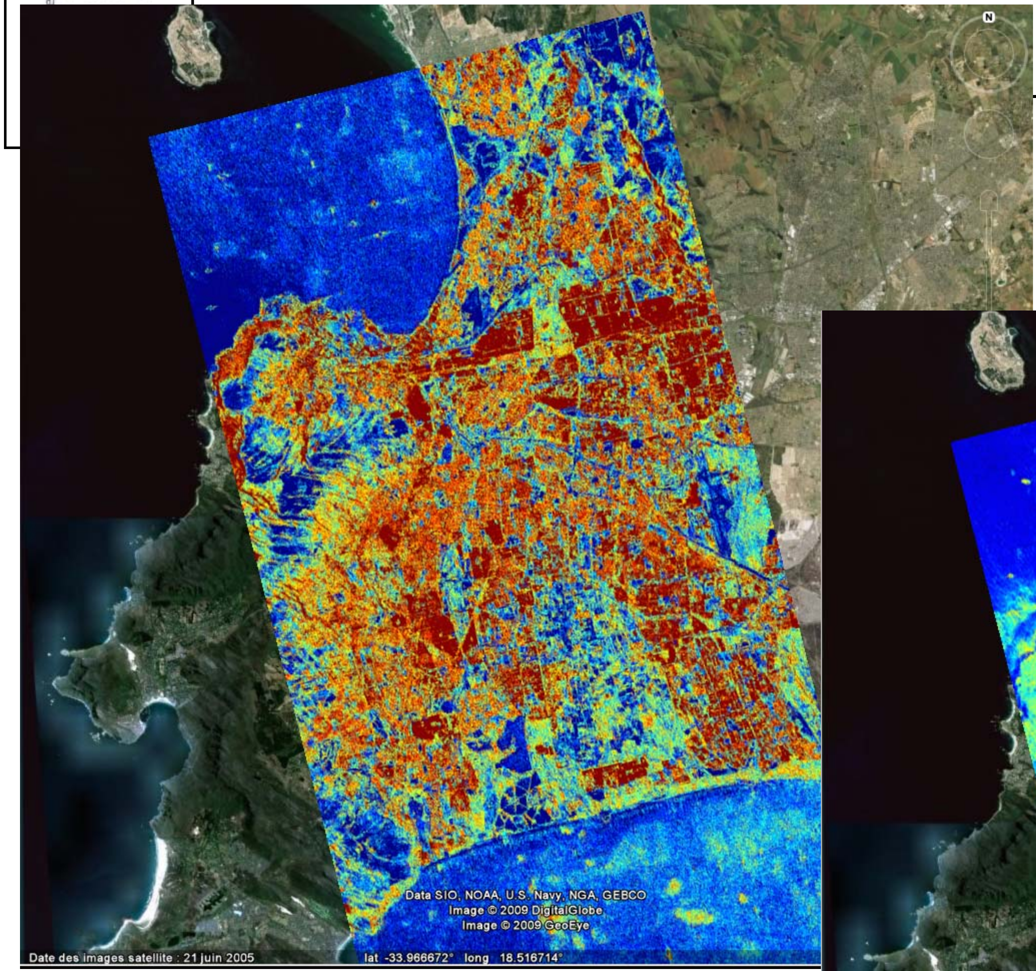

entropy

alpha

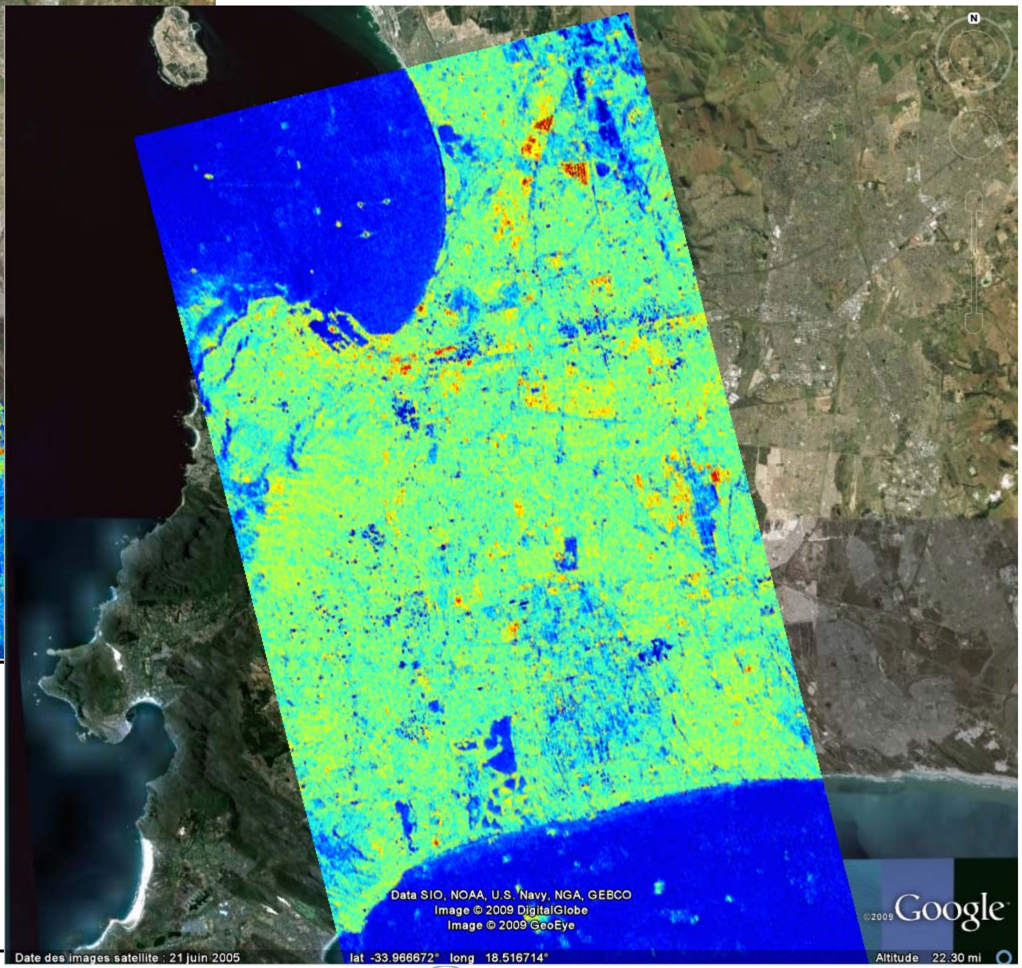

GeoInformazione TOR VERGATA

$$P\left(\langle[T]\rangle/[T_m]\right)=\frac{L^{Lp}\left|\langle[T]\rangle\right|^{L-p}e^{-LTr\left([T_m]^{-1}\langle[T]\rangle\right)}}{\pi^{\frac{p(p-1)}{2}}\Gamma(L)\ldots\Gamma(L-p+1)\left|[T_m]\right|^{L}}$$

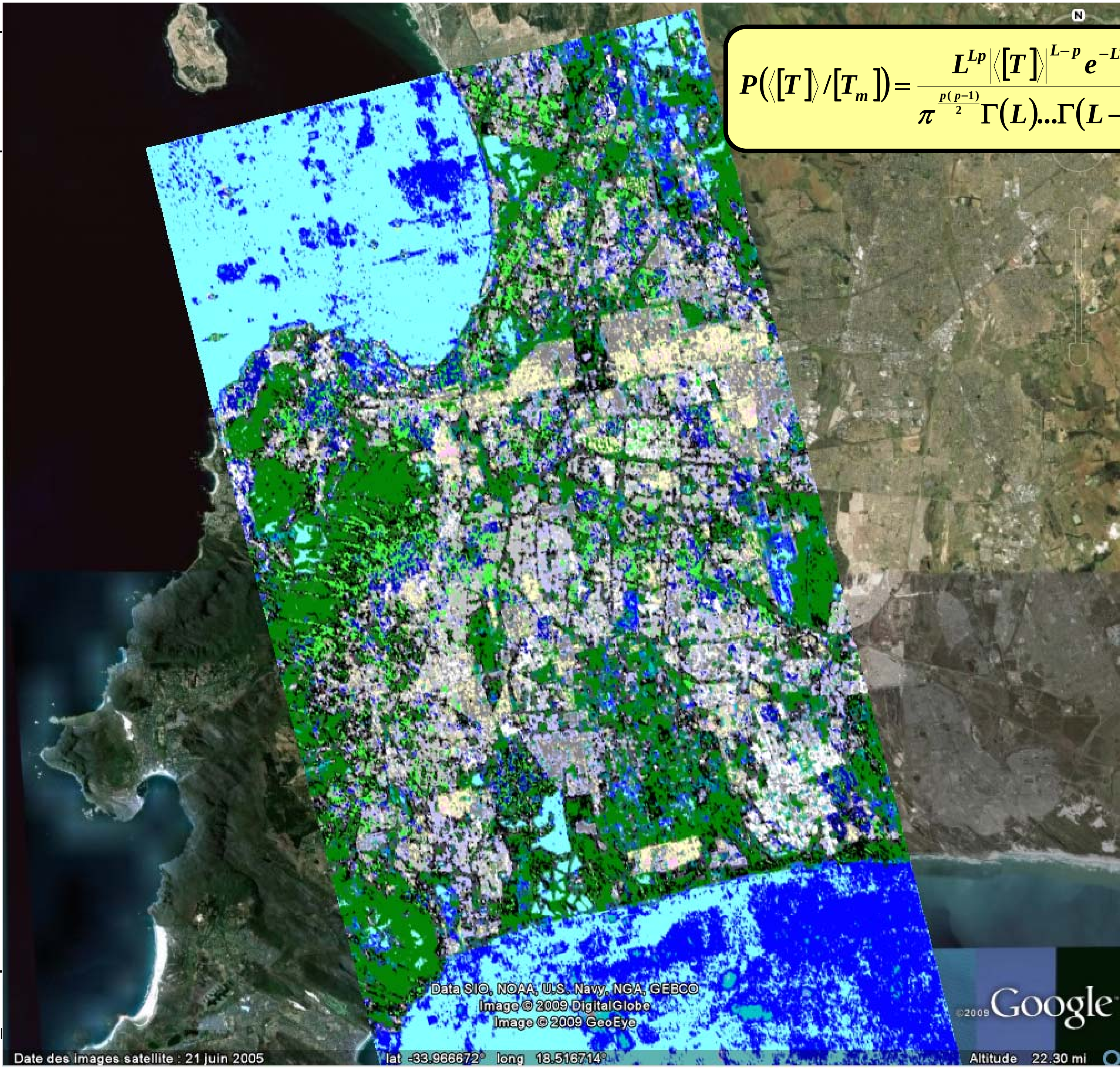

RADARSAT-1

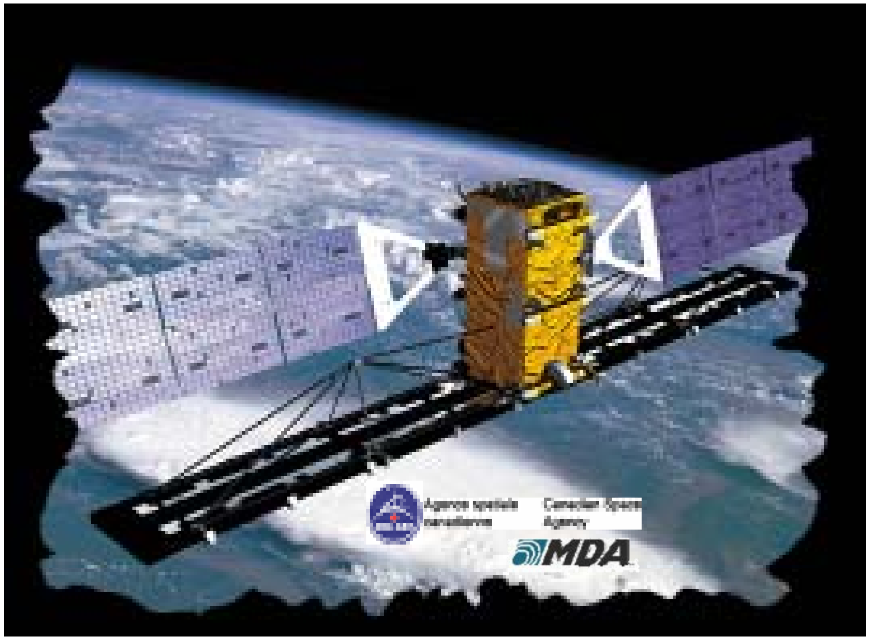

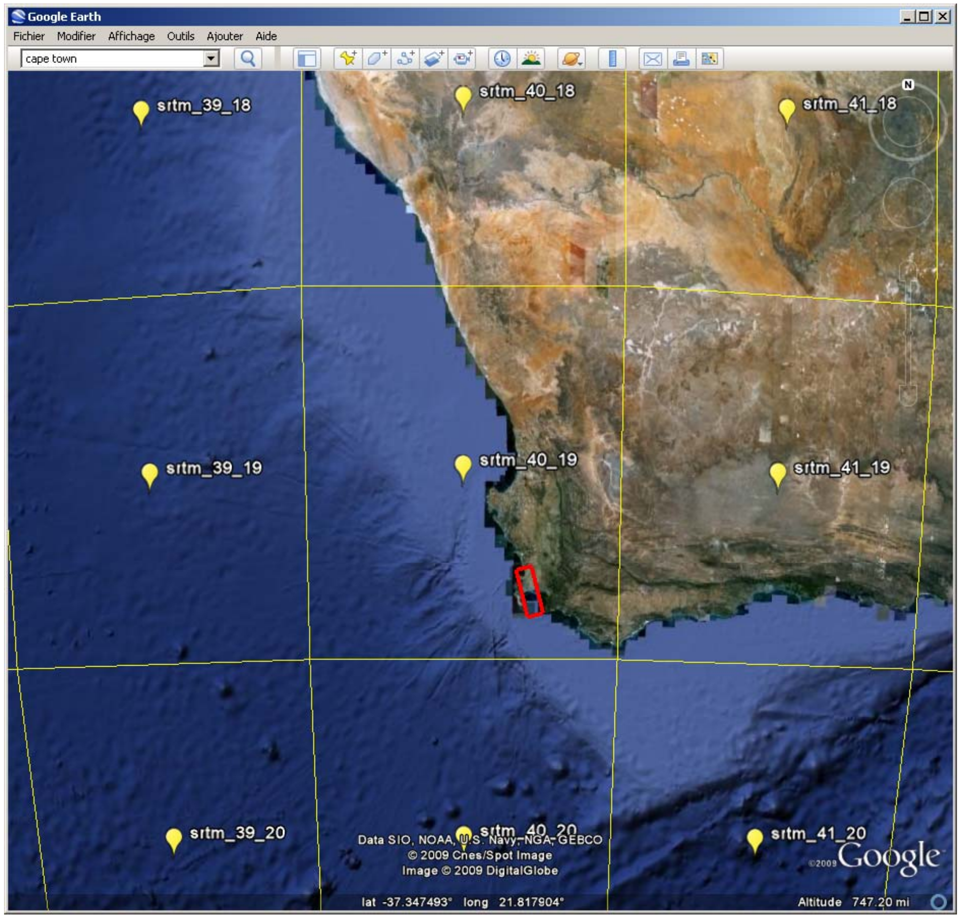

- **RADARSAT-2 Quad POL**
- **RADARSAT-2 Fine Mode**

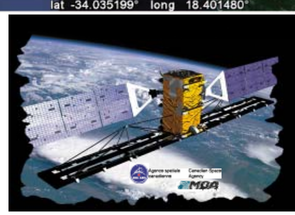

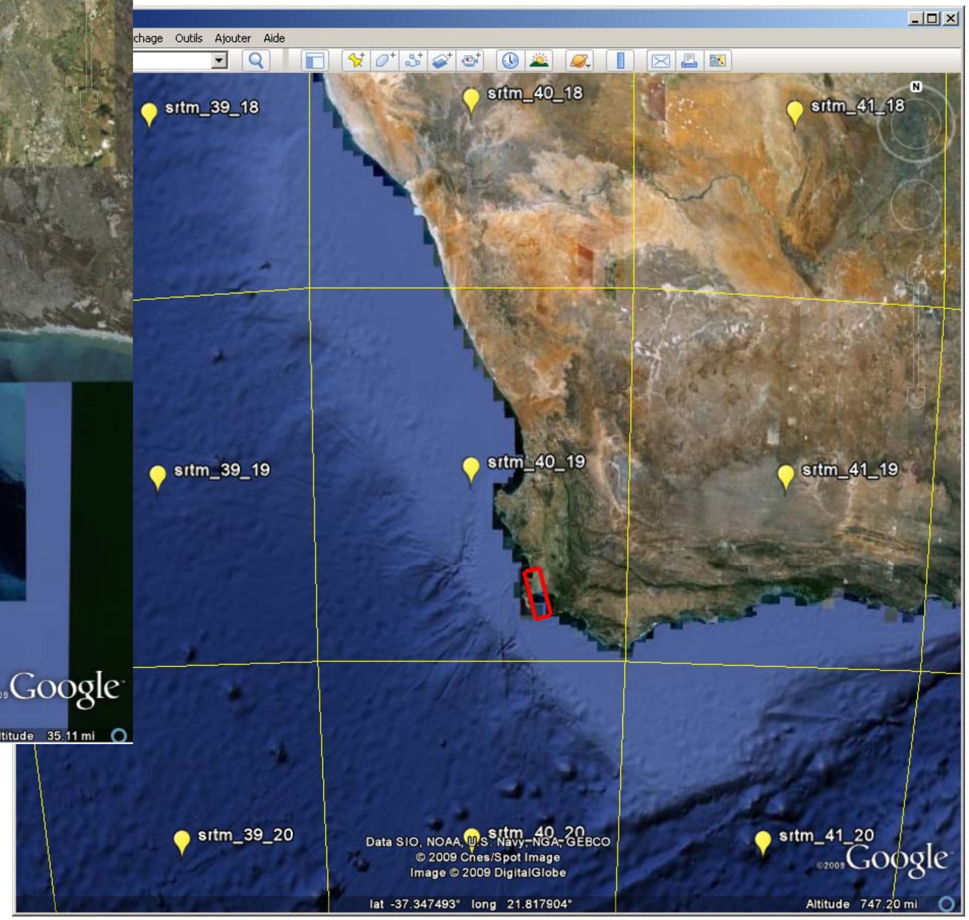

Cape Town – April 2009

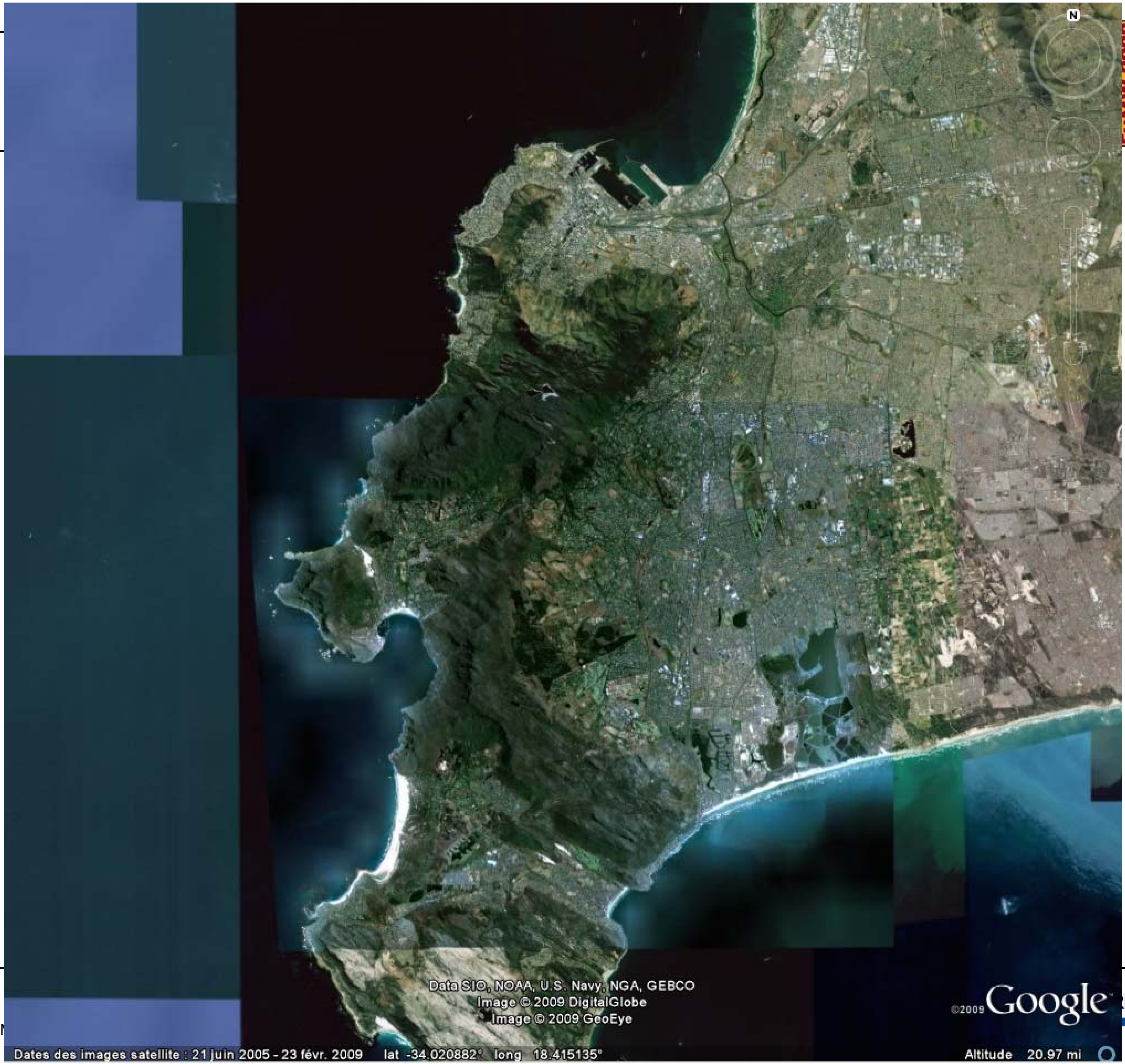
Data SIO, NOAA, U.S. Navy, NGA, GEBCO
Image © 2009 DigitalGlobe
Image © 2009 GeoEye
©2009 Google
Dates des images satellite : 21 juin 2005 - 23 févr. 2009 lat -34.020882° long 18.415135°
Altitude 20.97 mi

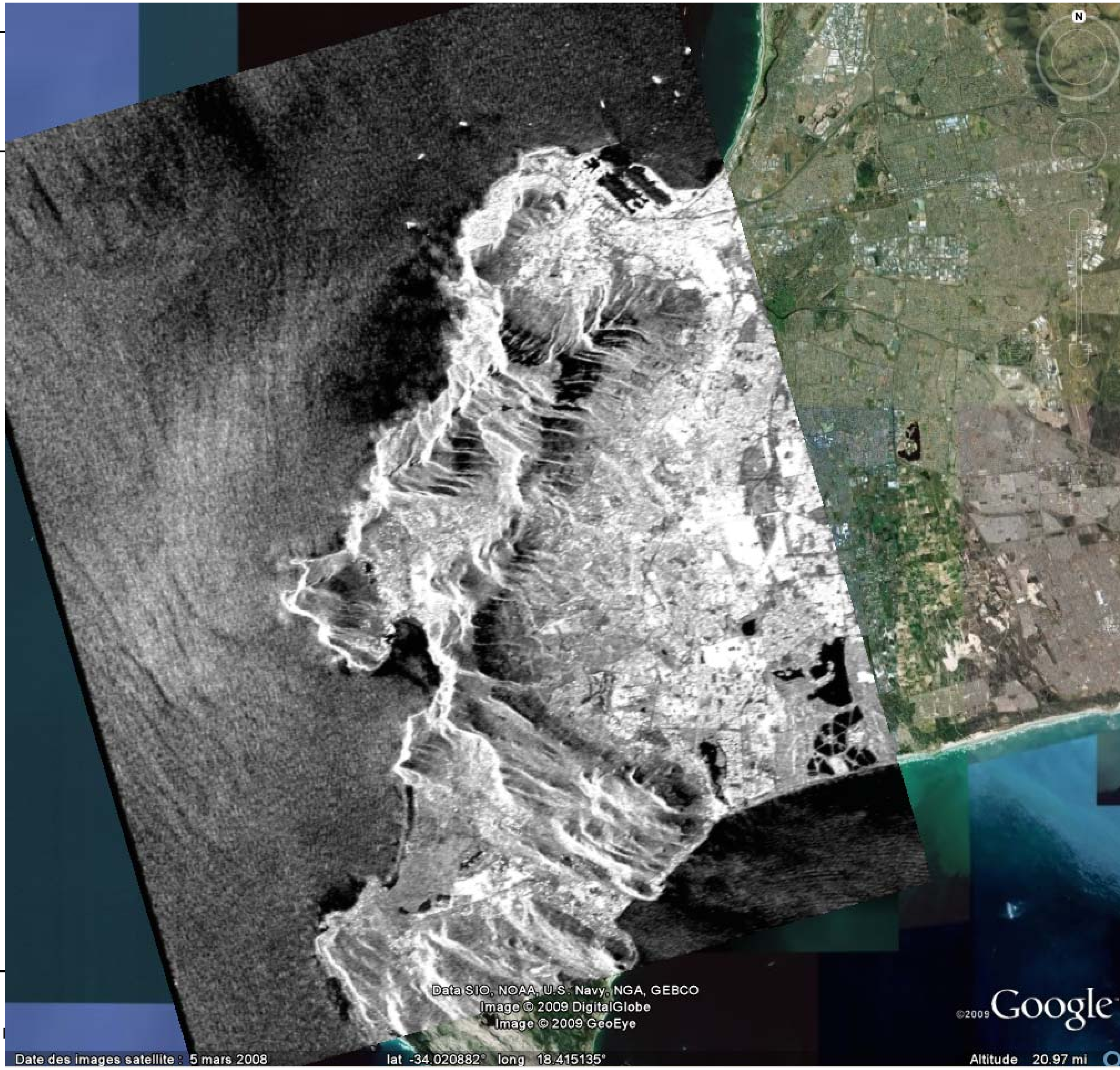
Data SIO, NOAA, U.S. Navy, NGA, GEBCO
Image © 2009 DigitalGlobe
Image © 2009 GeoEye
©2009 Google
Date des images satellite : 5 mars 2008
lat -34.020882° long 18.415135°
Altitude 20.97 mi
N

|HH+VV|
|HV|
|HH-VV|

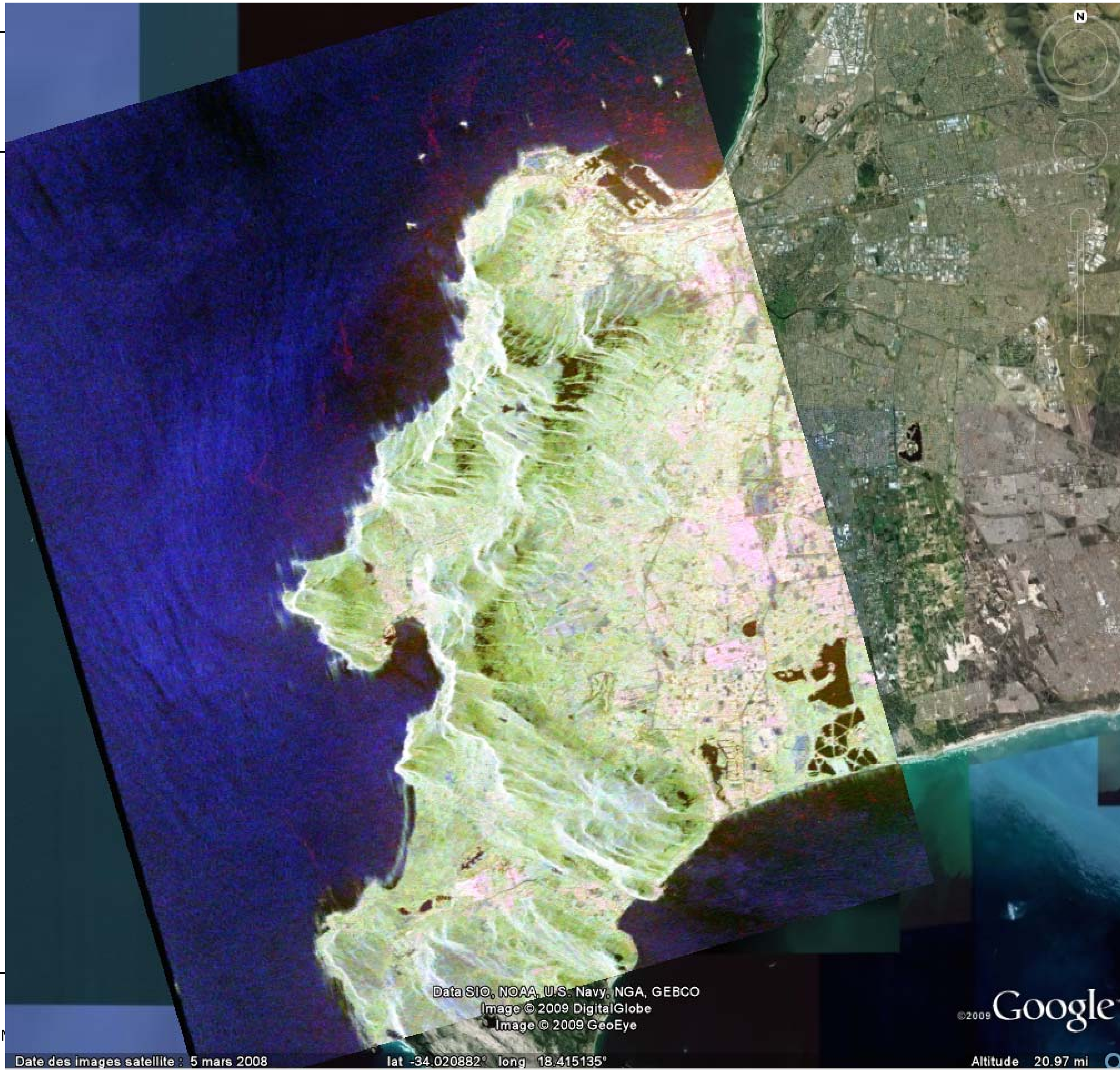
N
Data SIO, NOAA, U.S. Navy, NGA, GEBCO
Image © 2009 DigitalGlobe
Image © 2009 GeoEye
©2009 Google
Date des images satellite : 5 mars 2008
lat -34.020882° long 18.415135°
Altitude 20.97 mi

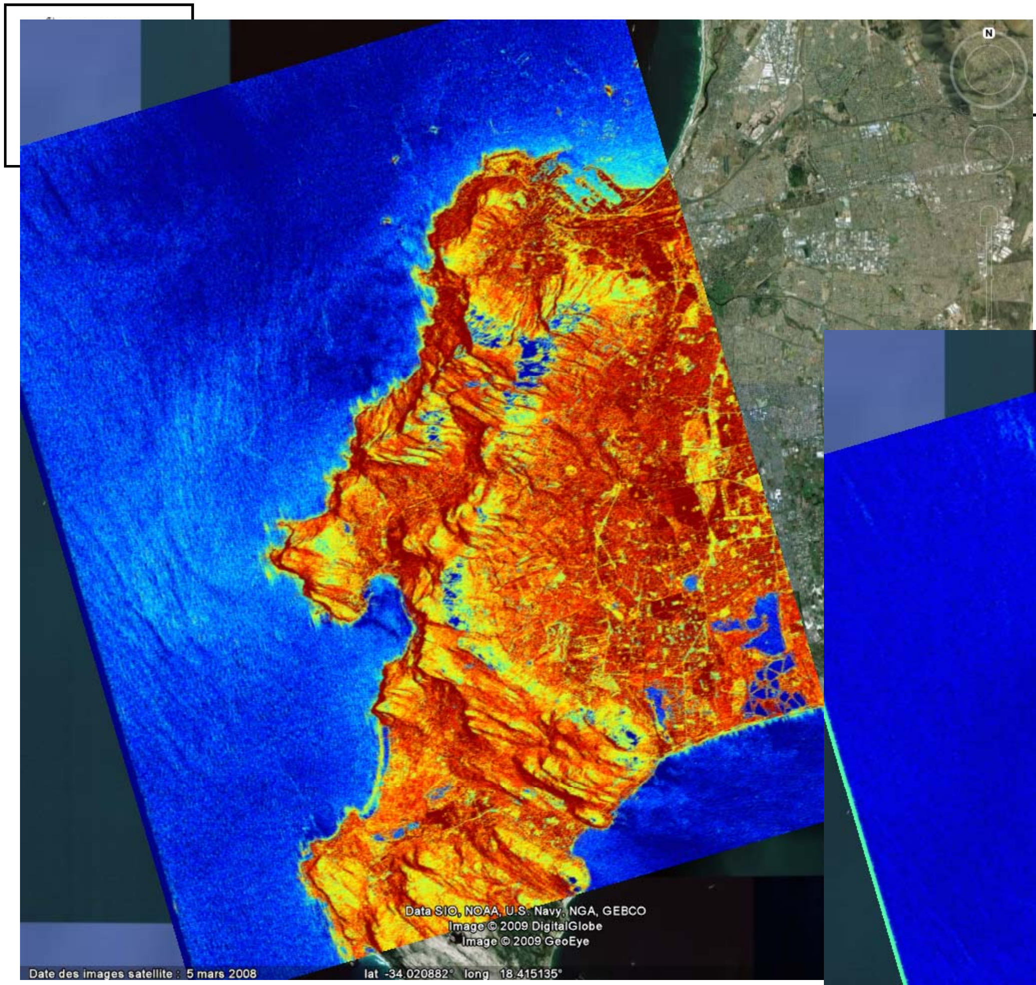

entropy

alpha

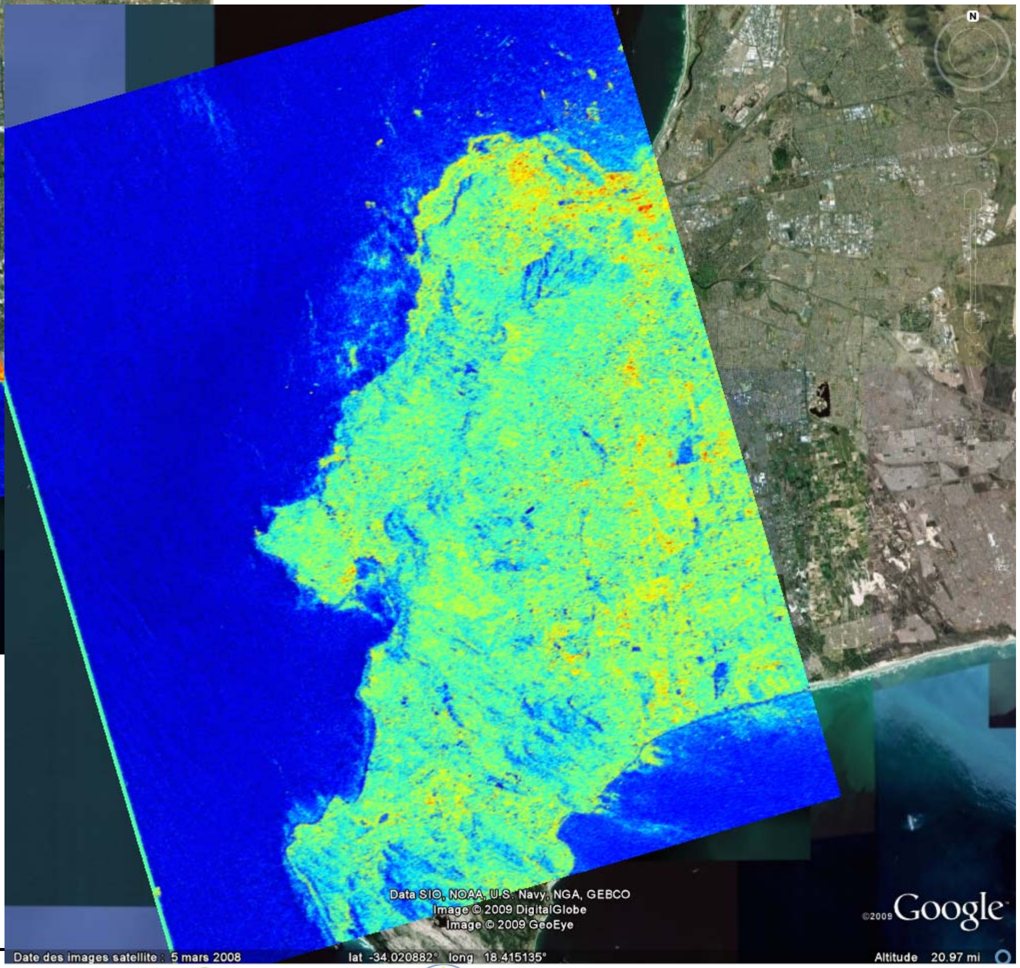

$$P\left(\langle[T]\rangle/[T_m]\right)=\frac{L^{Lp}\left|\langle[T]\rangle\right|^{L-p}e^{-LTr\left([T_m]^{-1}\langle[T]\rangle\right)}}{\pi^{\frac{p(p-1)}{2}}\Gamma(L)\ldots\Gamma(L-p+1)\left|[T_m]\right|^{L}}$$

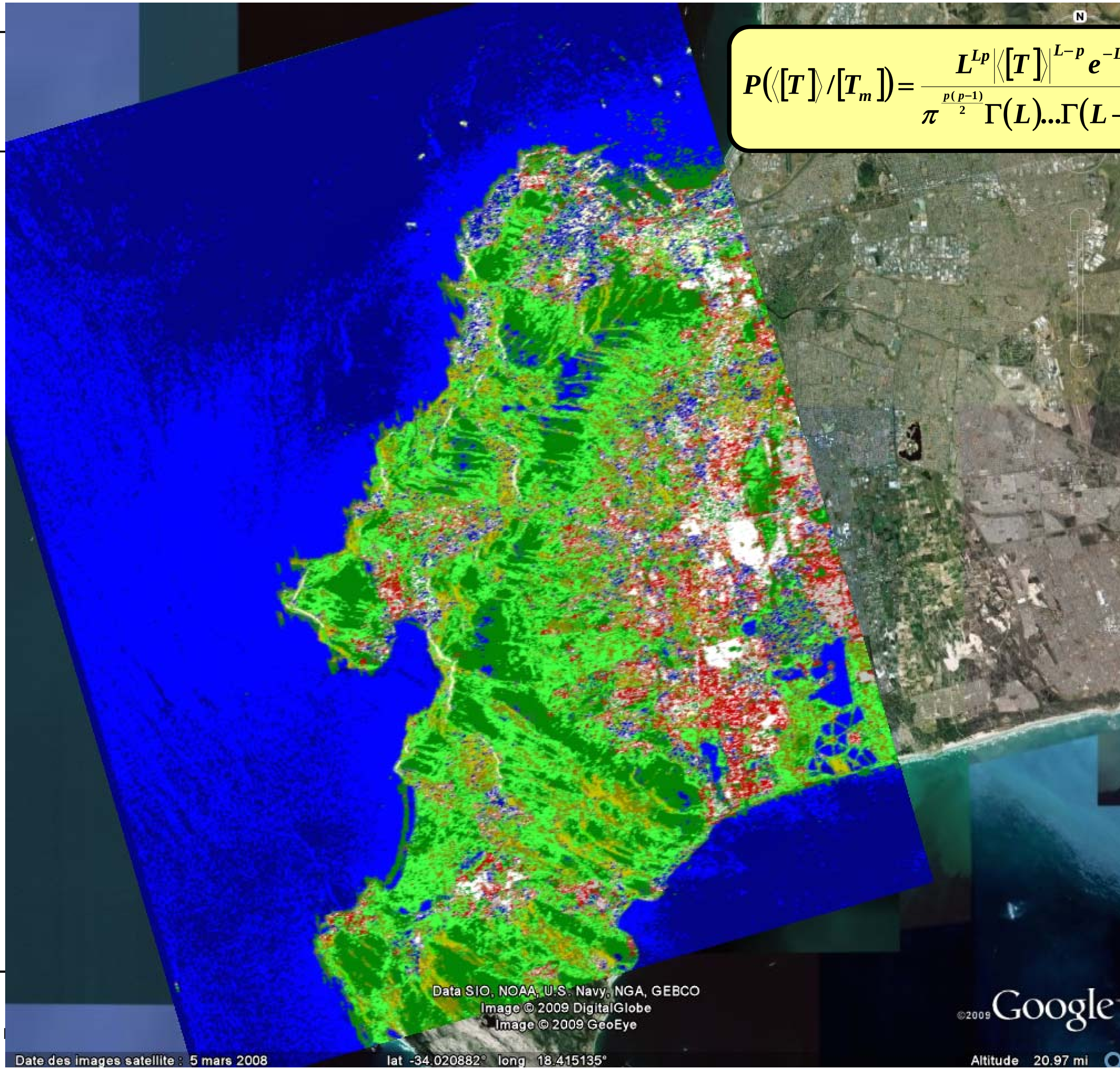

FULL POLARIMETRIC SAR INTERFEROMETRY

INTRODUCTION to POLINSAR

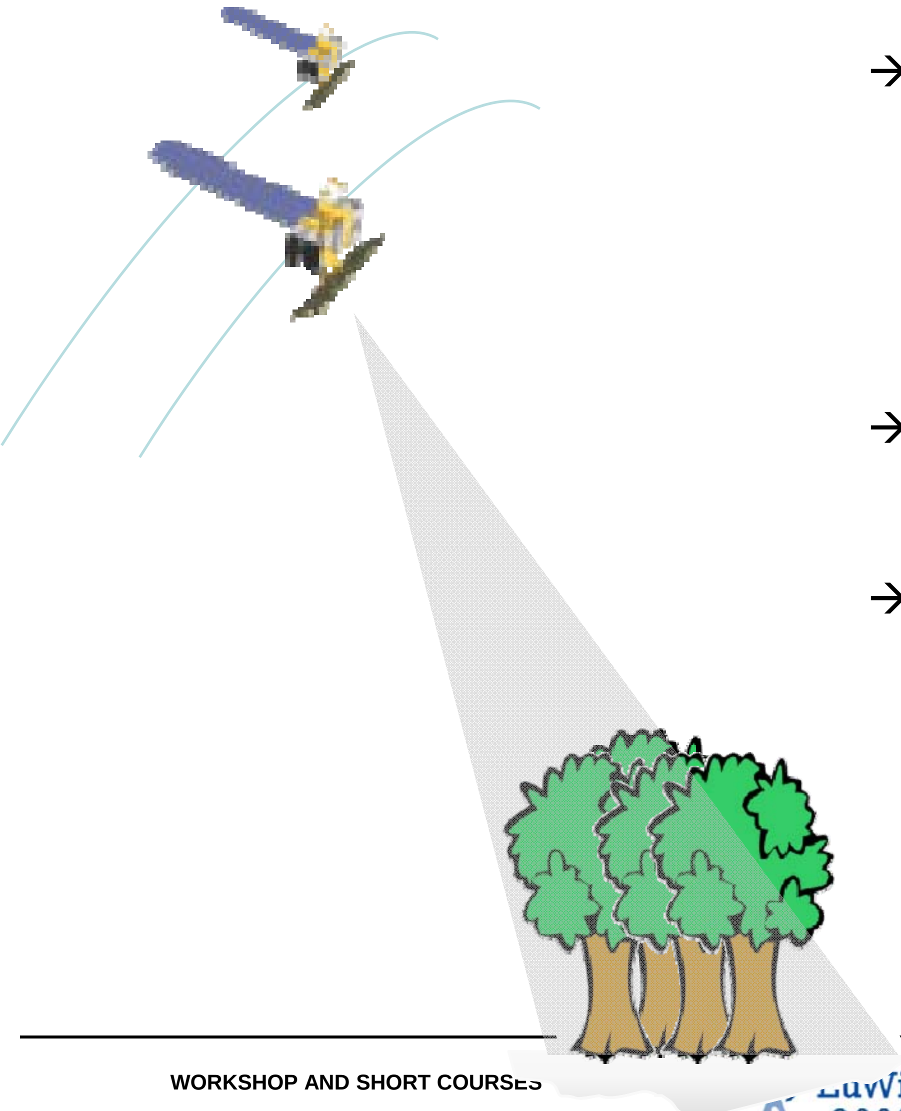

→ PolInSAR basic idea

- InSAR coherence has different sensitivity according to polarization
- To discriminate among different components of the vertical structure of vegetation

→ Key observable

- Complex degree of coherence $\tilde{\gamma}$

→ ALOS PALSAR

- L-band
- 46 days revisit time

INTRODUCTION to POLINSAR

vertical distribution of scatterers

→ Complex coherence model (Truhaft and Siqueira, Cloude and Papathanassiou):

$$\tilde{\gamma}_t = \frac{\langle S_1^A S_2^{B*} \rangle}{\sqrt{\langle S_1^A S_1^{B*} \rangle \langle S_1^A S_2^{B*} \rangle}} = e^{jk_z z_0} \frac{\int_0^{h_v} \rho(z) e^{jk_z z} dz}{\int_0^{h_v} \rho(z) dz}$$

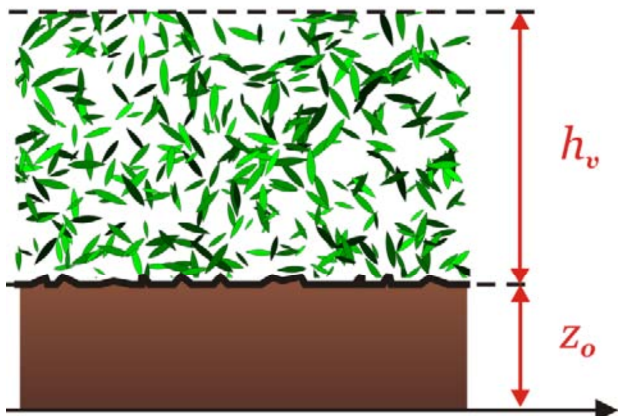

→ Complex coherence model (Truhaft and Siqueira, Cloude and Papathanassiou):

$$\tilde{\gamma}_t = \frac{\langle S_1^A S_2^{B*} \rangle}{\sqrt{\langle S_1^A S_1^{B*} \rangle \langle S_1^A S_2^{B*} \rangle}} = e^{jk_z z_0} \frac{\int_0^{h_v} \rho(z) e^{jk_z z} dz}{\int_0^{h_v} \rho(z) dz}$$

SINC

$$= e^{jk_z z_0} e^{jk_z \frac{h_v}{2}} \mathrm{Sinc}\left(k_z \frac{h_v}{2}\right)$$

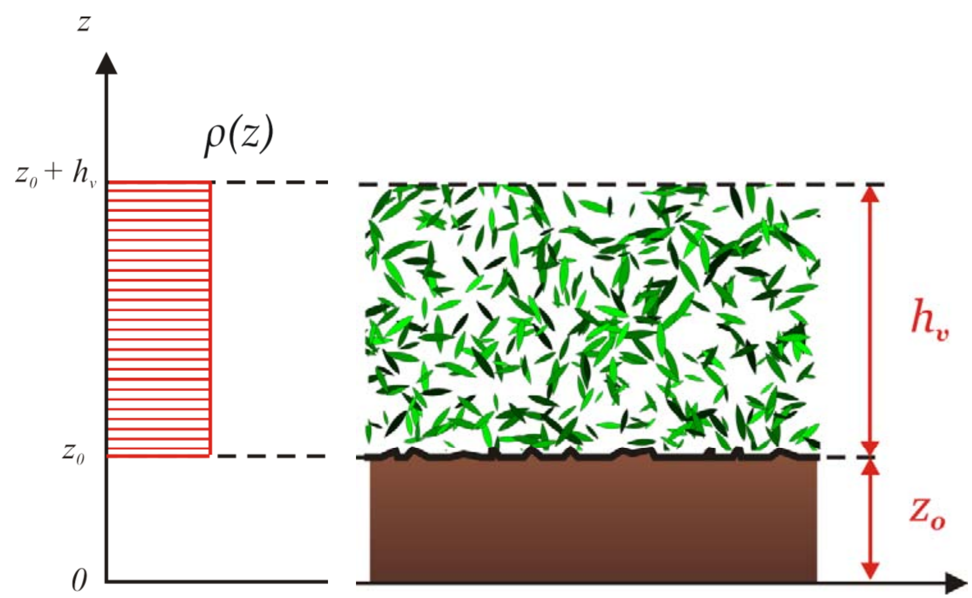

Introduction

Vertical distribution of scatterers

→ Complex coherence model (Truhaft and Siqueira, Cloude and Papathanassiou):

$$\tilde{\gamma}_t = \frac{\langle S_1^A S_2^{B*} \rangle}{\sqrt{\langle S_1^A S_1^{B*} \rangle \langle S_1^A S_2^{B*} \rangle}} = e^{jk_z z_0} \frac{\int_0^{h_v} \rho(z) e^{jk_z z} dz}{\int_0^{h_v} \rho(z) dz}$$

SINC

$$= e^{jk_z z_0} e^{jk_z \frac{h_v}{2}} \mathrm{Sinc}\left(k_z \frac{h_v}{2}\right)$$

RVoG

$$= e^{jk_z z_0} \frac{\tilde{\gamma}_{vol} + \eta(\vec{w})}{1 + \eta(\vec{w})}$$

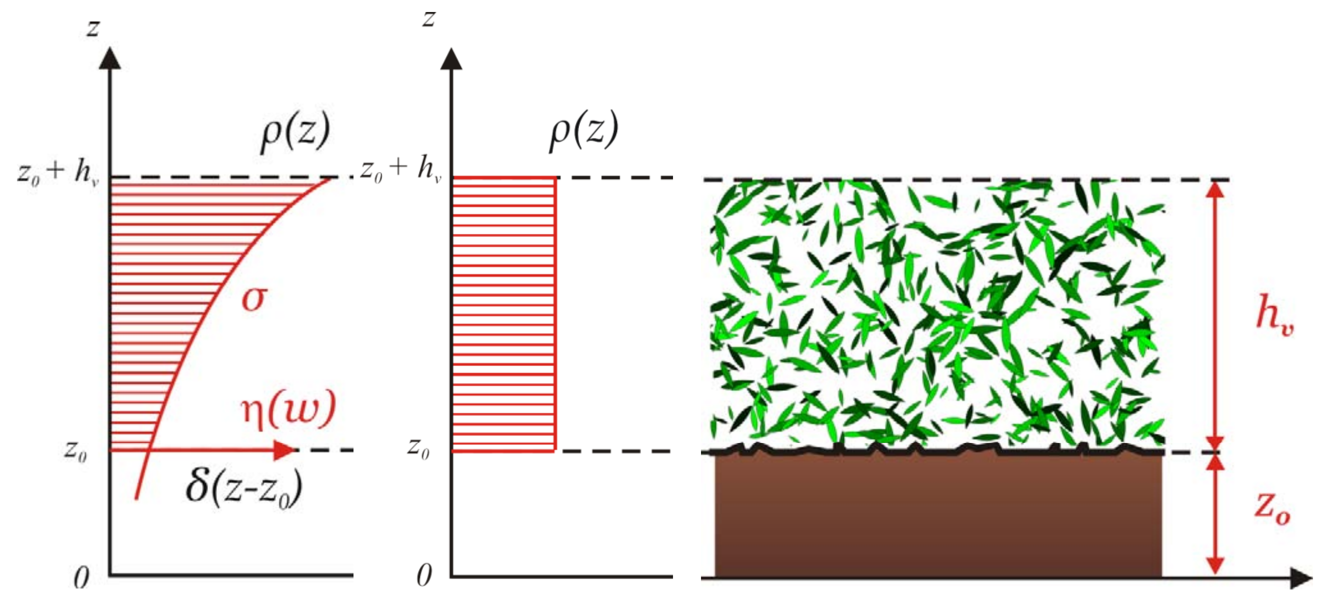

Introduction

Vertical distribution of scatterers

→ Complex coherence model (Truhaft and Siqueira, Cloude and Papathanassiou):

$$\tilde{\gamma}_t = \frac{\langle S_1^A S_2^{B*} \rangle}{\sqrt{\langle S_1^A S_1^{B*} \rangle \langle S_1^A S_2^{B*} \rangle}} = e^{jk_z z_0} \frac{\int_0^{h_v} \rho(z) e^{jk_z z} dz}{\int_0^{h_v} \rho(z) dz}$$

SINC $= e^{jk_z z_0} e^{jk_z \frac{h_v}{2}} \mathrm{Sinc}\left(k_z \frac{h_v}{2}\right)$

RVoG $= e^{jk_z z_0} \frac{\tilde{\gamma}_{vol} + \eta(\vec{w})}{1 + \eta(\vec{w})}$

PCT $= e^{jk_z z_0} e^{jk_z \frac{h_v}{2}} \sum_n a_{n0}(w) f_n$

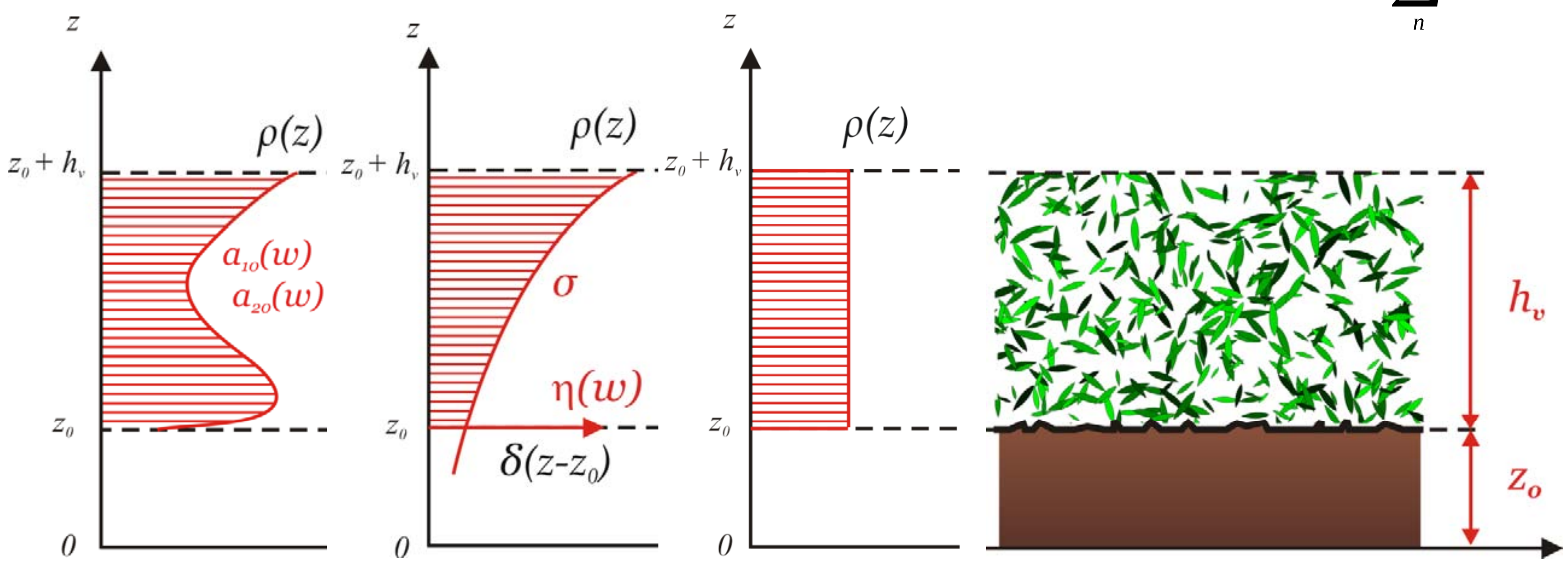

INTRODUCTION to POLINSAR

vertical distribution of scatterers

→ Polarization diversity allows to identify top- (ϕ_A) and bottom-phase center (ϕ_B)

main issues

→ Temporal decorrelation

  – Up to a certain extent, low impact on the average *phase height, but..*

$$h_v \neq \frac{1}{k_z}(\phi_A - \phi_B)$$

→ Effects of volume penetration

→ Terrain-induced distortions

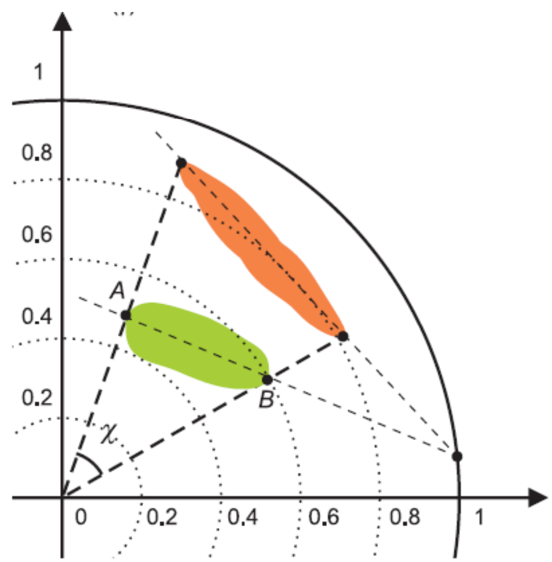

OBJECTIVES

1. ***To quantify the amount of terrain slope distortion and volume penetration using PolSARProSIM simulations and RVoG predictions***
2. ***To perform ALOS-PALSAR observations and to retrieve slope-corrected forest height estimates***

Volume and slope effects

top/bottom scattering phase center

→ Polarization diversity allows to identify top- (⊗) and bottom-phase center (⊗)

→ Complex coherence includes the contribution of volume and slope distortion

$$\tilde{\gamma} = \gamma \, e^{j\phi} = \tilde{\gamma}_v \, \tilde{\gamma}_s \, \tilde{\gamma}_n$$

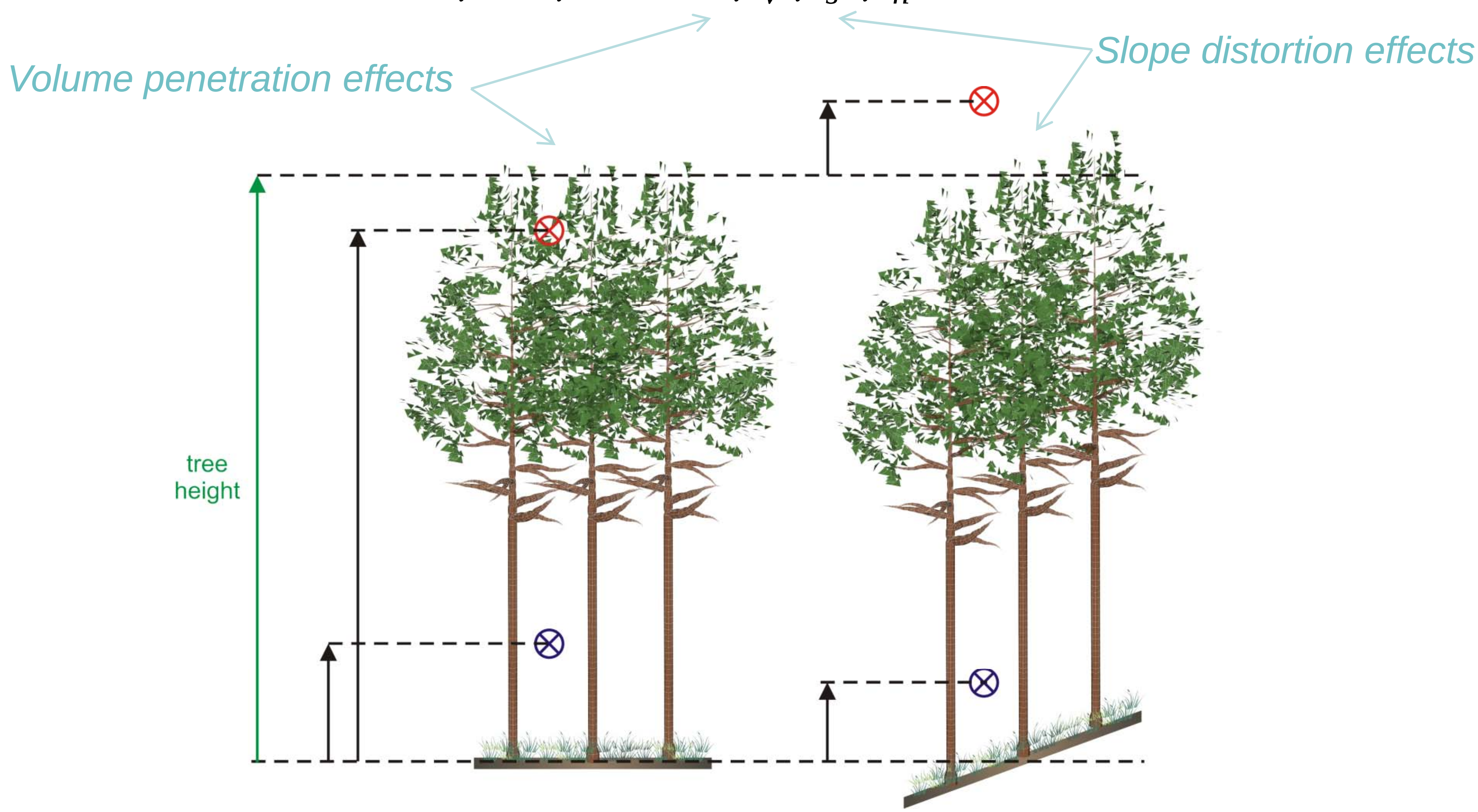

PolSARProSIM

results

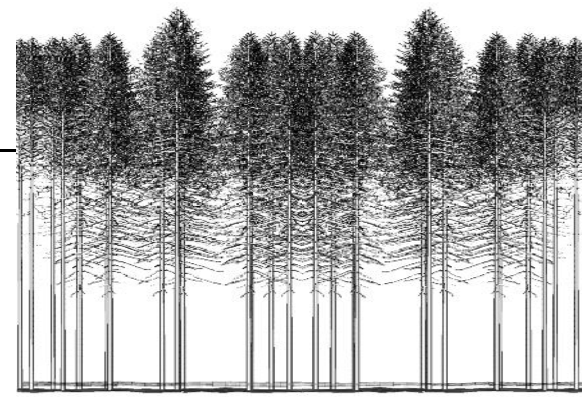

→PolSARProSIM
- Maxwell-based scattering model
- Fully coherent PolInSAR simulator
- Only target decorrelation

→ Input Parameters
- Satellite altitude, baseline, inc. angle
- Forest height h, density, tree type
- Soil roughness, moisture, terrain slope

→ Output Parameters
- Interferometric height h_{int}
- Individual scattering mechanisms → σ, η

→ Simulated scenario
- ALOS/PALSAR acquisition geometry
- Moderate density and soil roughness
- L-band
- Pine forest

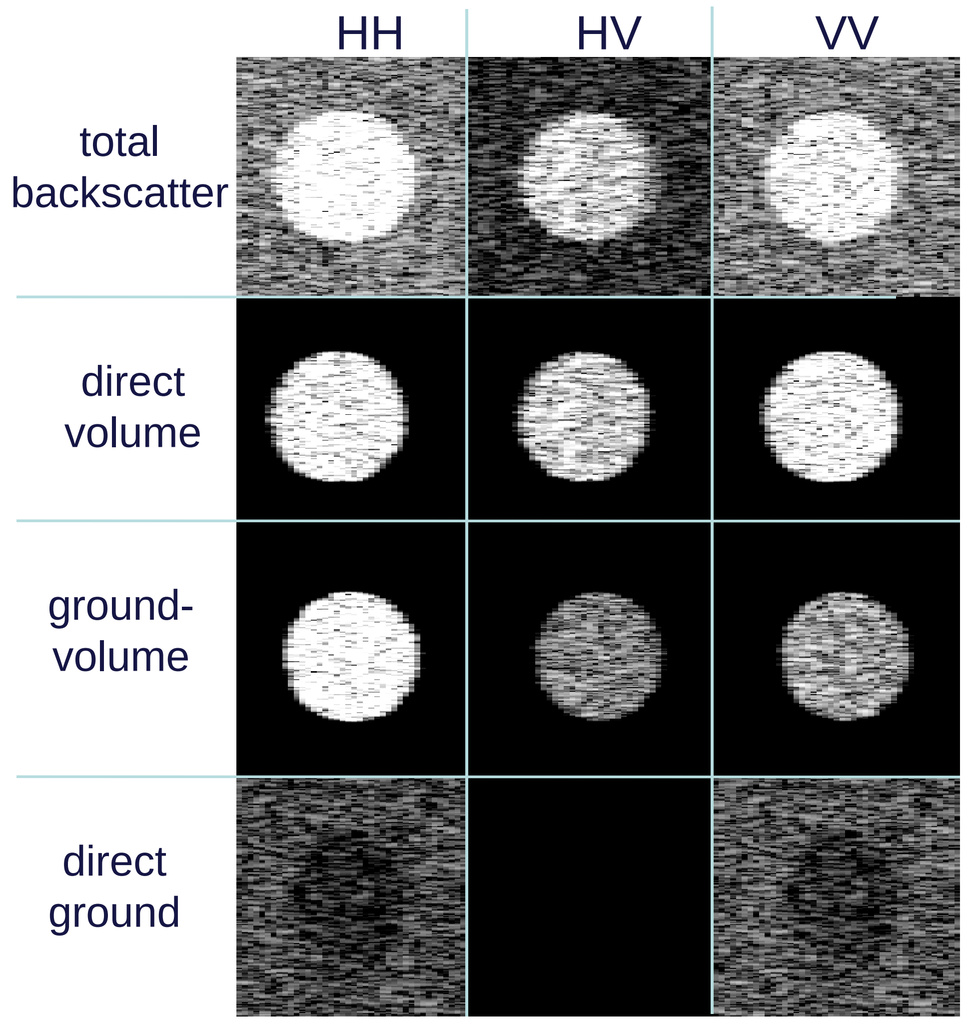

FOREST HEIGHT ESTIMATION

volume penetration

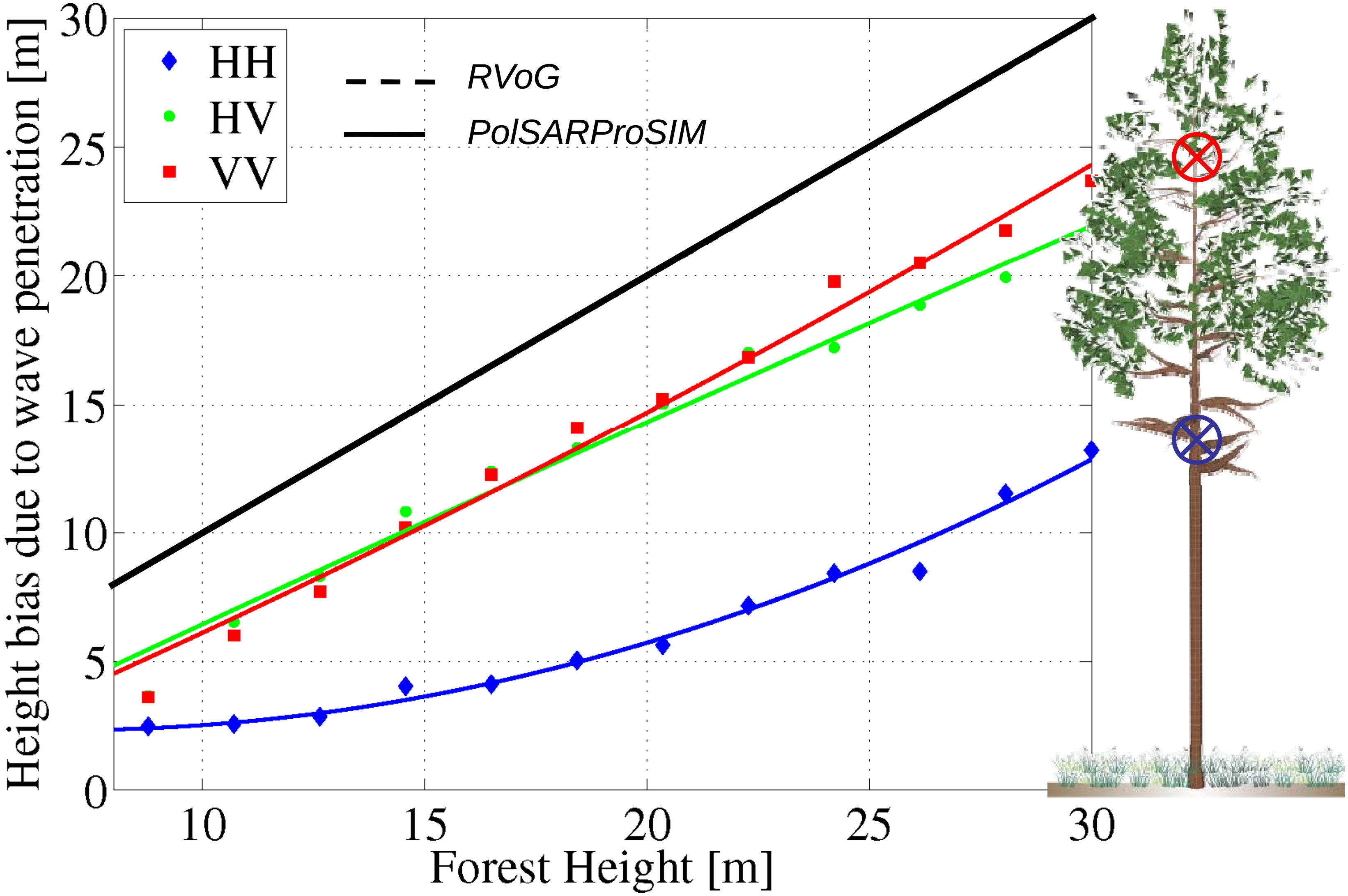

FOREST HEIGHT ESTIMATION

volume penetration

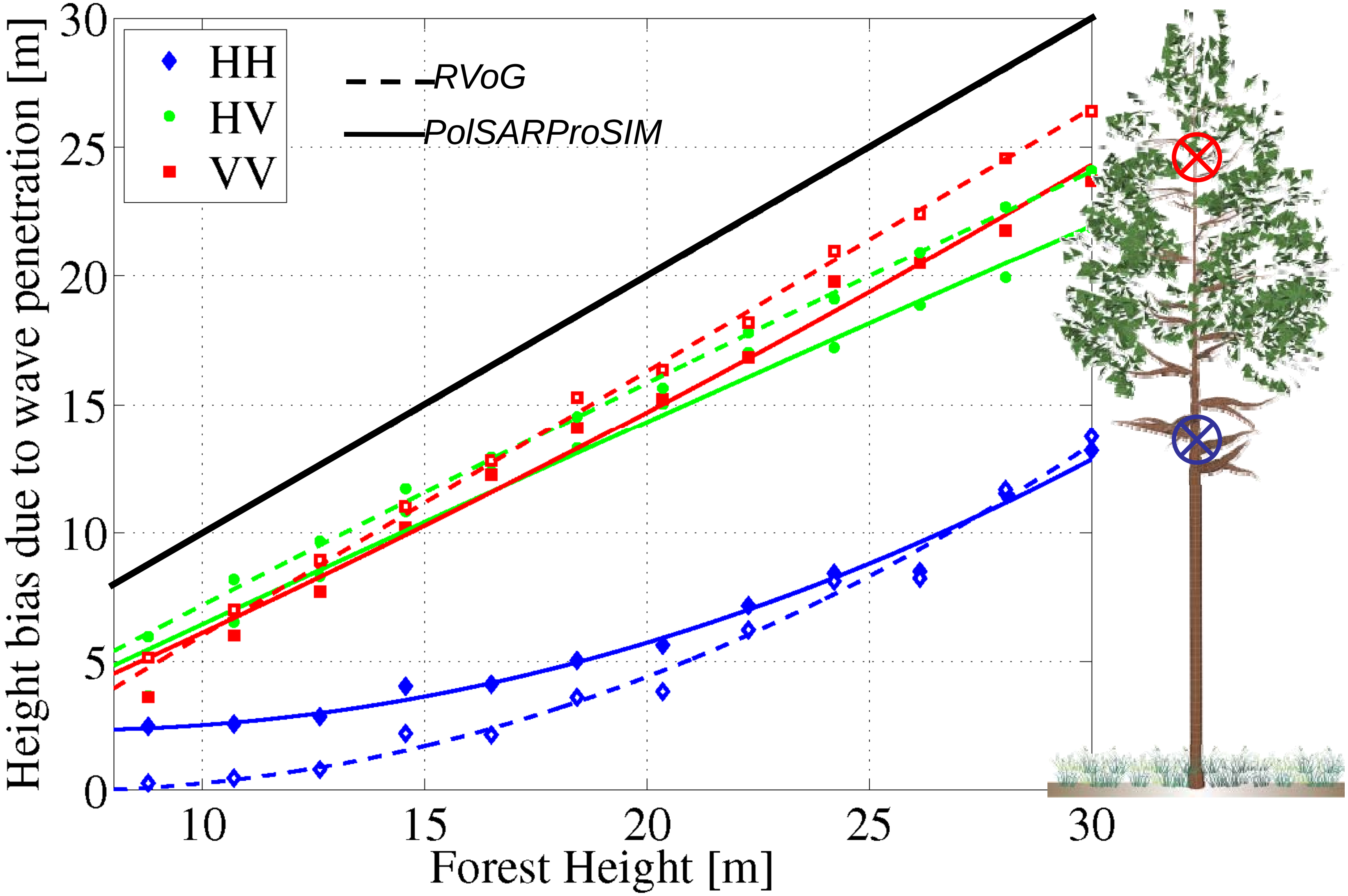

FOREST HEIGHT ESTIMATION

azimuth terrain slope

$h_v = 15$ m

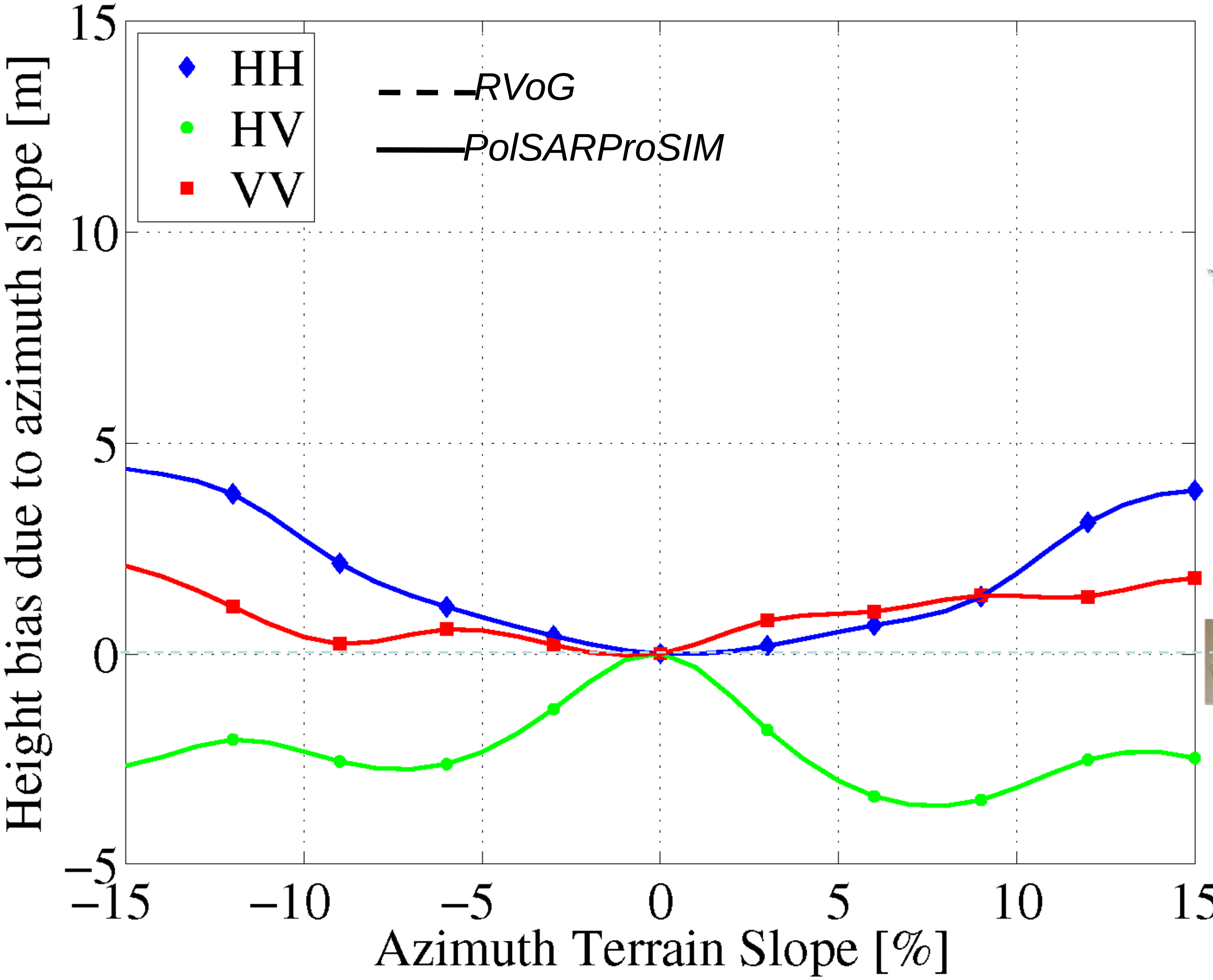

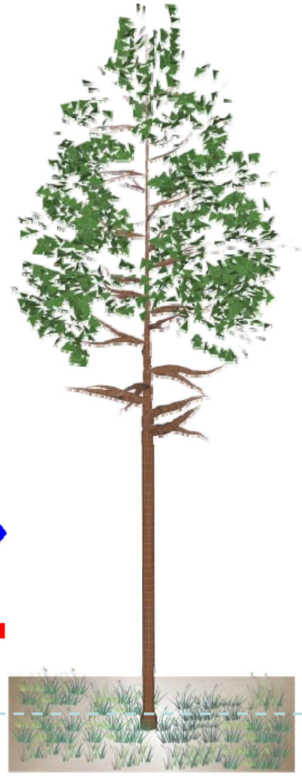

FOREST HEIGHT ESTIMATION

azimuth terrain slope

$h_v = 15$ m

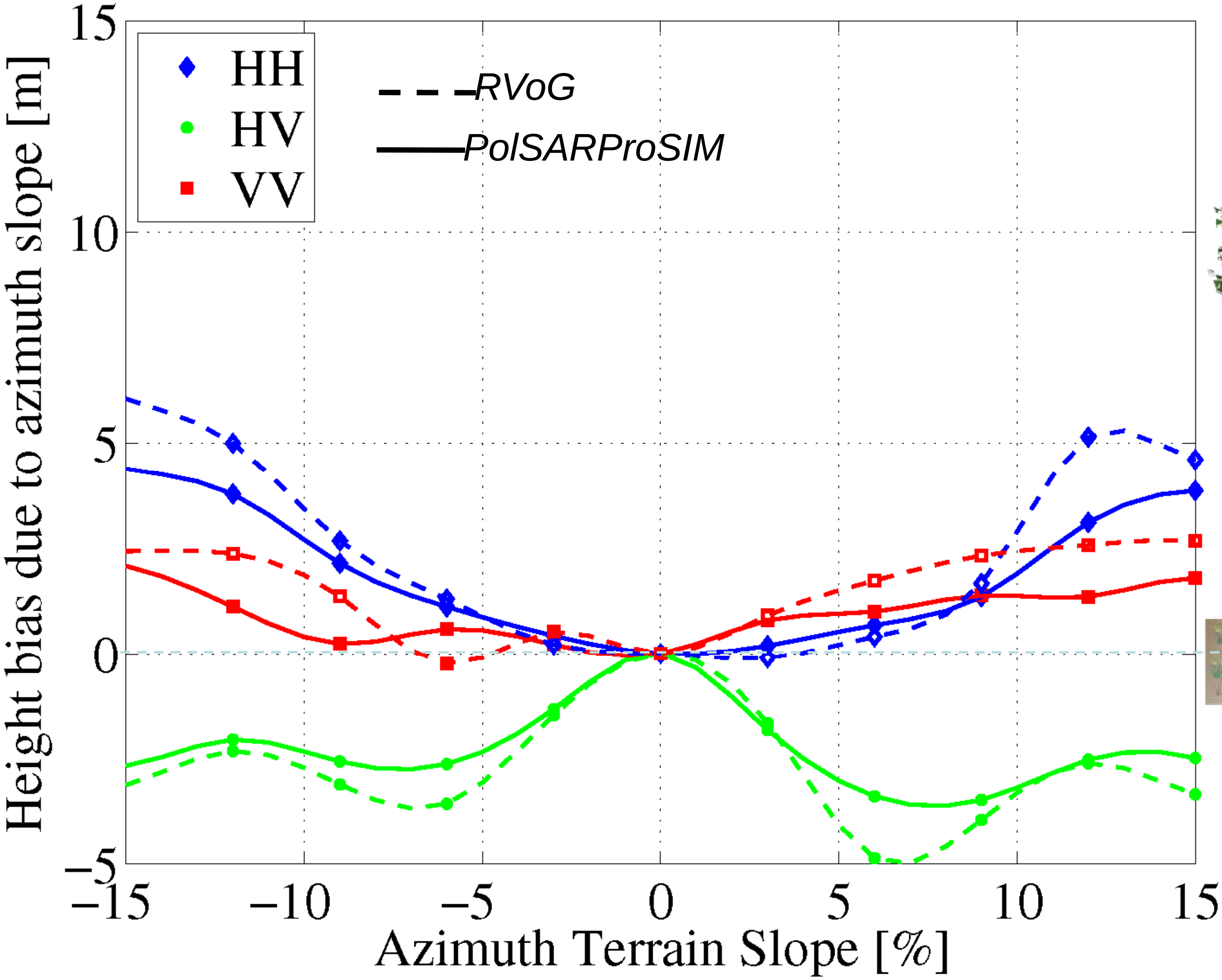

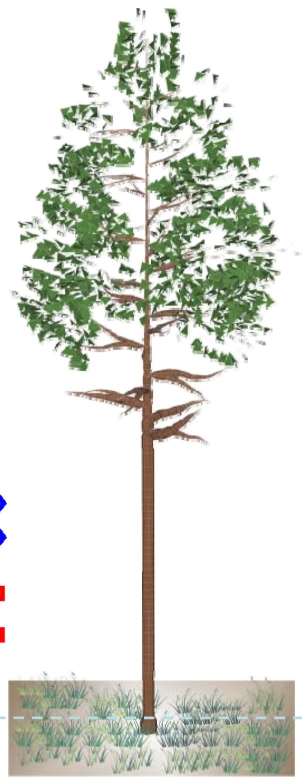

FOREST HEIGHT ESTIMATION

range terrain slope

$h_v = 15$ m

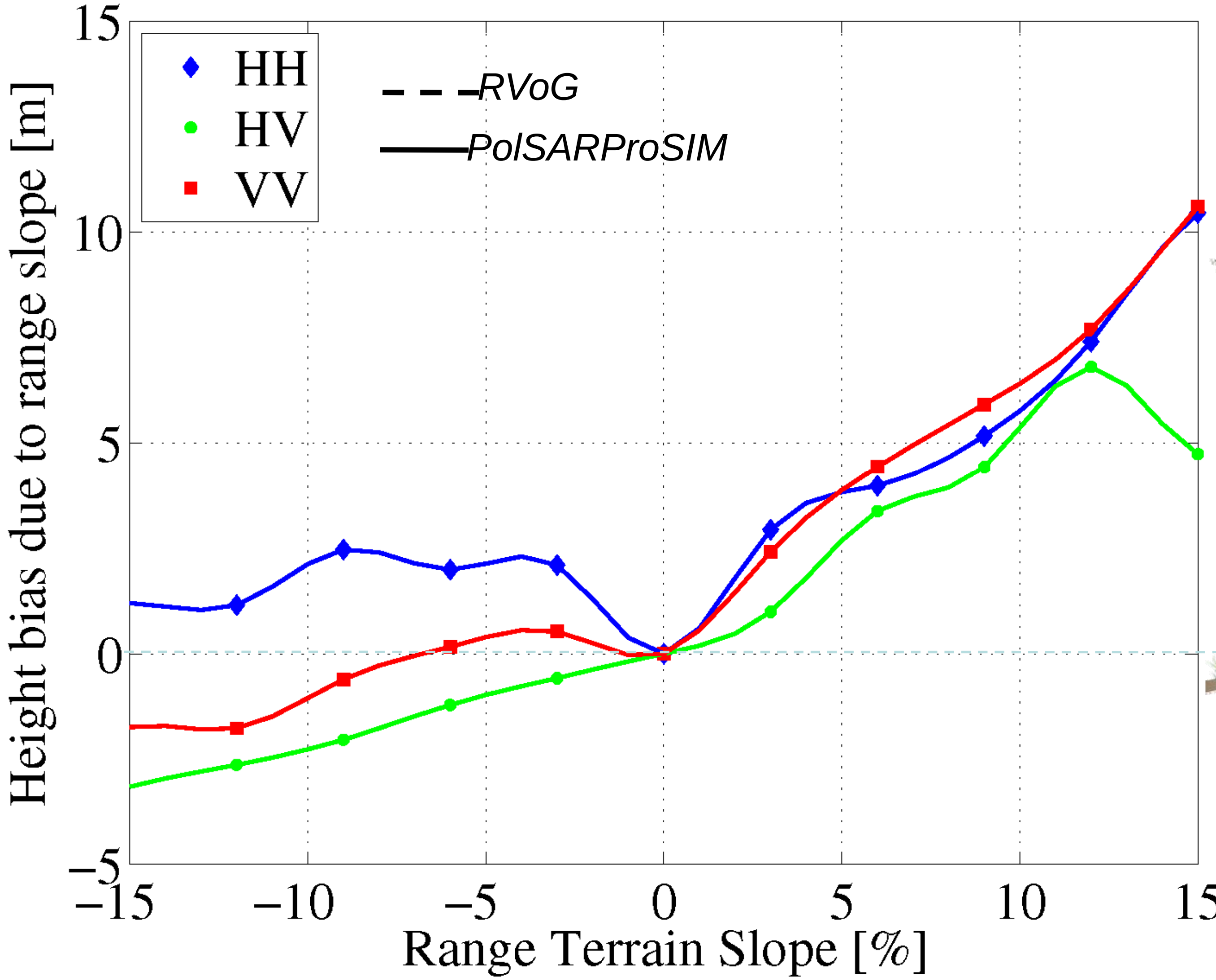

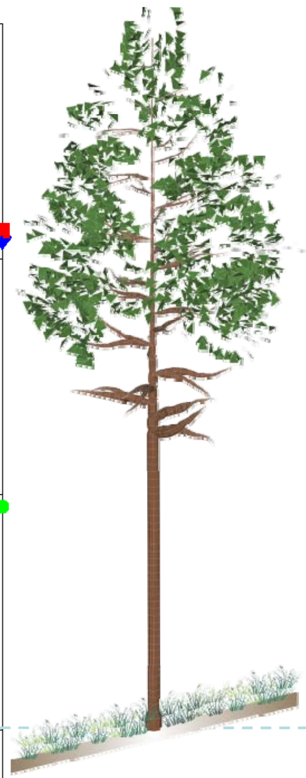

FOREST HEIGHT ESTIMATION

range terrain slope

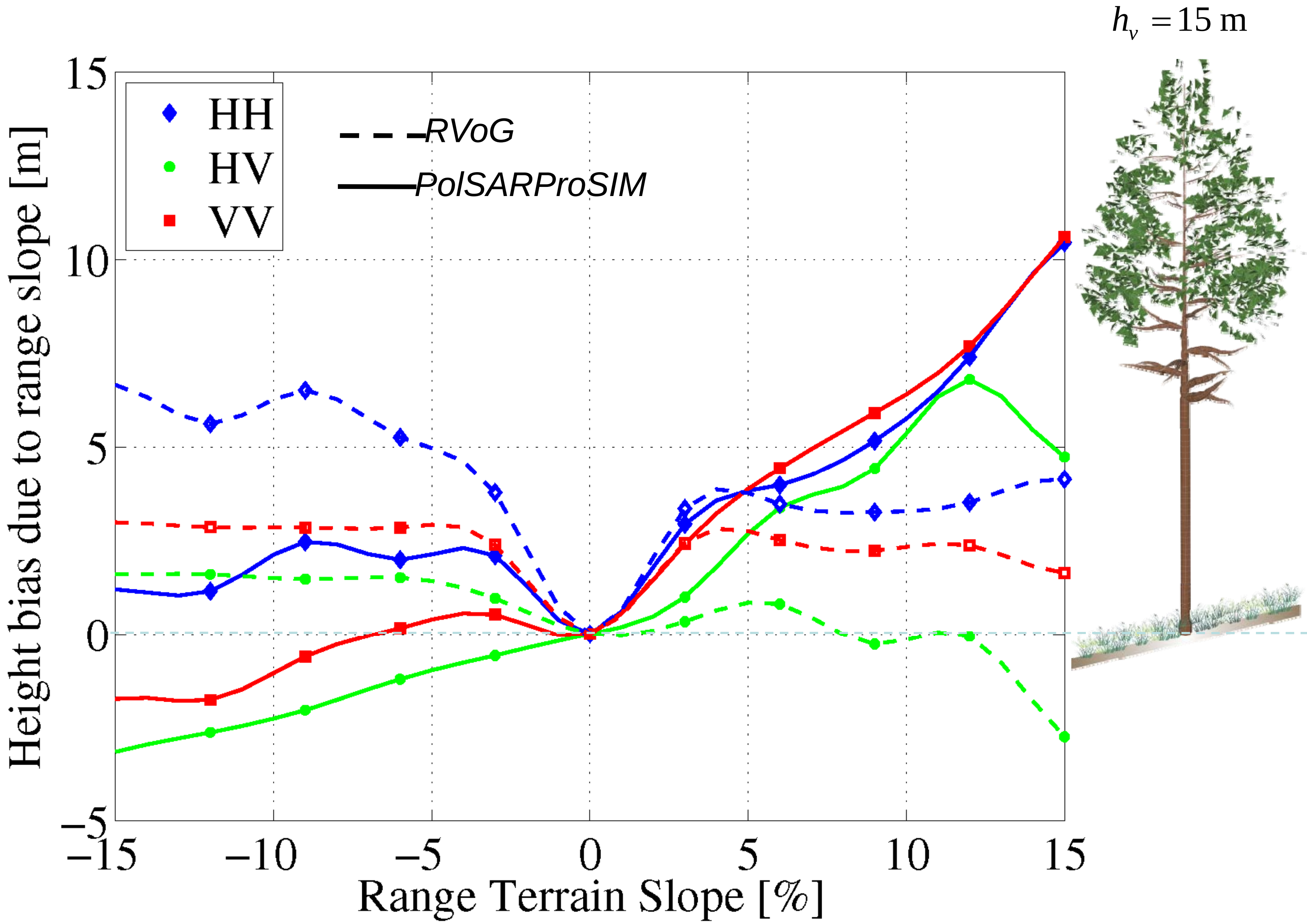

FOREST HEIGHT ESTIMATION

PolSARProSIM → **POLINOMIALS of terrain slope distortion and penetration depth**

↓

DEM → **Correct for slope distortion**

$$\tilde{\gamma}_s(\alpha) = \frac{\tilde{\gamma}'_s(\alpha)}{\tilde{\gamma}'_s(0)} \qquad \tilde{\gamma}_{s0} = \frac{\tilde{\gamma}}{\tilde{\gamma}_s^{A}(\alpha)}$$

↓

Estimate height (1)

$$h_{v1} = \frac{1}{k_z}\arg\left[\frac{\tilde{\gamma}^{A}\,\tilde{\gamma}^{B*}}{\tilde{\gamma}_s^{A}(\alpha)\,\tilde{\gamma}_s^{B*}(\alpha)}\right]$$

↓

Correct for volume effects

$$\phi_1(h_v) = \arg\left(\frac{\tilde{\gamma}^{A*}}{\tilde{\gamma}_s^{A*}(\alpha)}e^{jk_z z_v}\right), \quad \phi_1(h_v) = \arg\left(\frac{\tilde{\gamma}^{B}}{\tilde{\gamma}_s^{B}(\alpha)}e^{-jk_z z_0}\right)$$

↓

Estimate height (2)

$$h_{v2} = \frac{1}{k_z}\arg\left[\frac{\tilde{\gamma}^{A}\,\tilde{\gamma}^{B*}}{\tilde{\gamma}_s^{A}(\alpha)\,\tilde{\gamma}_s^{B*}(\alpha)}e^{j\phi_1(h_{v1})}e^{j\phi_2(h_{v1})}\right]$$

(loop back to **Correct for volume effects**)

POLINSAR ALOS PALSAR

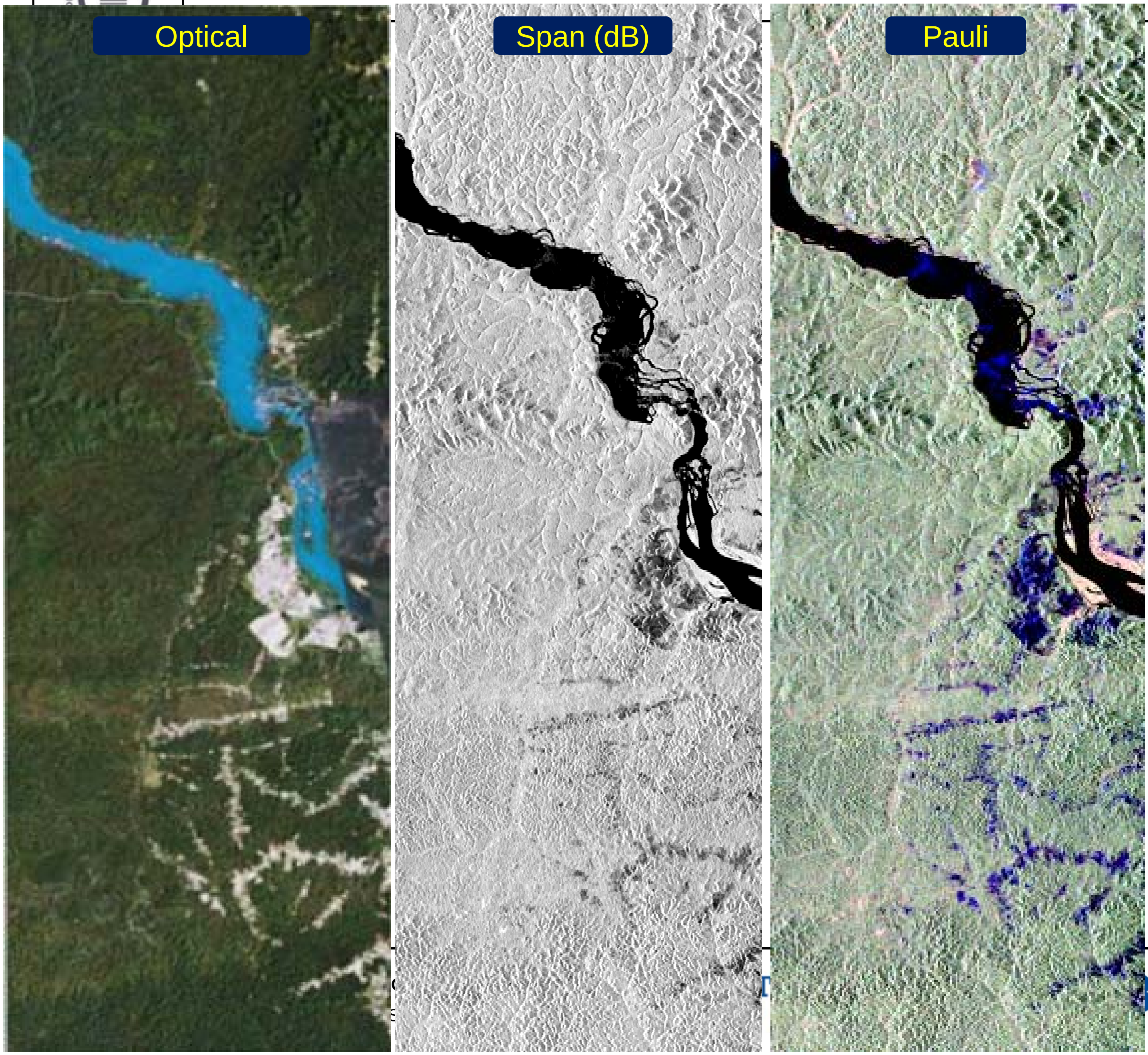

- → Full-PolInSAR
- → Amazon/Brasil
- → Ascending pass
- → Baseline = 130 m

POLINSAR ALOS PALSAR

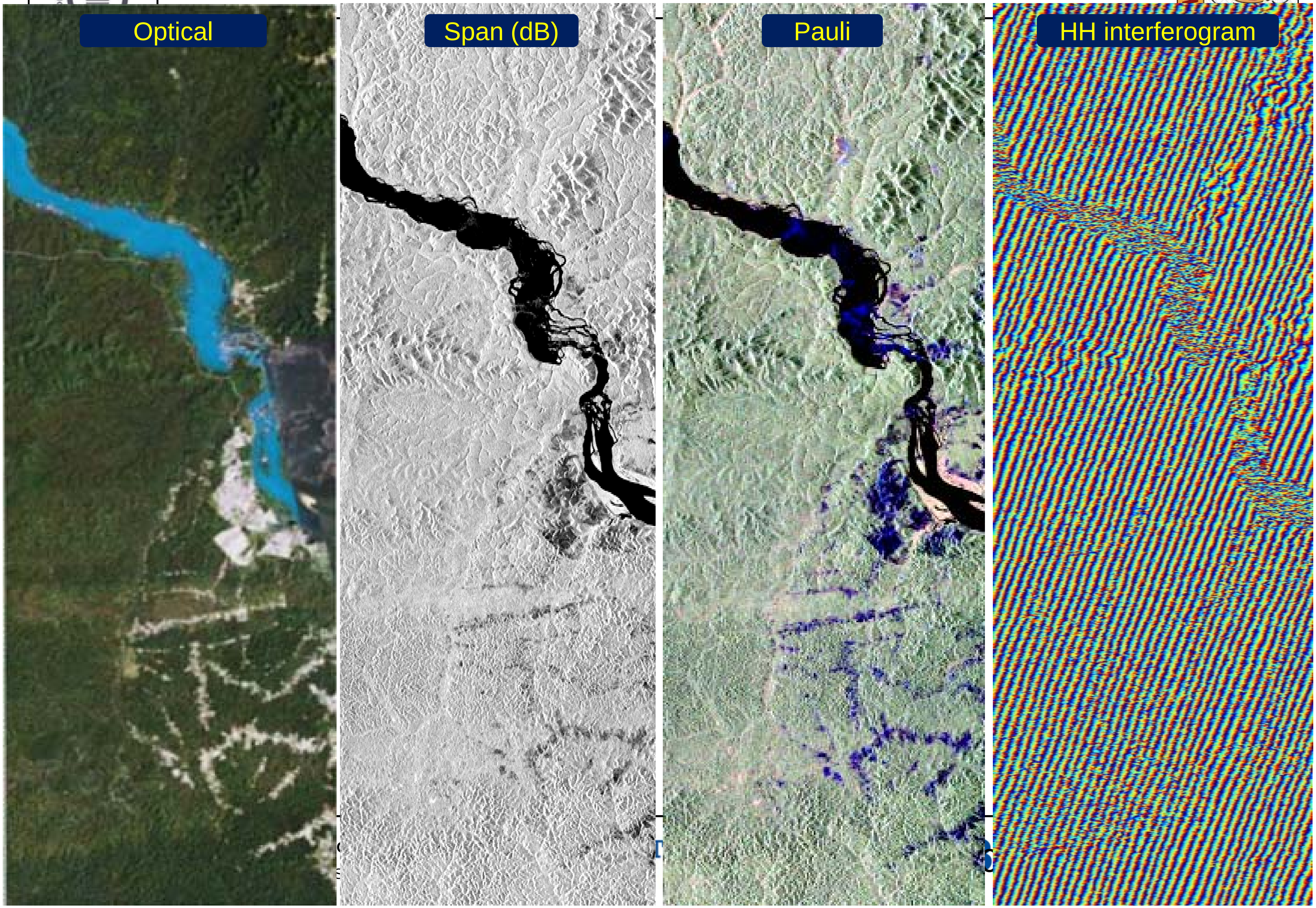

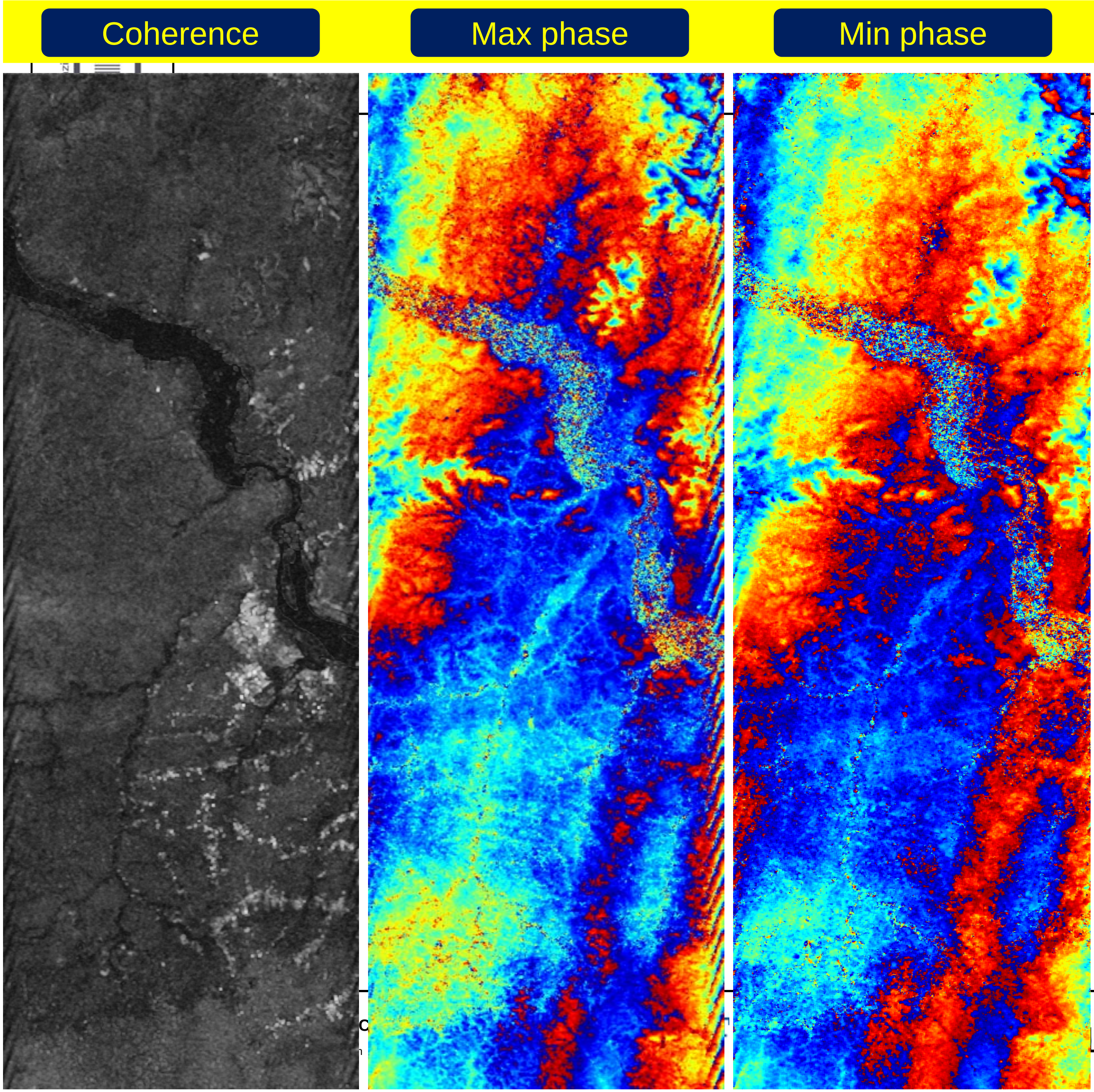

Coherence
Max phase
Min phase

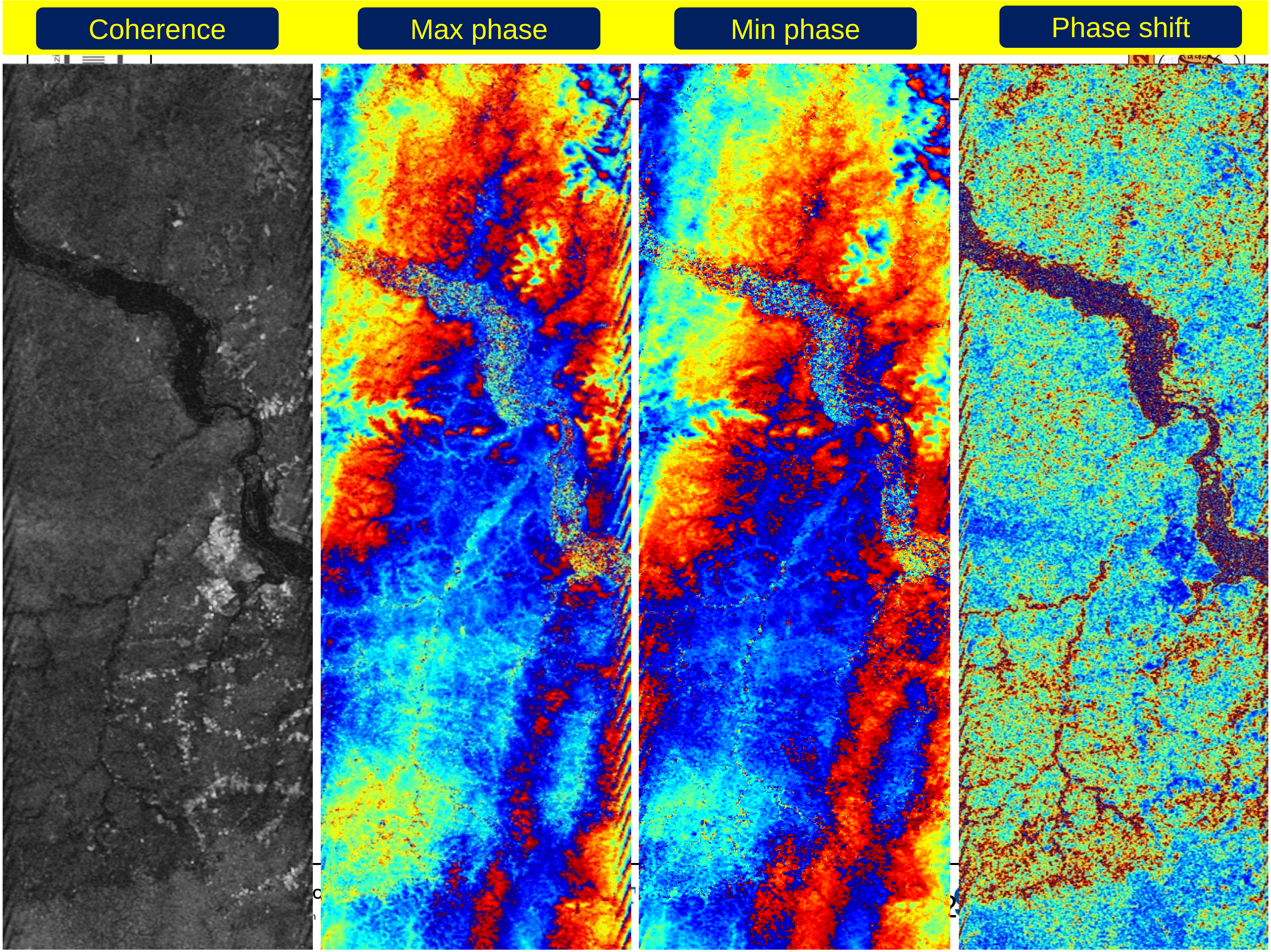
Coherence
Max phase
Min phase
Phase shift

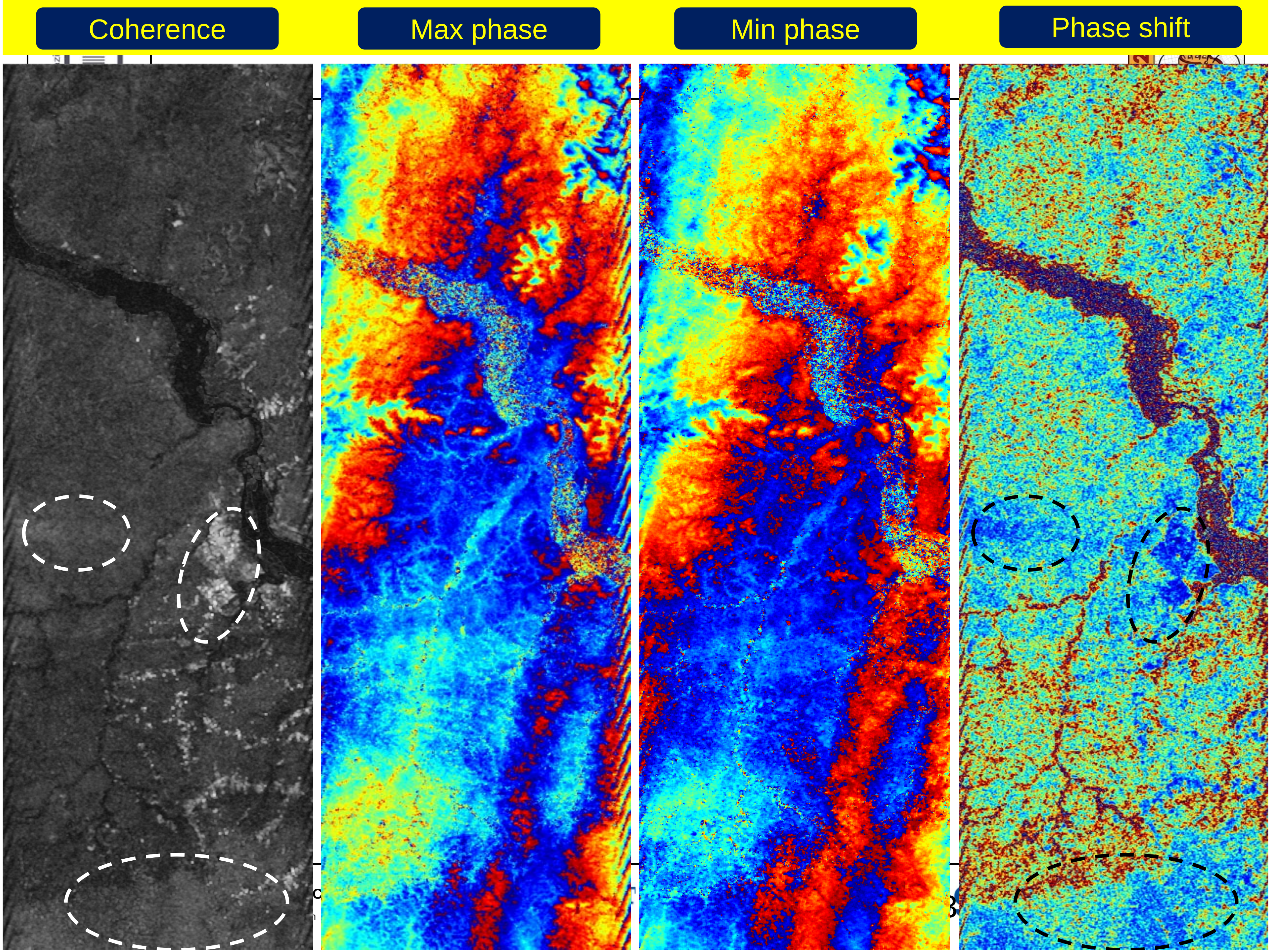
Coherence
Max phase
Min phase
Phase shift

POLINSAR ALOS PALSAR

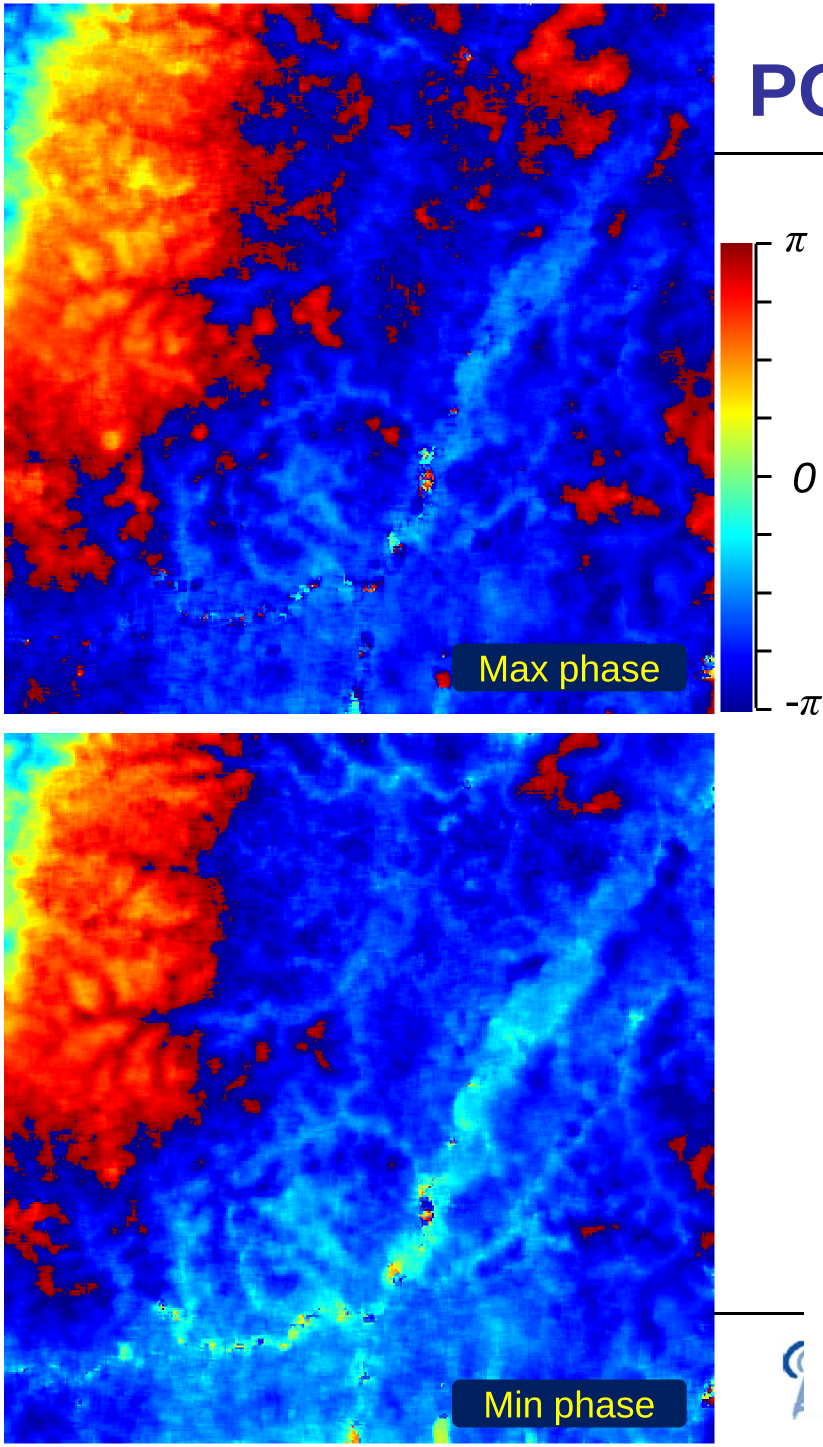

Max/Min Phase difference scaled by vertical wavenumber:

$$h_{v0} = \frac{1}{k_z}\arg\left[\tilde{\gamma}^{A}\,\tilde{\gamma}^{B*}\right]$$

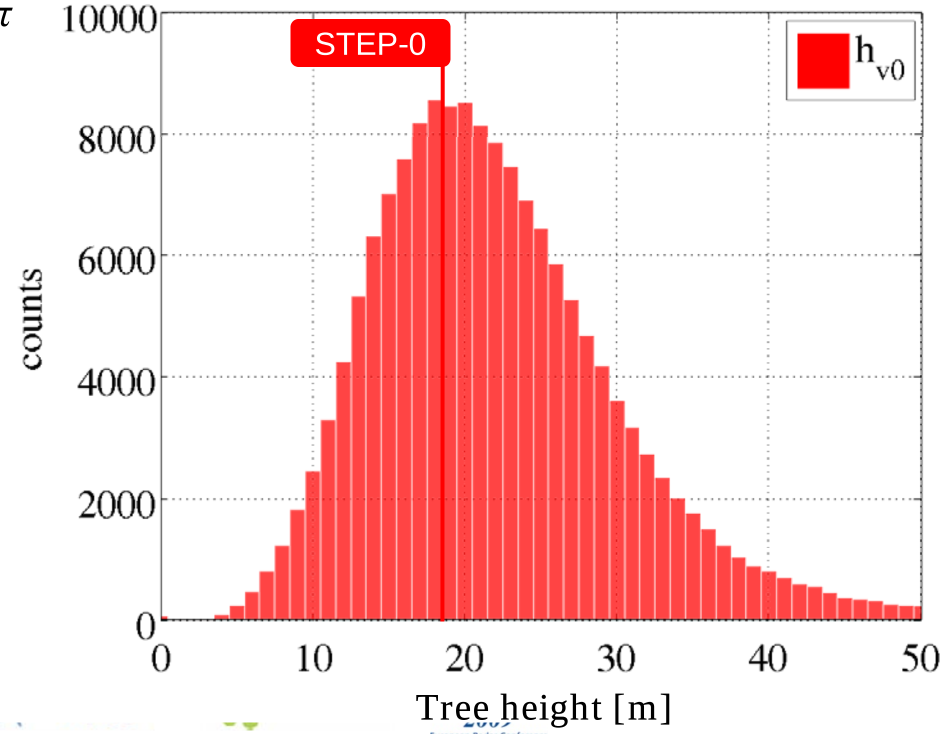

POLINSAR ALOS PALSAR

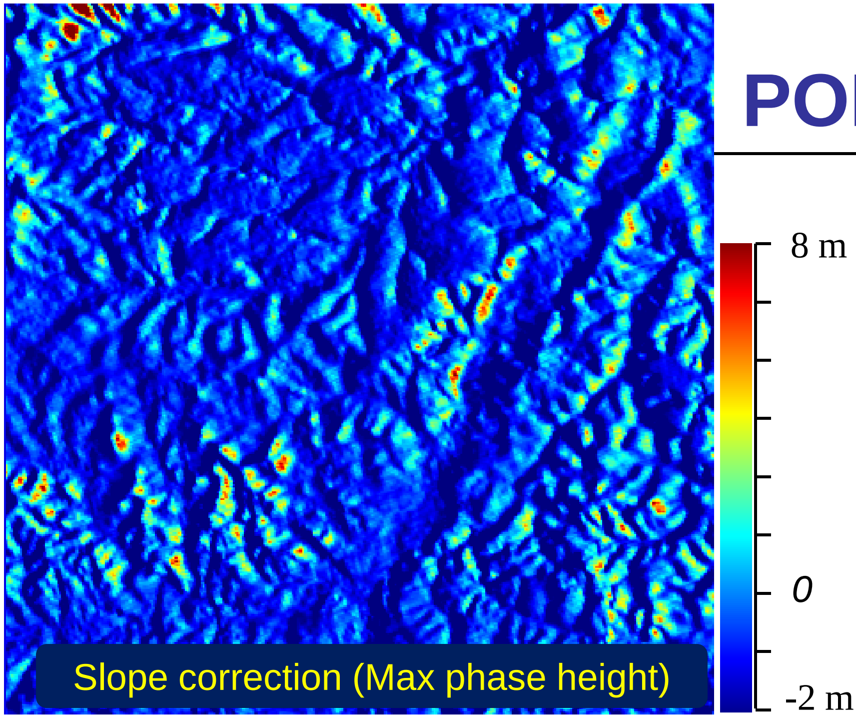

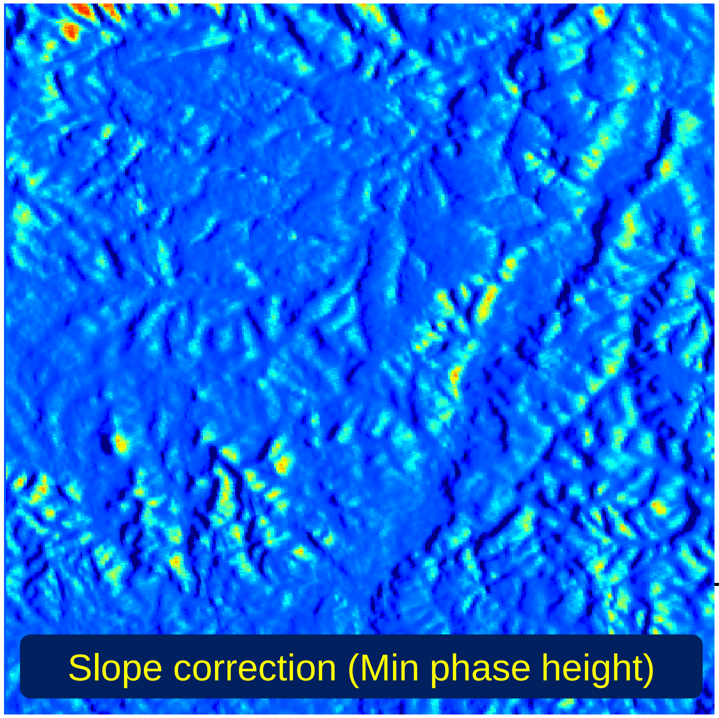

Slope correction maps for Max/Min phase height generated by combining SRTM DEM and PolSARProSIM simulations

$$h_{v1} = \frac{1}{k_z} \arg\left[\frac{\tilde{\gamma}^{A} \tilde{\gamma}^{B*}}{\tilde{\gamma}_s^{A}(\alpha)\, \tilde{\gamma}_s^{B*}(\alpha)} \right]$$

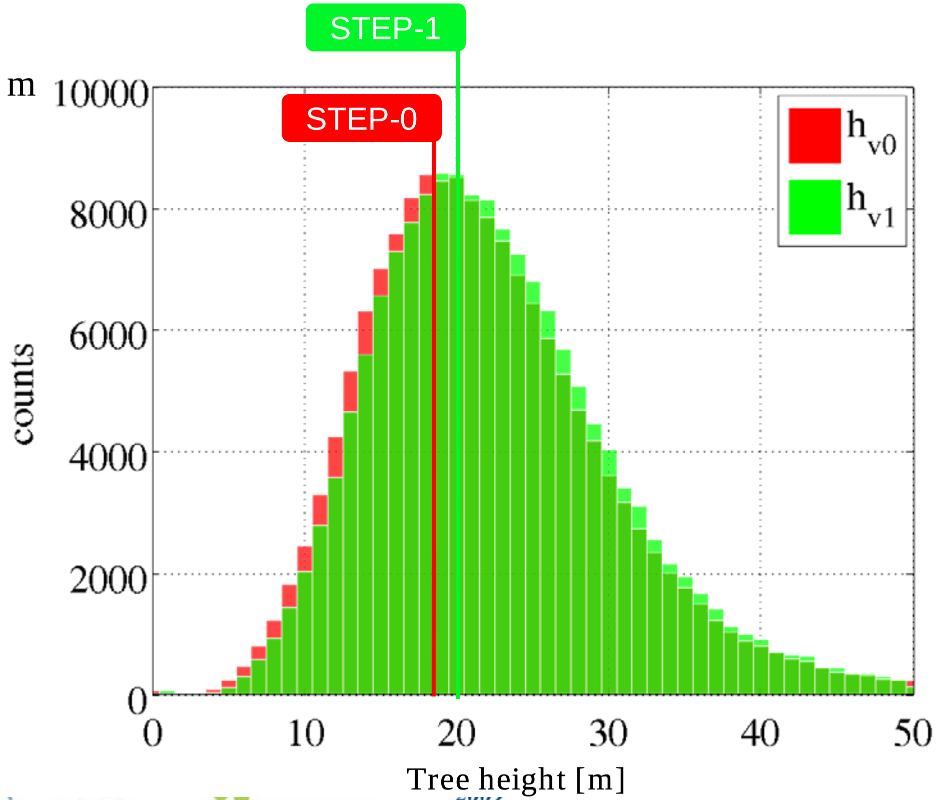

POLINSAR ALOS PALSAR

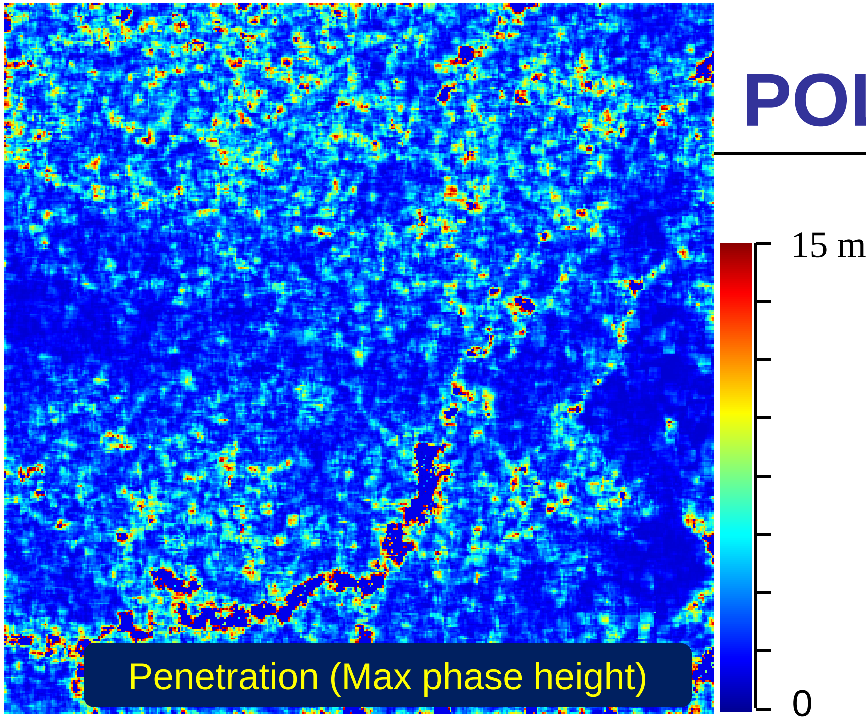

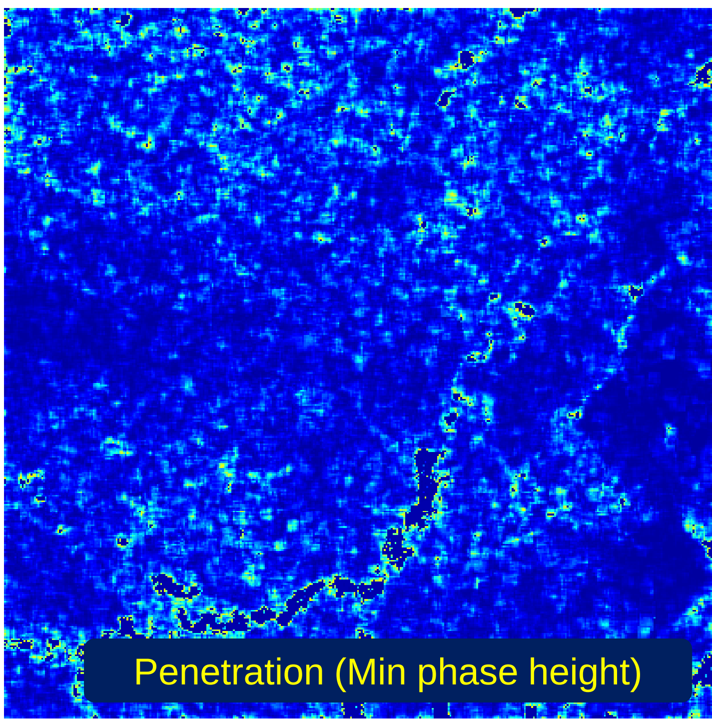

Penetration correction maps for Max/Min phase height generated by combining height estimates at STEP-1 and PolSARProSIM simulations

$$h_{v2} = \frac{1}{k_z} \arg\left[\frac{\tilde{\gamma}^{A} \tilde{\gamma}^{B*}}{\tilde{\gamma}_s^{A}(\alpha)\, \tilde{\gamma}_s^{B*}(\alpha)} e^{j\phi_1(h_{v1})} e^{j\phi_2(h_{v1})} \right]$$

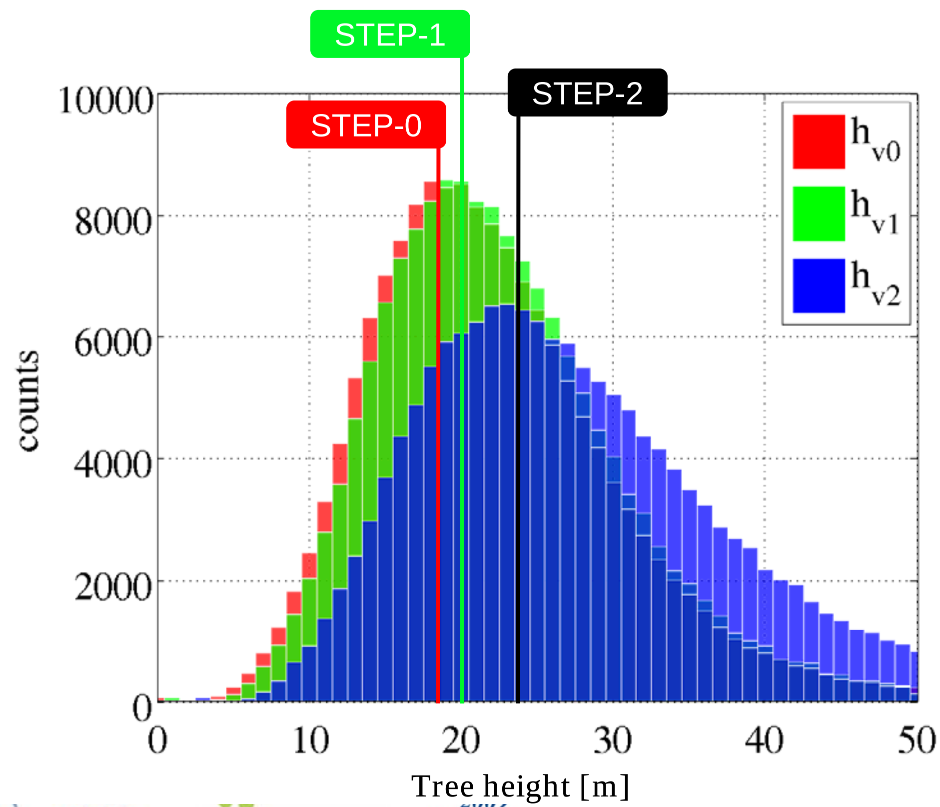

COMPACT POLARIMETRY
AND
COMPACT POLINSAR

COMPACT/HYBRID MODES

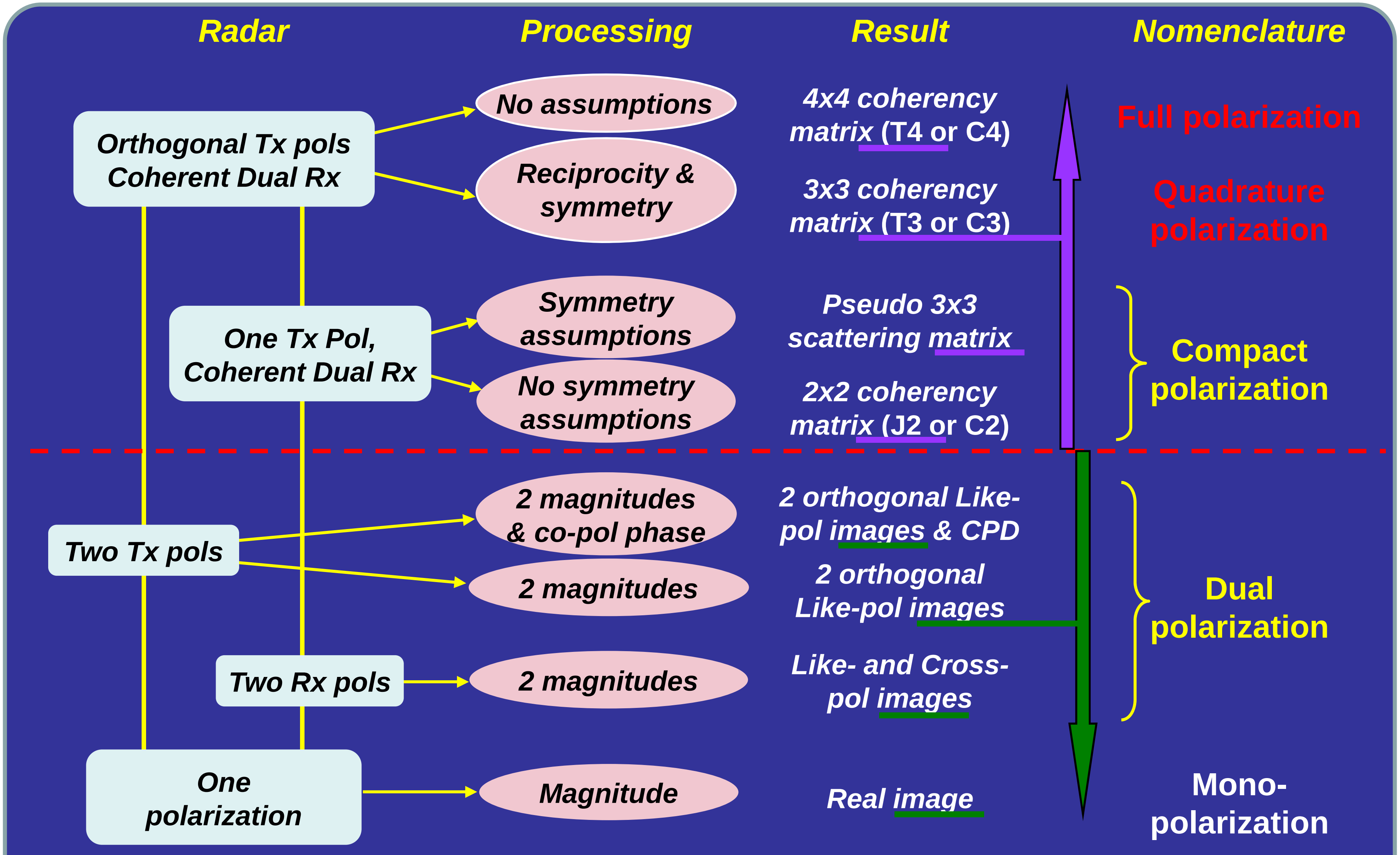

Courtesy of Dr. R. K. Raney – POLINSAR09

COMPACT/HYBRID MODES

Transmit CP (*note the 90º hybrid*)

Receive (*coherently*) linear (H & V)

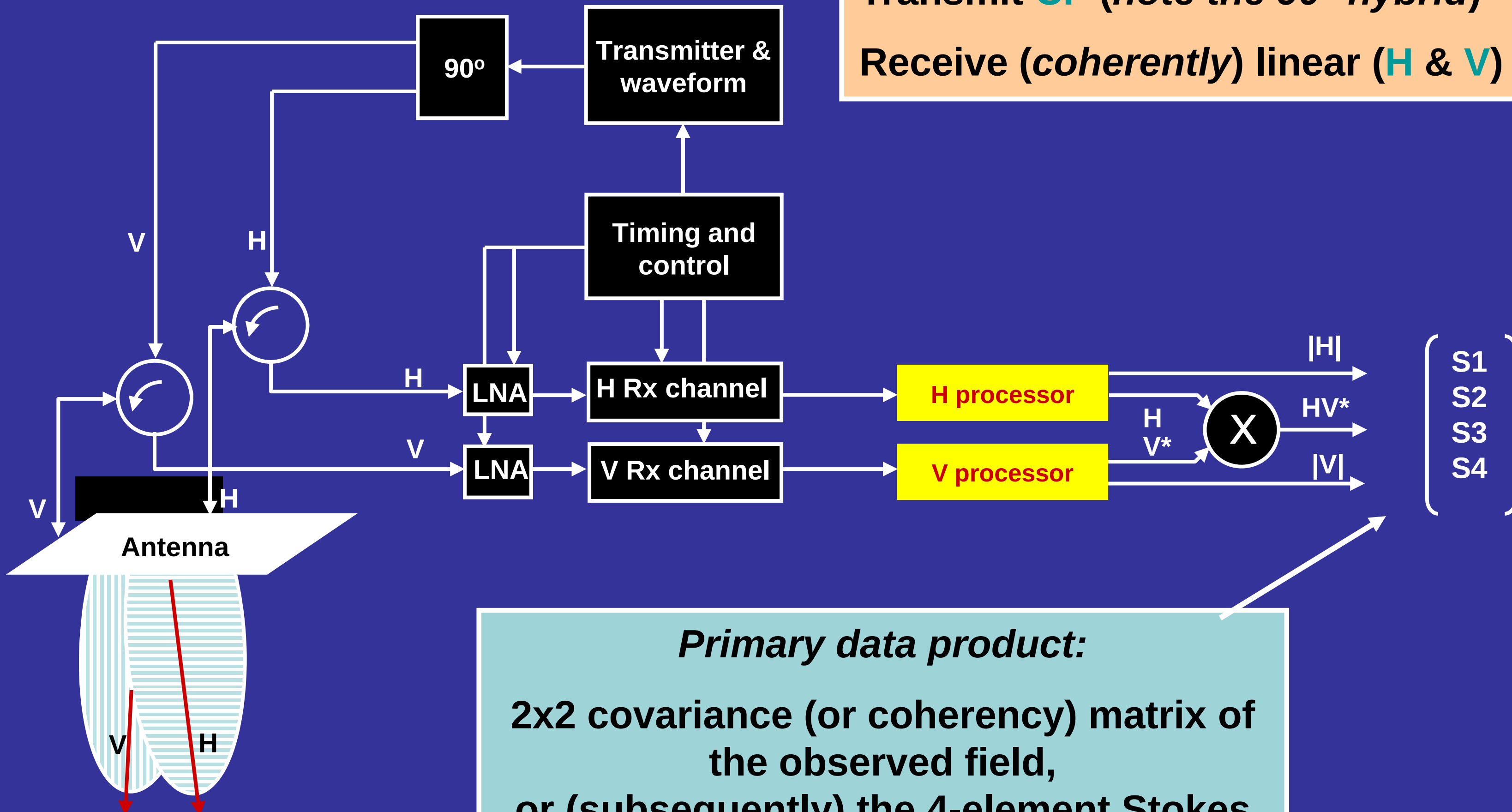

Primary data product:

2x2 covariance (or coherency) matrix of the observed field, or (subsequently) the 4-element Stokes vector

Courtesy of Dr. R. K. Raney – POLINSAR09

COMPACT/HYBRID MODES

Transmit RC and LC polarizations, interleaved, at 2x Nyquist PRF

Receive (*coherently*) linear (H & V) after each transmission

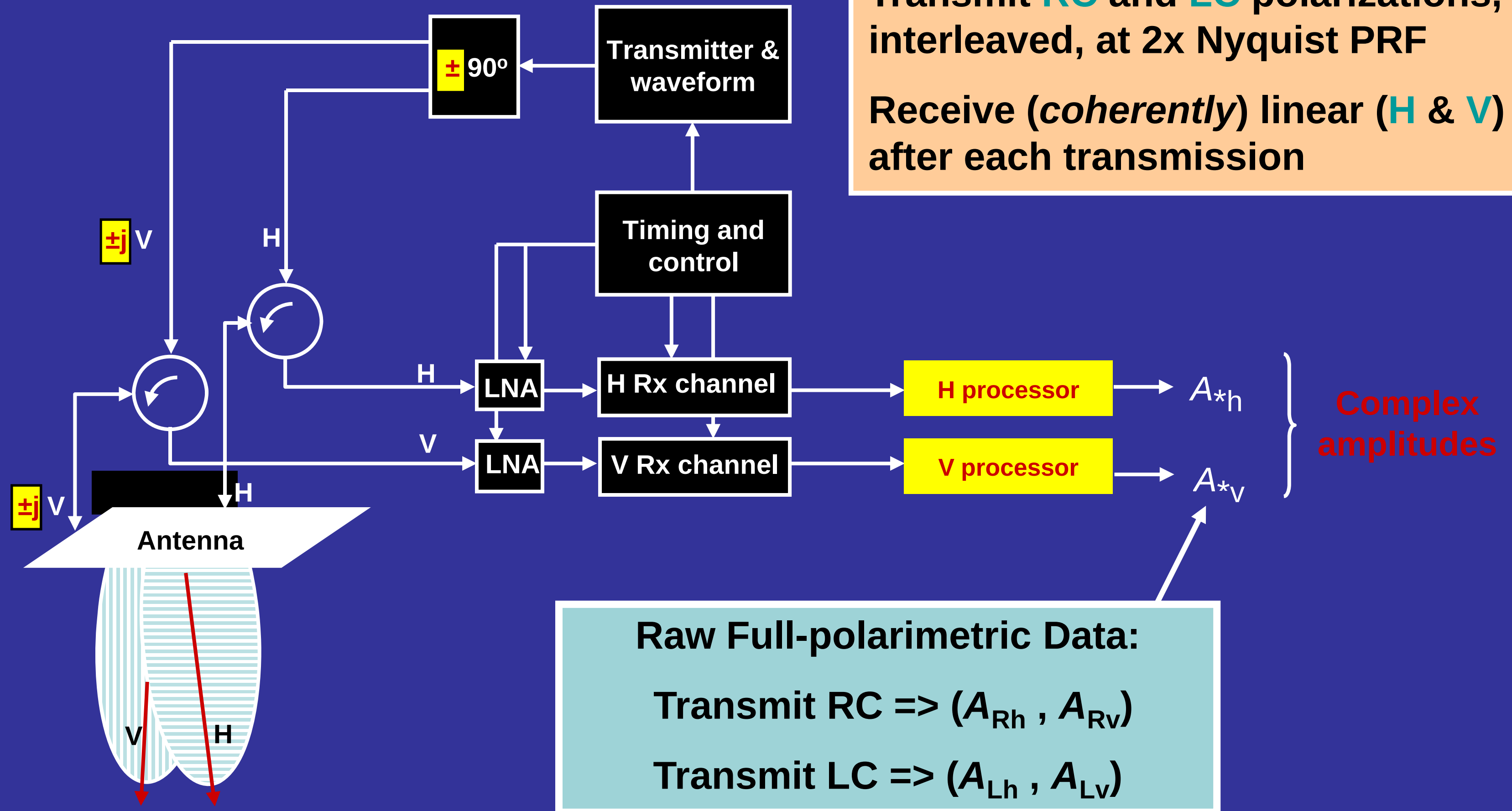

A_{*h}

A_{*V}

Raw Full-polarimetric Data:

Transmit RC => (A_{Rh} , A_{Rv})

Transmit LC => (A_{Lh} , A_{Lv})

Courtesy of Dr. R. K. Raney – POLINSAR09

COMPACT/HYBRID MODES

Freeman Decomposition
QP: Quad Polarization

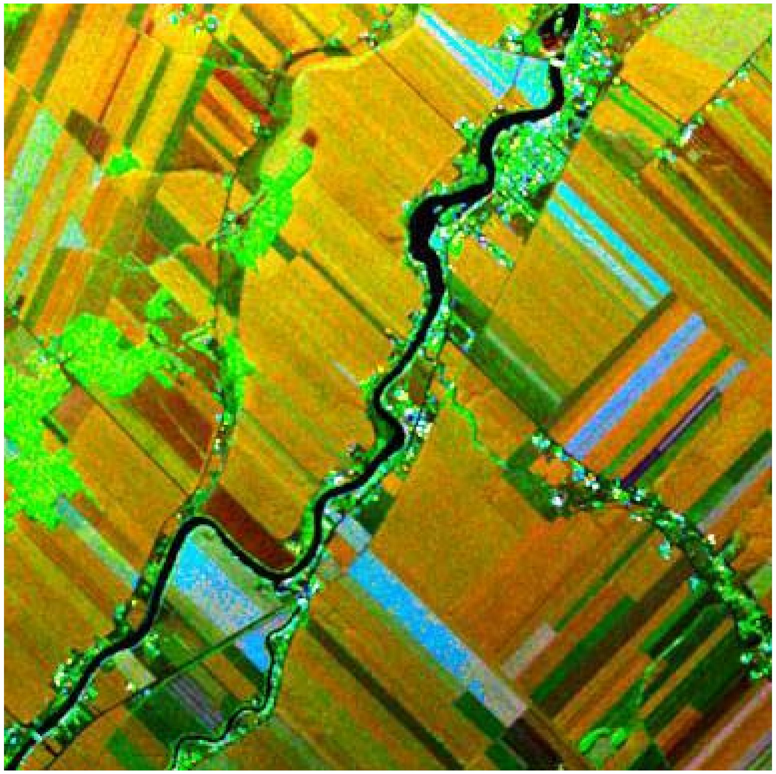

R: Surface
G: Volume
B: Double Bounce

m-δ Feature Decomposition
CL Hybrid-Polarity

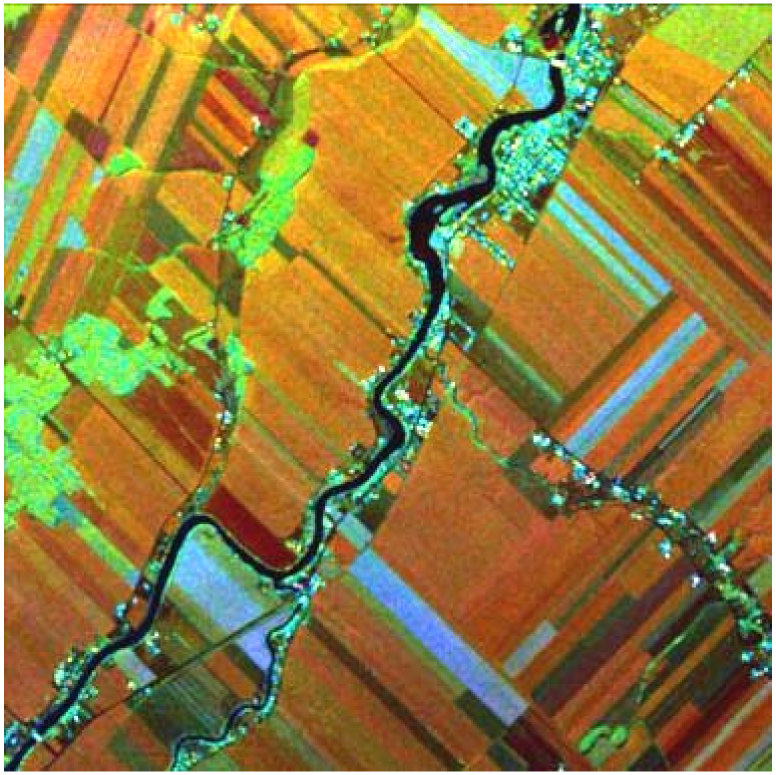

$$R = \sqrt{S_o m \frac{(1-\sin\delta)}{2}}$$

$$G = \sqrt{S_o (1-m)}$$

$$B = \sqrt{S_o m \frac{(1+\sin\delta)}{2}}$$

Courtesy of Dr. F. Charbonneau (CCRS) – POLINSAR09

COMPACT/HYBRID MODES

Compact / Hybrid Pol Data are usually synthesized from full-pol SLC data

Synthesis of Compact / Hybrid Pol Data more close to the reality
On received signal before the SAR Receiver (a)

Taking into account:
Attenuation (co-, x-channels), A / D Conversion, SAR processor

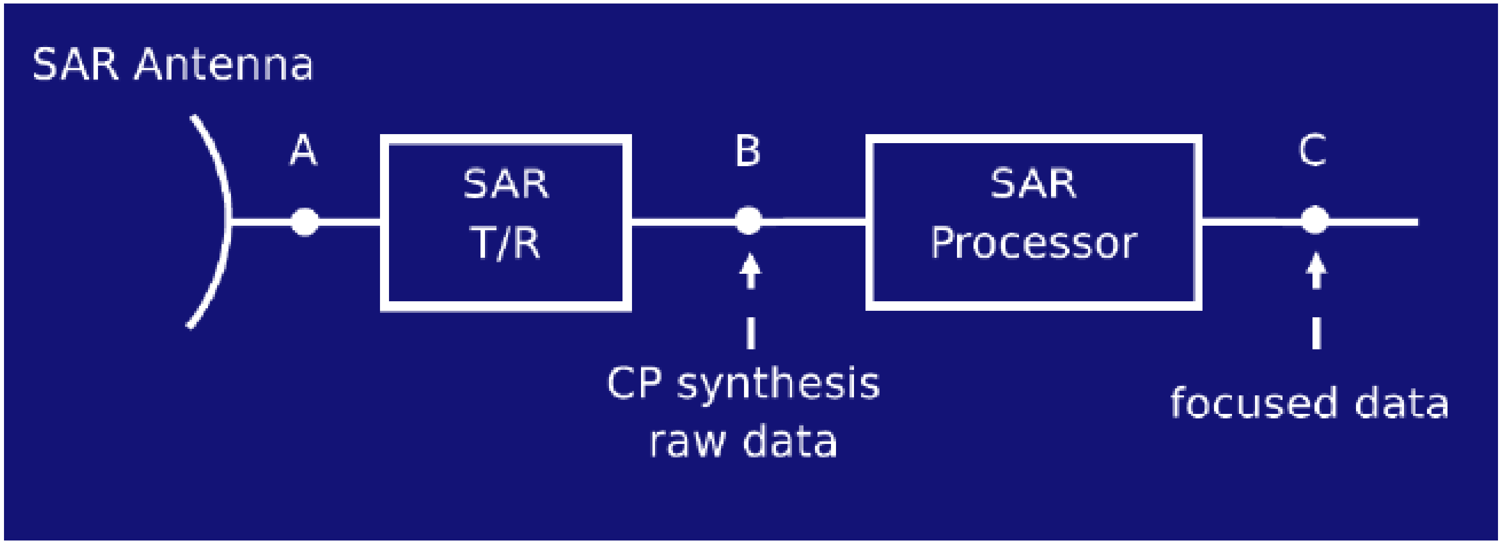

COMPACT/HYBRID MODES

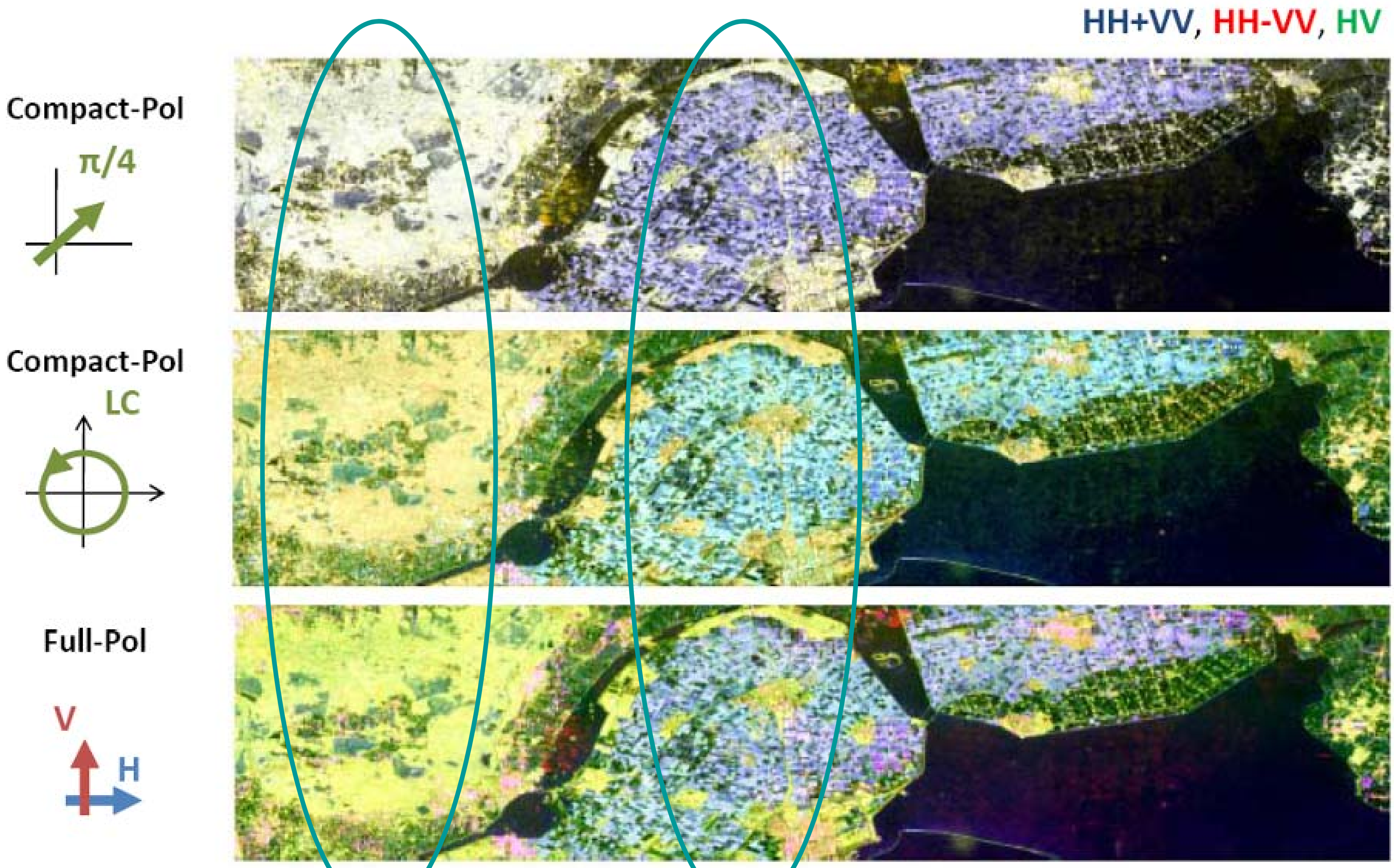

COMPACT/HYBRID MODES

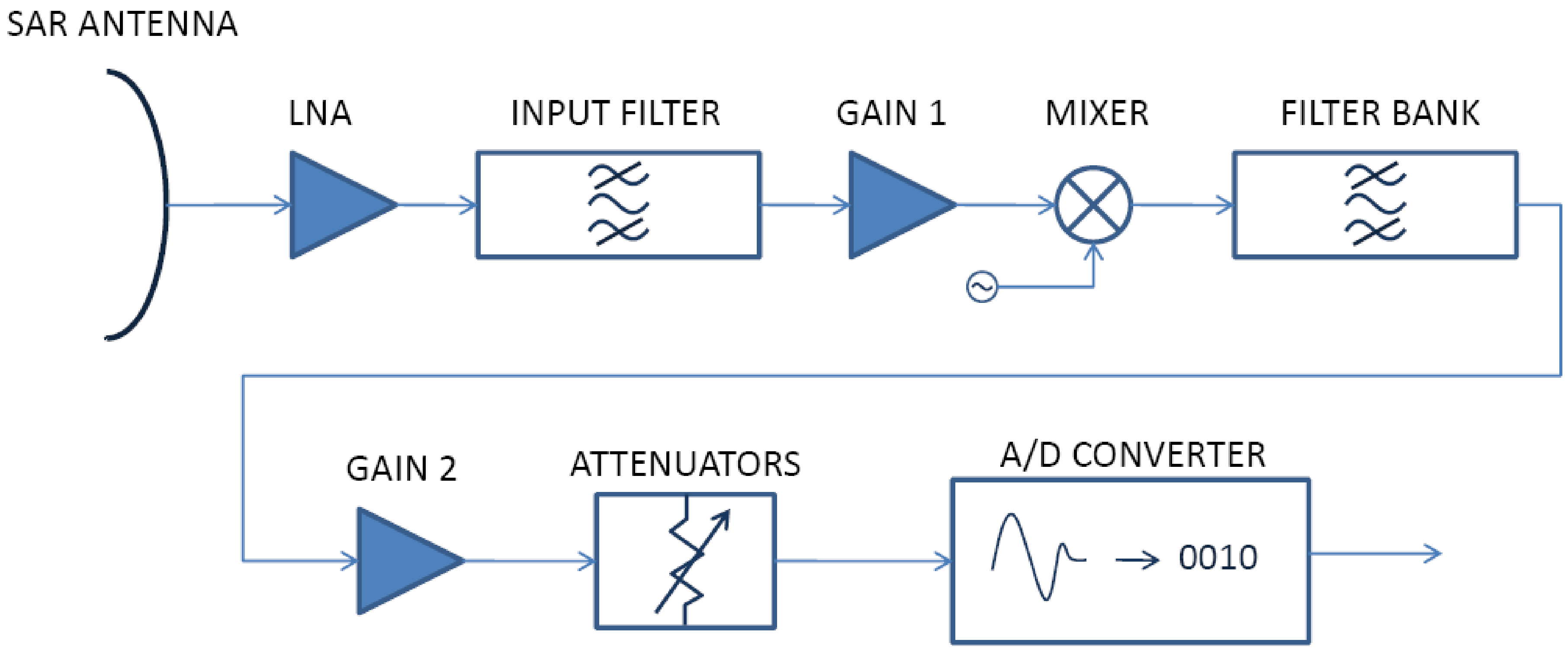

Co-polar (HH/VV) → 21 dB

X-polar (HV/VH) → 30 dB

???...!!!

COMPACT PolInSAR

To compare the PolInSAR performance of Compact-Pol with Full-Pol using L-band data

Compact PolSAR/PolInSAR ⟷ **Full PolSAR/PolInSAR**

L-band data
Forest height retrieval

How

Reconstruction of the pseudo full PolInSAR information aims

- to extract the HH-HV-VV channels from compact-pol data
- to easily compare them with the full-pol channels

COMPACT PolInSAR

Reconstruction of full polarimetric information

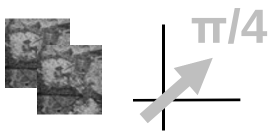

CP (π/4 mode)

CP scattering vector

$$k_{\pi/4}$$

2×2 CP covariance matrix

$$J_2 = \left\langle k_{\pi/4} \, k_{\pi/4}^{*T} \right\rangle$$

Reconstruction of FP

3×3 reconstructed FP coherency matrix

$$T_3$$

PolSAR algorithms

→ Reconstruction based on symmetry properties of geophysical media

→ Performance of CP (π/4 mode) evaluated on PolSAR classification results (Souyris, 2005)

COMPACT PolInSAR

Reconstruction of full PolInSAR information

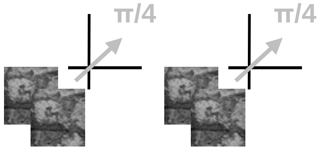

C-PolInSAR (π/4 mode)

2 CP scattering vectors

$$k_{(\pi/4)_1}$$
$$k_{(\pi/4)_2}$$

4×4 CP covariance matrix

$$J_4$$

Reconstruction of F-PolInSAR

6×6 reconstructed F-PolInSAR coherency matrix

$$T_6 = \begin{bmatrix} T_{11} & \Omega_{12} \\ \Omega_{12}^{*T} & T_{22} \end{bmatrix}$$

PolInSAR algorithms

COMPACT Pol-InSAR

Reconstruction of full PolInSAR information

CP scattering vectors

$$k_{(\pi/4)_1} = \begin{pmatrix} S_{HH_1} + S_{HV_1} \\ S_{VV_1} + S_{HV_1} \end{pmatrix}$$

$$k_{(\pi/4)_2} = \begin{pmatrix} S_{HH_2} + S_{HV_2} \\ S_{VV_2} + S_{HV_2} \end{pmatrix}$$

4×4 C-PolInSAR covariance matrix

$$J_4 = \left\langle \begin{bmatrix} k_{(\pi/4)_1} \\ k_{(\pi/4)_2} \end{bmatrix} \begin{bmatrix} k_{(\pi/4)_1} \\ k_{(\pi/4)_2} \end{bmatrix}^{*T} \right\rangle = \begin{bmatrix} J_{11} & J_{12} \\ J_{12}^{*T} & J_{22} \end{bmatrix}$$

$$J_{12} = \begin{bmatrix} j_{11} & j_{12} \\ j_{21} & j_{22} \end{bmatrix}$$

$$\begin{cases} j_{11} = S_{HH_1} S_{HH_2}^* + S_{HH_1} S_{HV_2}^* + S_{HV_1} S_{HH_2}^* + S_{HV_1} S_{HV_2}^* \\ j_{12} = S_{HH_1} S_{VV_2}^* + S_{HH_1} S_{HV_2}^* + S_{HV_1} S_{VV_2}^* + S_{HV_1} S_{HV_2}^* \\ j_{21} = S_{VV_1} S_{HH_2}^* + S_{VV_1} S_{HV_2}^* + S_{HV_1} S_{HH_2}^* + S_{HV_1} S_{HV_2}^* \\ j_{22} = S_{VV_1} S_{VV_2}^* + S_{VV_1} S_{HV_2}^* + S_{HV_1} S_{VV_2}^* + S_{HV_1} S_{HV_2}^* \end{cases}$$

8 observables < 18 unknowns

COMPACT Pol-InSAR

Reconstruction of full PolInSAR information

→Additional equations from symmetry properties (Nghiem, 1992)

→Two approaches:

- rotation symmetry
- reflection symmetry

C-PolInSAR observables
+
Reflection symmetry
+
rotation invariance of x-pol terms

→

6×6 reconstructed
F-PolInSAR coherency matrix

$$T_6^{\mathrm{ref}}$$

Cross-coherency matrix:

$$\Omega_{12} = \frac{1}{4}\begin{pmatrix} j_{11}+j_{12}+j_{22}+5j_{21} & 2(j_{11}-j_{22}) & 0 \\ 2(j_{11}-j_{22}) & 2(j_{11}+j_{22})-4j_{21} & 0 \\ 0 & 0 & j_{11}+j_{22}-j_{21}-j_{12} \end{pmatrix}$$

COMPACT Pol-InSAR

Performance evaluation scheme

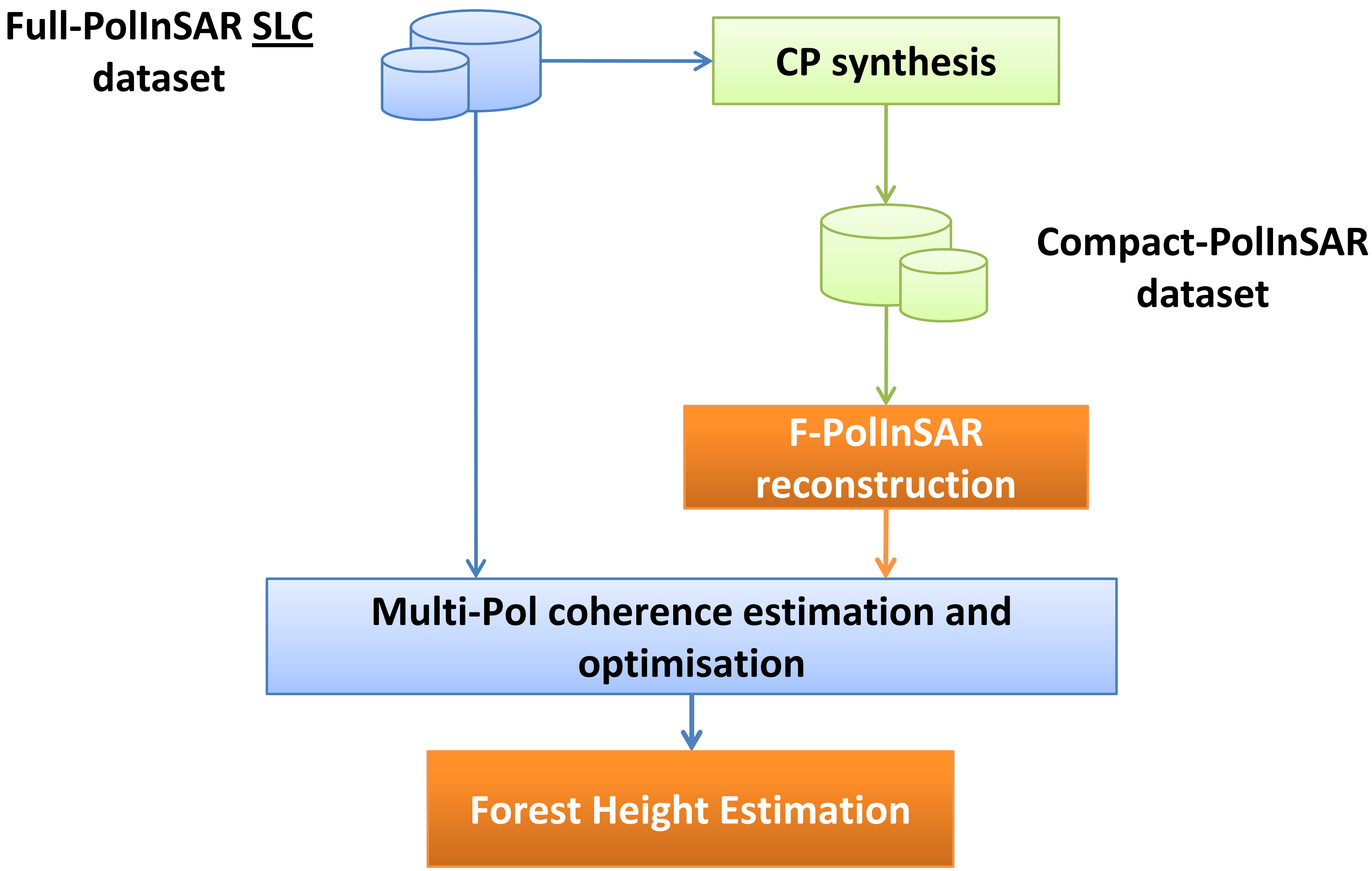

Reconstructed FP information

Airborne E-SAR data (Traunstein, Germany)

HH
VV
HV

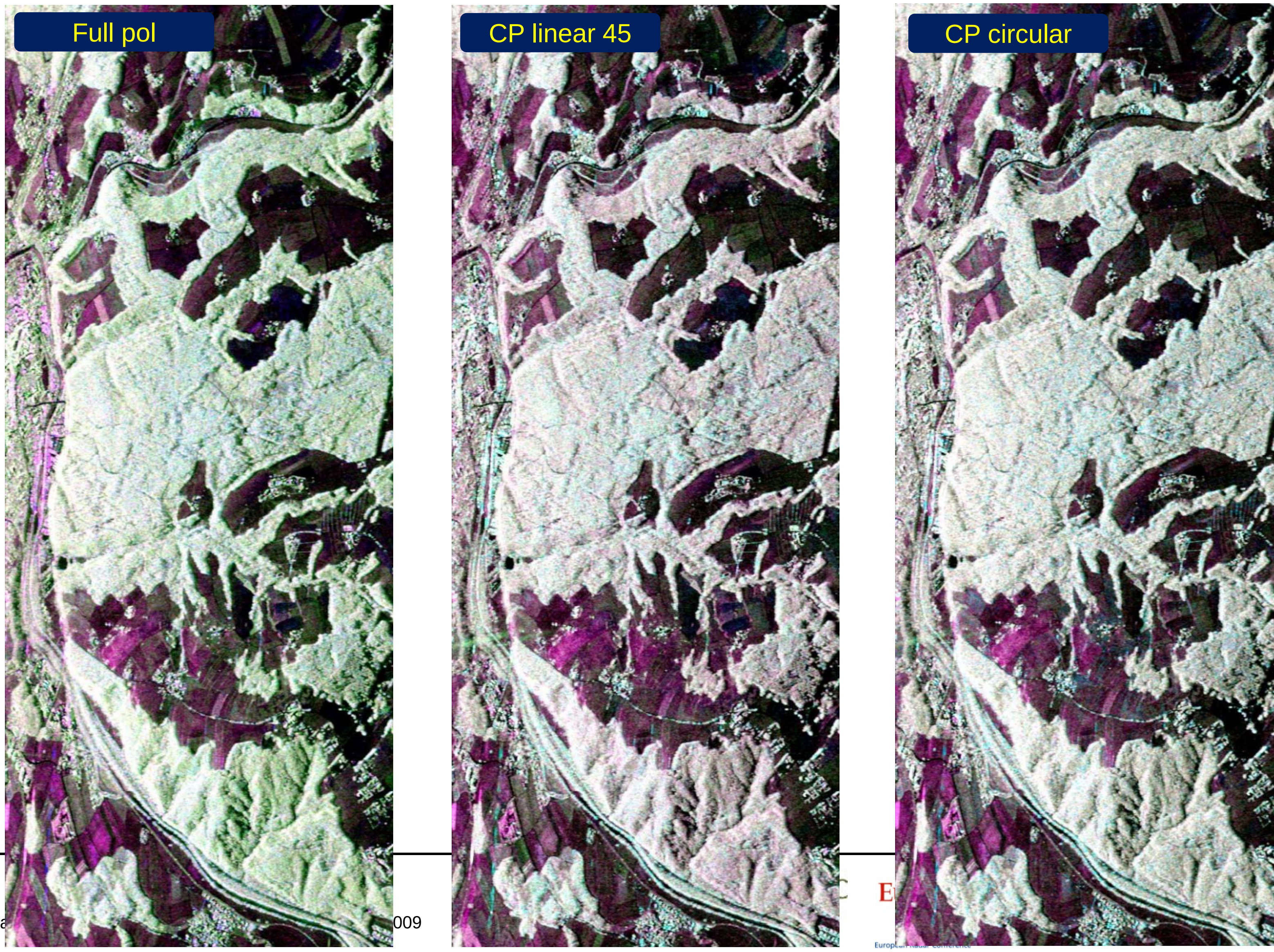

Reconstructed FP information

Airborne E-SAR data (Traunstein, Germany)

Reconstructed FP information

Airborne E-SAR data (Traunstein, Germany)

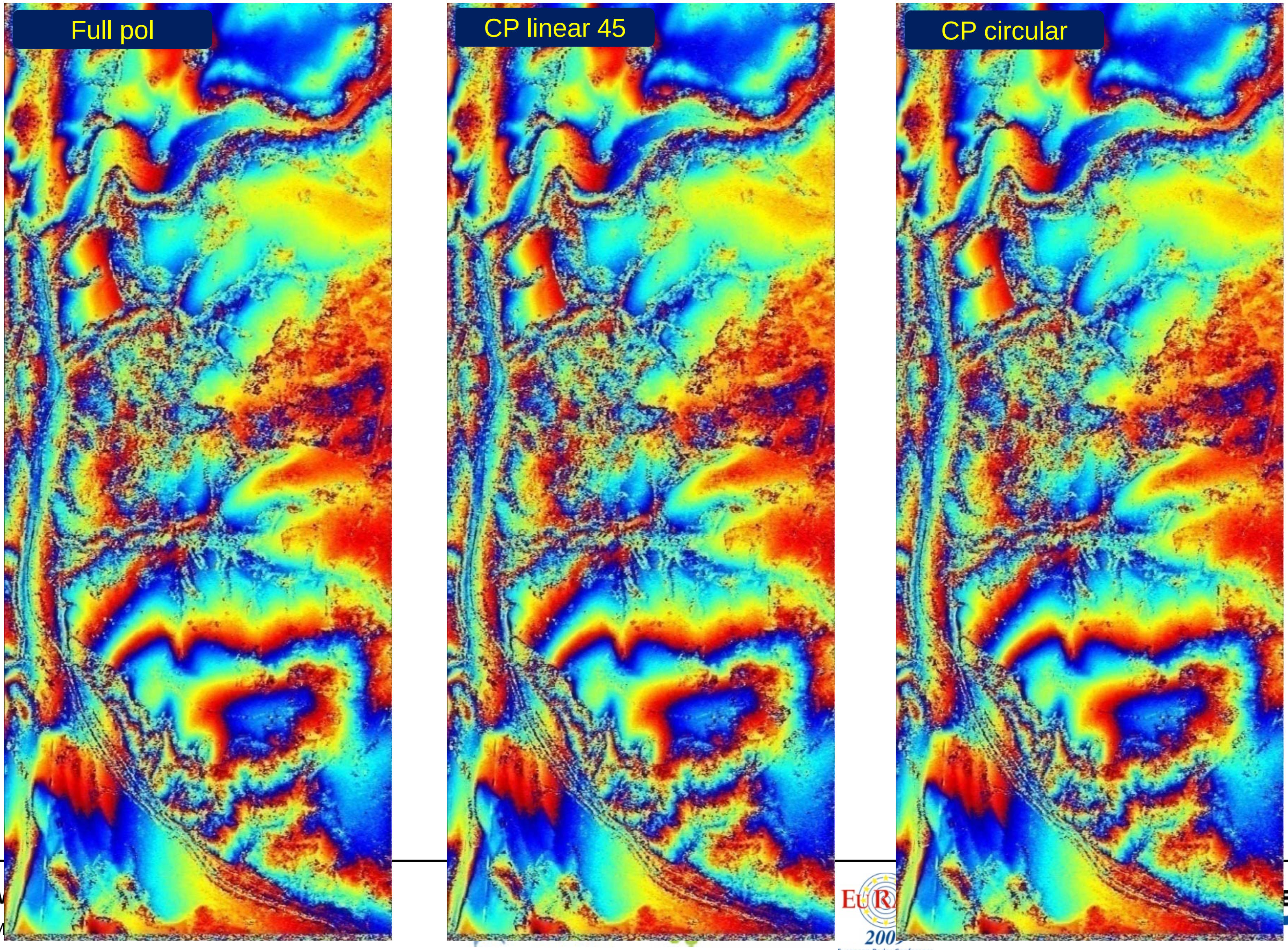

Reconstructed Full-PolInSAR

Row profiles

PolInSAR coherence HH

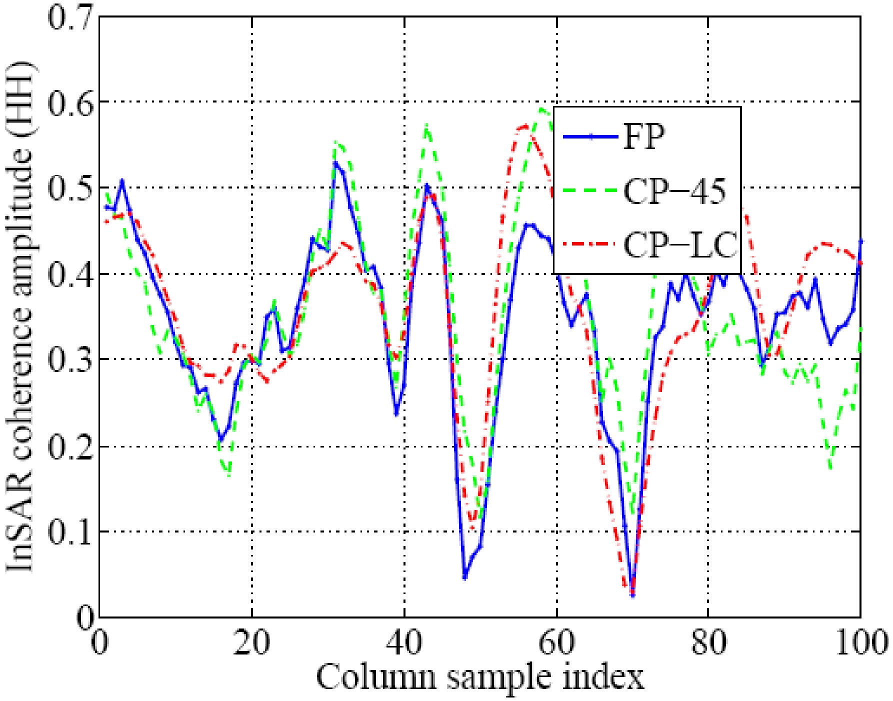

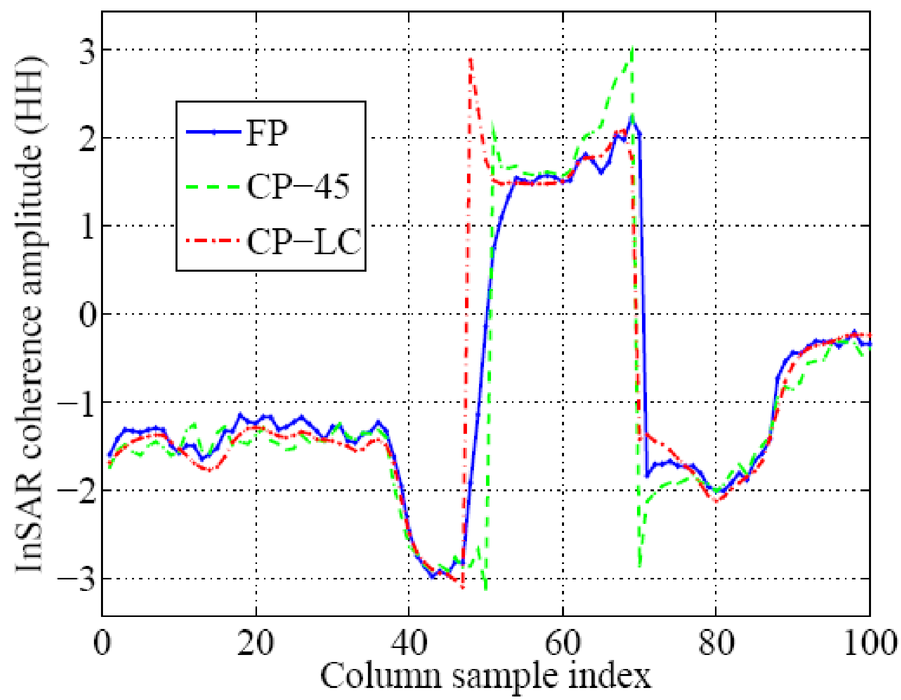

COMPACT/HYBRID MODES

NOT A SUBSTITUTE FOR COMPLETE FULL-POL SAR

- ☹ **SAR Processor does not introduce important distortions**
- ☹ **A/D Converters increase the Signal-to-Quantization Noise on HV/VH (6dB)**
- ☹ **Attenuation imbalance (9dB): Important Effect for the HV reconstruction**
- ☹ **Compact / Hybrid Polarimetric Reconstruction procedures cannot cope with point scatterers.**
- ☹ **Compact / Hybrid Polarimetric Reconstruction procedures cannot cope with quantitative Surf / Vol models, even in the "well posed" reflection symmetry case.**
- ☺ **A class of mixed Surf / Vol problems can however be identified**
- ☺ **Compact PolInSAR gives good performance in presence of "well posed" symmetry case.**